STRUCTURAL HEALTH MONITORING OF HIGHWAY BRIDGES IN ZAMBIA BY USING SENSOR TECHNOLOGY – A CASE STUDY OF NANSENGA BRIDGE

By

KASUMBA HOPESON

A Thesis submitted to the University of Zambia in fulfilment of the requirements for the Degree of Master of Engineering in Structural Engineering

THE UNIVERSITY OF ZAMBIA

LUSAKA

2019

COPYRIGHT- DECLARATION

I hereby declare that the work presented in this thesis is a result of my research work and that it has not previously been submitted for a degree, diploma or other qualification at this or another University. However, part of the work has been published by the 5th international conference on (DII) development and investment in infrastructure strategies for Africa.

_____ _____

Signature **Date**

CERTIFICATE OF APPROVAL

This thesis of **Hopeson Kasumba** has been approved as fulfilling the requirements for the award of Master of Engineering Degree in **Structural Engineering by** the University of Zambia

Examiner 1 Name	Signature	Date
_____	_____	_____
Examiner 2 Name	Signature	Date
_____	_____	_____
Examiner 3 Name	Signature	Date
_____	_____	_____
Supervisors Name	Signature	Date
_____	_____	_____
Chairperson	Signature	Date
_____	_____	_____

ABSTRACT

Structural Health Monitoring by use of Visual inspections of bridge structures can be subjective and inaccurate. Recent developments in sensing, communication and information technologies, however, have completely modernized the inspection procedures and significantly increased the efficiency in terms of labor and time. In recent years, innovations have led to the development of high-tech-based systems that range from sensing the structural condition or loading, to knowledge- based decision making. With such advanced technologies, a large number or portions of infrastructure can be managed in a fast and cost effective manner.

Bridge infrastructure are integral elements to transportation infrastructure, therefore Structural Health Monitoring (SHM) is essential to assess the integrity of load carrying capacity, safety and economic maintenance interventions. Damage to bridge structures can arise from a number of situation such as; prolonged use with increased imposed loads, environmental effects, inadequate maintenance and construction errors. This research focused on multiscale structural health monitoring of bridges in Zambia using wireless sensor technologies, with case studies on the Nansenga Bridge located on the Turnpike-Livingstone Road (T1). A rational decision making tool for conducting effective and efficient SHM of highway bridges has been proposed through this research

Nondestructive testing and evaluation techniques were used to collect data on the current condition of the Bridge. Due to lack of Design data and as built drawings on older bridges, a redesign of Nansenga Bridge was conducted to BS5400 parts 2&4 of 1978 in order to verify the incorporated rebar sizes, placement and spacing. With verified collected data, a Finite Element (FE) model of Nansenga was developed using FEM design 17 software, whereby moving load was applied to study both linear and dynamic responses of the bridge. Highly distressed regions from FE simulations agreed with onsite localized damage detected on the bridge deck and girders. Crack widths of 1.00mm to 1.75mm, which exceed maximum allowable width of 0.30mm, were detected thereby exposing both concrete and reinforcement to abnormal stress conditions. This excessive damage requires immediate attention by the agency responsible for roads as this bridge is on a Trunk Road, T1, linking Zambia to other SADCC countries (South Africa, Botswana and Namibia). Ultrasonic pulse velocity tests indicated crack depths of 50mm to 300mm on the Nansenga Bridge beams.

Key words:Structural Health Monitoring, Sensors, Non Destructive Testing,Finite element modelling

ACKNOWLEDGEMENT

I would like to first thank the almighty God for giving me a health life in undertaking this study.
I further give many thanks to my supervisor, Dr Michael Mulenga for his guidance, brilliant ideas and continuous support throughout my masters of structural engineering by research. I can never forget how blank I was about structural health monitoring during our first meeting in his office. Being alone in class with no one to ask made me doubt if I will ever complete this research but his guidance gave me strong faith to move on until I saw myself speak and understand the language.

I would also like to thank Eng. Hamunzala for his guidance on literature for finite element analysis, at the point when I almost applied to change the program of study he came and provided me with Abaqus software.

I further extend my appreciation to Eng Dbanga and Denis Kristen of strusoft (Sweden) for introducing me to FEM design software; it wouldn't have been possible to get this far. I would also like to thank the staff at Road Development Agency (RDA) bridge unit for information on Zambian bridges.

Lastly but not the least, I would like to thank my friends, staff at Hopkas engineering consultants Ltd, family and children (Chanda Kasumba, Hopeson Kasumba Jnr and Luse Kasumba) for their support and encouragement, and not forgetting Eng. Peter Kapala my mentor for encouraging me to pursue research on structural health monitoring.

CONTENTS

LIST OF APPENDICES

LIST FIGURES

List of Tables

ABBREVIATIONS

AE	Acoustic Emission
B-WIM	Bridge weigh-in-motion
CCDs	Charge-Coupled Devices
DAQ	Data Acquisition
DLA	Dynamic Load Analysis
DSM	Digital Surface Model
DSP	Digital Signal Processor
EIZ	Engineering Institution of Zambia,
EM	Electromagnetic
EMI	Electromechanical Impedance
EO	Electro-Optical
FBG	Fibre Bragg Gratings
FEM	Finite Element Modelling
FEMU	Finite Element Model Updating
FEMR	Finite Element Model Refinement
FOS	French acronym for Structural Monitoring using
FOSs	Fiber Optic Sensors
GPR	Ground-Penetrating Radar
IBIS-S	Image By Interferometric Survey Sensor

IfSAR	Interferometric Synthetic Aperture Radar
LG	Long Gauge
MEMS	Micro Electromechanical Systems
MWM	Meandering Winding Magnetometer
NDE	Non-Destructive Evaluation
NDT	Non-Destructive Testing
OBR	Optical Backscatter Reflectometer
OFDR	Optical Frequency Domain Reflectometry
OTDR	Optical Time-Domain Reflectometer
POF	Plastic Optical Fibre
RADAR	Radio Detection and Ranging
RDA	Road Development Agency
R-WIM	Railway Weigh-In-Motion
SATCC	Southern African Transport and communication commission
SAR	Synthetic Aperture Radar
SEM	Scanning Electron Microscopy
SFAP.	Small Format Aerial Photography
SG	Short Gauge
SHM	Structural Health Monitoring
WIM	Weigh In Motion

WSSN	Wireless Smart Sensor Network

CHAPTER 1: INTRODUCTION

1.1 Definition of a bridge and Structural Health Monitoring

A bridge is a structure built to span a physical obstacle such as a body of water, valley, or road, for the purpose of providing passage over the obstacle. According to (RDA-SBD) Road Development Agency standard bidding document and (SATCC) Southern African Transport and Communication Commission, a Bridge is defined as a structure with a span greater than 6m between the inner faces of the abutments for carrying traffic or other moving loads over a depression or obstruction such as a channel, road or railway.

The life of a highway bridge is far from being monotonous and predictable. Much like our own existence, its evolution depends on many uncertain events, both internal and external. Some uncertainties arise right during construction, creating structural behaviors that are not predictable by design and simulations. Once in use, bridges are subjected to evolving patterns of loads and other actions. Often, the intensity and type of solicitation are very different from the ones taken into account during its design and in many cases they are mostly unknown in both nature and magnitude. The sum of these uncertainties created during design, construction and use, poses a great challenge to the engineers and institutions in charge of structural safety, maintenance and operation. Further, defining service levels and prioritizing maintenance budgets relying only on models and superficial observation can lead to dangerous mistakes and inefficient use of resources.

Regular visual inspections can certainly reduce the level of uncertainty, but still serious limitations exist resulting from observation of the structure's ’surface’’ condition during short times spaced by long periods of inactivity. In this research, bridge monitoring was embarked on to demonstrate acquisition of more reliable data based on the current conditions of bridges in Zambia, by applying both the wired and wireless sensor structural health monitoring (SHM) technologies, assessing extent of damage to bridge components like Abutments, Piers, bridge deck, beams, girders, anchored cables and towers, upon which bridge management and maintenance interventions can be based.

1.2 Why structural health monitoring of bridges in Zambia

The Zambian government has the overall responsibility for the construction, maintenance and functionality of their own bridges through road authorities, mainly the RDA and local authorities. The local authorities are often responsible for bridges in their jurisdiction, and may lack experience that would guide them in decision making. In addition, finances are limited and the authorities are looking for new and cost-effective solutions that will help them make informed decision on interventions. Some of the decisions on maintenance and new constructions of bridges are political, and these decisions often delay the execution of projects. In many instances, due to lack of alternatives, there is need to use the old bridges even if they are badly deteriorated. Using SHM techniques, such structures can be assessed before any management decision, to guarantee the safety of users and monitoring the integrity.

1.3. Economic and Life-Safety

Economic and life-safety issues are the primary driving force behind the development of structural health-monitoring technology. Marchesiello and Gorman (1999) state the need for accurate numerical models for bridge applications in which some modal frequencies are closely spaced, as illustrated in Equation 1.

$$\mathrm{CPM} = \frac{Capacity}{\sum_{i=1}^{n}\sum_{j=1}^{m}[C_{ij} + L_{ij}]}\ , \qquad \text{Equation (1.1)}$$

where the "*Capacity"* in the numerator gives a measure of the structure's remaining useful life and C_{ij} represents the cost of the structure's component *j* to resist the i^{th} failure mode or hazard and L_{ij} is the life of the structure.

1.4 Damage

Damage can be defined as changes introduced into a system that adversely affect its current or future performance. Damage alters the stiffness, mass, flexibility, and damping parameters of a structure. A review by Doebling and Farrar (1998), damage has been intentionally introduced into a structure in an effort to simulate damage without having to wait for it to occur. In other cases, the authors postulate a damage-sensitive feature and then develop an experiment to demonstrate the effectiveness

of this feature. In these cases, there is no need to formally define damage. Most laboratory investigations fall into this category. When a SHM system is deployed on an *in situ* structure, it is imperative that the investigators first clearly define and quantify the damage that they are looking for; then, they can increase the likelihood that the damage will be detected with sufficient warning, and to make optimal use of their sensing resources. Several analysis procedures exist to model the complex behavior of concrete, including concrete cracking, tension stiffening, and nonlinear multiaxial material properties. Finite element techniques, for example, are developed to permit a more rational analysis of cracking. Equation 1.2 defines a local damage index:

$$d_n = \frac{S_n - \bar{S}_n}{S_n} = 1 - \frac{\bar{S}_n}{S_n} \quad , \qquad \text{Equation (1.2)}$$

where S_n is the original cross section area, and $\acute{S}_n$ is the effective resisting area after crack formation.

The local damage index, d_n, represents the surface density of cracking, and it is initially zero when the concrete is in its intact state. Based on this local damage index, a modified constitutive relation between stress and strain can be formulated. The modified constitutive model accounts for the reduction of the moment resisting area caused by the cracking, and the different responses in tension and compression are taken into account.

1.5 Statement of the problem

- Structural assessment of bridges in Zambia has been ineffective because it has been based only on visual inspections, lacking determination of the exact location and maximum extent of damage.
- Tools for planning, construction, maintenance and management of bridge infrastructure are inadequate

1.6 Significance of study

This study is aimed at demonstrating SHM with a view to:

- Improving the credibility of bridge inspections and subsequent ratings through less subjective techniques and data;
- Improving data consistence enabling the development of better decision-making tools;
- Improving and augment visual assessment, and provide early detection and warning;
- Assessing long-term performance result in modified specifications and inspection standards, and optimization of inspection schedules; and
- Allowing more rational decision making on maintenance or replacement scheduling which could result in the optimization of maintenance cost and increased reliability of high way bridges.

1.7 Objectives of this research

1.7.1 Main Objective

The main objective of the research was to:

- Propose an effective and efficient decision making tool for monitoring high way bridges in Zambia.

1.7.2 Specific Objectives

The specific objectives were to:

1. Review types of Structural Health Monitoring in use in Zambia
2. Review improved and cost-effective technologies on SHM of bridges that could be applied in Zambia
3. Apply sensor technologies for SHM on Zambian highway bridge with a case study of Nansenga Bridge
4. Demonstrate the application of SHM systems in order to illustrate the salient features of the subject area and highlight the numerous results that could be achieved.
5. Highlight the general results and applicability of SHM
6. Propose a rational decision making tool for bridge infrastructure interventions in Zambia based on SHM of technology

1.8 Research questions to be answered

To address the specific objectives, the research questions for this study were as follows:

I. What systems exist for inspection and monitoring of highway bridges in Zambia?
II. What technologies exist for SHM elsewhere?
III. Is there need for SHM of highway bridges in Zambia?
IV. Is the current inspection and monitoring of highway bridges in Zambia effective and efficient?
V. Is there deterioration in bridge infrastructure in Zambia? (existence)
VI. On the selected bridge:
    a) Where is the damage in the structure? (location)
    b) What kind of damage is present? (type)
    c) How severe is the damage? (extent)

VII. Is there a rational decision making tool for planning, construction, maintenance and management of bridge infrastructure in Zambia?

1.9 Thesis structure

This thesis has six chapters, chapter one covers introduction which defines the study, the problem and significance of the research. Chapter two presents literature review with recent technologies and recommendations by other researchers in the field of structural Health monitoring relevant to this study. The methodology of this research has been covered in chapter three were stages involved in undertaking this study successfully have been explained. Chapter four presents results of data collected, design control, finite element and experimental SHM field tests. Discussion of results has been done in chapter five comparing and highlighting numerous results that were achieved in order to meet the objective of this research. Conclusions and recommendations are presented in chapter six of this thesis confirming the achievements and challenges of the research associated with meeting the objectives of the research.

CHAPTER 2: LITERATURE REVIEW

2.1 Structural Health Monitoring of Bridges in Zambia

From 1964 to date, Zambia has not applied effective bridge monitoring technology apart from visual inspections. According to a Road Development Agency (RDA) Bridge inventory report of 2010 conducted by Rankin Engineering Consultants which gave an update on the status of bridges in Zambia, Rankin Engineering conducted only visual inspections on bridges around the country and established that the country had 454 major bridges (bridges longer than 60m) and 3321 culverts. Out of these major bridges, 28 located on feeder roads were beyond repair, 49 were too expensive to repair. One of the major bridges surveyed was the Kafue Hook Bridge, on the Lusaka-Mongu Road (M9). One hundred and twenty six (126) bridges were in a marginal condition while the conditions of the rest ranged from satisfactory to good. According to National Bridge Inventory Systems (NBIS) USA, bridges must be inspected every 2years and it took Zambia more than 45years to conduct the first inspection and condition rating. According to the National Highway Institute within the Federal Highway Administration (FHWA) guidance document, USA, the condition rating of 1995 indicated that 0.00 to 9. 45% of the Zambian major bridges do not satisfy the structural integrity and were risky to users**.**

2.2 Structural Health Monitoring Technologies and advancement

Structural health monitoring is a non-destructive *in-situ* structural sensing and evaluation method that uses a variety of sensors attached to, or embedded in a structure to monitor the structural response, analyze the structural characteristics for the purpose of estimating the severity of damage/deterioration and evaluating the consequences thereof on the structure in terms of response, capacity, and service-life (Karbhari et al 2005,).The sensors obtain various types of data (either continuously or periodically), which are then collected, analyzed and stored for future analysis and reference. The data can be used to identify damage at its onset, to assess the safety, integrity, strength, or performance of the structure.

SHM may also include the use of many devices, techniques and systems that are traditionally designated as Non-Destructive Testing (NDT) and Non-Destructive Evaluation (NDE) tools. There

is no formal delineation between each approach, but there is a difference between NDT/NDE and SHM. NDT/NDE normally refers to a one-time assessment of the condition of materials at a single point and the effect or extent of the deterioration in the structure using equipment external to the structure. SHM normally refers to activities focused on assessing the condition of the structure or its key components based on response to various types of loads. It generally involves on-going or repeated assessment of this response. Some sensor systems may need to be embedded in or attached to the structure for the complete monitoring period.

Structural health monitoring is commonly considered only as acquisition of data from a structure about its response to external and internal excitations. More importantly, SHM also includes the interrogation of this data to quantify the change in state of the structure and thence the prognosis of aspects such as capacity and remaining service-life. The former is hence a necessary, but not sufficient, part of the latter. Also, the concept of monitoring prescribes that it be ongoing, preferably, an autonomous process rather than one that is used at preset time intervals, through human intervention. Thus SHM is essentially the basis for condition-based, rather than time-based monitoring and the system should be integrated into the use of real time data on aging and degradation, in the assessment of structural integrity and reliability. In addition to the need for current condition assessment and long-term monitoring for better management of existing structures, the following factors also contribute to the recent rapid development and advancement of SHM technologies in civil engineering (Bisby 2006):

- The recent advancements in sensing technologies with high speed and low-cost electronic circuits, and development of highly efficient signal validation and processing methods (e.g. fiber optic sensors (FOSs) and smart materials);
- Ongoing developments in communication technologies, wide usage of internet and wireless technologies;
- Developments of powerful data transmission and collection systems, data archiving and retrieval systems; and advances in data processing, including damage detection models and artificial intelligence algorithms.
- SHM of infrastructure provides early warning of structural damage or decay, thus improving the health of our infrastructure systems.

2.3 Classification of SHM

According to Sikorsky (1999), SHM systems can be classified both in terms of their level of sophistication and by the types of information (and decision making algorithms) which they are capable of providing. These classifications are particularly instructive in understanding the goals of SHM and some of the concepts that are discussed later in this report. The classifications of SHM systems can be summarized as follows (Sikorsky1999):

- **Level I:** At this level, SHM system is capable of detecting damage in a structure, but cannot provide any information on the nature, location, or severity of the damage. It cannot assess the safety of the structure.
- **Level II:** Slightly more sophisticated than Level I. Level II systems can detect the presence of damage and can also provide information on its location.
- **Level III:** A Level III SHM system can detect and pinpoint damage, and quantify the damage to indicate the extent of its severity.
- **Level IV:** This is the most sophisticated SHM system. At this level, the system is capable of providing detailed information on the presence, location, and severity of damage. It is able to use this information to evaluate the safety of the structural system. Obviously, as the level goes higher, more information could be obtained from the SHM system although the system is becoming more complicated and costly.

2.4. Types of SHM

In addition to the sophistication and objective, SHM can also be classified into at least four types or categories in terms of the type of field testing undertaken and the timescale on data acquisition, as shown in Figure 2.1 (Bisby 2006).

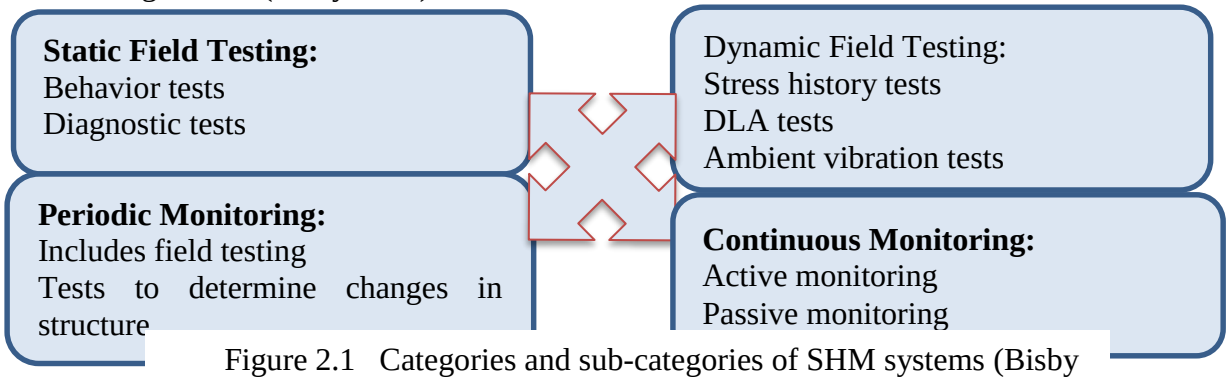

Figure 2.1 Categories and sub-categories of SHM systems (Bisby

These various types are not independent to each other, as more than one type of testing or monitoring may be employed in a complete SHM program. More details, along with the associated content in static and dynamic field testing are presented in the following sections.

2.4.1 Static Field Testing

Since field testing of bridges is a critical part of a complete SHM program, this and the following sections are devoted to bridge field-testing. In a broad sense, bridge tests are either static or dynamic, which indicate how the structure is excited (static load, dynamic load, or ambient vibrations) to obtain its response.

Static field testing is commonly used to determine the load carrying capacity of a structure, and to provide data about a structure's behavior and ability to sustain live loads. During static tests, loads are slowly placed and sustained on the structure (i.e. trucks or calibrated test vehicles travelling at crawl speed across the bridge) and the structural response is measured and recorded by a network of sensors. These types of loads do not cause any dynamic effects such as impact, vibrations or resonance and hence the interpretation of data is less complex and more easily calibrated against theoretical models and calculations. Static testing is easy to perform and enables examination of structural behavior and health, although the tests do not capture the full load response actually experienced by most structures, particularly for the case of bridges where moving loads excite the dynamic response of the structure.

2.4.2 Dynamic Field Testing

Every structure has its own typical dynamic behavior, known as the 'vibration signature'. Vibration, i.e. the periodic to-and-fro motion of a structure of its members is characterized by three basic parameters: how quickly the motion is repeated (frequency), the magnitude of the motion is (amplitude), and how soon it dies out without new supply of excitation energy (damping). Changes in a structure, such as damage and deterioration leading to decrease in the load-carrying capacity, affect the dynamic response of it. Subsequently, the measurement and monitoring of dynamic response characteristics can be used to evaluate structural integrity.

Dynamic field testing is mostly applicable to bridges since bridge structures are generally subjected to moving traffic loads. To perform a dynamic testing, the bridge needs first to be excited by operational conditions or artificial vibrations. One of the following methods are usually used;

I. moving traffic (ambient vibration);
II. controlled moving truck loads; or,
III. forced vibration using impact hammer or shakers.

Dynamic response (acceleration or velocity versus time) of the bridge can be acquired by instrumentation of the structure with various sensors. Data and information from the monitoring sensors are accumulated and integrated for analysis, interpretation and decision-making Patjawit and Nukulchai (2005), In general, tests with forced vibration are conducted on smaller bridges. For larger truss, suspension and cable-stayed bridges, ambient tests become the only practical means of exciting the structure. In a typical dynamic field testing using a moving controlled vehicle, a test truck moves across a "bump" of a predetermined size on the bridge being tested. The test is usually carried out several times with the test vehicle travelling at a range of velocities. The vehicle hitting the bump introduces an impulsive dynamic load into the structure, which excites the bridge's dynamic response.

2.4.3 Periodic Monitoring

Structural health monitoring of civil engineering structures can be either be periodic or continuous. Periodic monitoring is conducted to investigate the structural response or any detrimental change that might occur in a structure at specified time or time intervals (e.g. weeks, months, or years apart). Analysis of the monitoring data may indicate damage or deterioration. For example, monitoring through static field testing or moving traffic, monitoring crack growth, monitoring before and after a repair, can all be done periodically. In periodic monitoring, sensors may be permanently installed on the structure or temporarily installed at the time of testing (Bisby 2006).

2.4.4 Continuous Monitoring

Continuous monitoring, as the name implies, refers to monitoring of a structure for an extended period of time (weeks, months, or years) without interruption. This type of monitoring has only recently been used in full scale field applications, due in part to the higher costs and complexity of SHM system (Bisby 2006). In continuous monitoring, data acquired at the structure are either collected or stored on site (logged) for transfer, analysis, and interpretation at a later time, or they are continuously communicated to an offsite (remote) location. In the most sophisticated of these types of SHM applications, field data are transmitted remotely to the engineer's office for *real-time monitoring* and interpretation. Customarily, continuous monitoring is only applied to those structures that are either extremely important or when there is a doubt about their structural integrity. The latter might be the case if the structure is likely to be exposed to extreme events, such as severe earthquakes and hurricanes, or if its design includes an innovative concept that does not have a history of performance to prove its long-term safety.

2.4.5 Components of SHM Systems

As mentioned previously, structural health monitoring refers to subjecting the structure to static or dynamic excitations, continuous or periodic monitoring of the structure's response using sensors that are either embedded in or attached to the structure. New advances in sensor and information technologies and the wide usage of Internet is making SHM a promising technology for better management of civil infrastructures. There have been many case studies worldwide in the past decade. While the specific details of each SHM system can vary substantially, SHM basically involves sensor and data acquisition, data transfer and communication, data analysis and interpretation, and data management. Thus a SHM system will typically consist of six common stages, as shown in Figure 2.2, namely:

- Data acquisition networks;
- Communication of data;
- Data processing;
- Storage of processed data;
- Diagnostic and prognostic analysis (i.e. damage detection and modeling algorithms, event Identification and interpretation); and

- Retrieval of information as required.

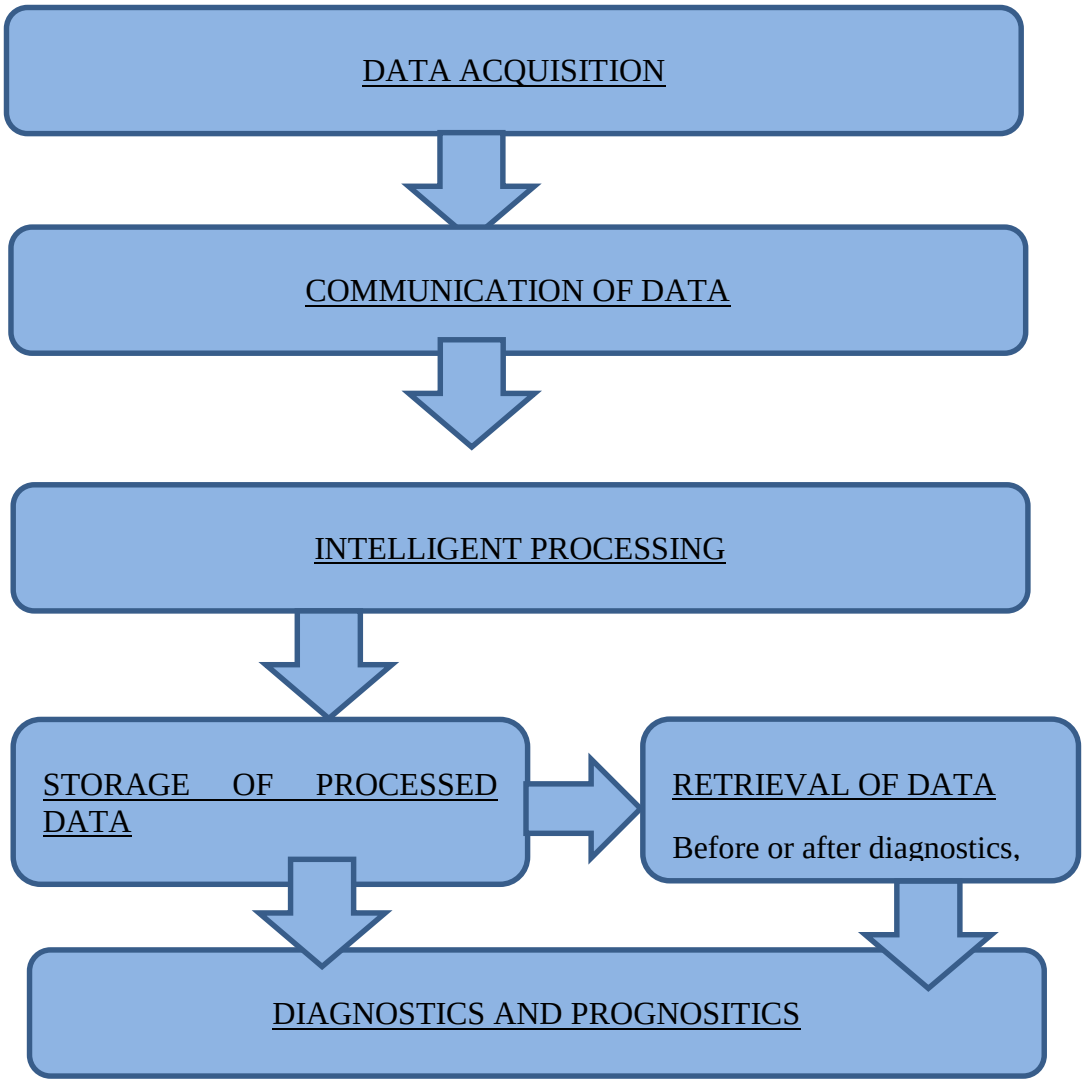

Figure 2.2 Components of a typical SHM (Bisby 2006)

A typical flow pattern between the six components of a SHM system is shown in Figure 2.2; however, other flow patterns are also possible, and the flow of information between system components can certainly take more than one path. Each of the various systems components is discussed in more details in this chapter.

2.5 Reported Advantages and Benefits of SHM

Structural health monitoring presents a number of key benefits for civil engineering structures. Some of the most commonly cited benefits of SHM include:

2.5.1 Early damage detection

Detection of structural damage at its onset permits early action which may prevent the structure from having to sustain loads for an extended period of time while in a damaged state. As a result, it becomes less necessary for structures to be *overdesigned*, which significantly lowers construction costs (Lau, 2003) and increases the overall efficiency of infrastructure projects. Early damage detection also allows repairs to be made at the onset of damage, which can drastically decrease the resulting repair costs and prevent further deterioration (Pines and Aktan, 2002). Additional cost savings are due to decreased site visits and manual investigations by maintenance workers, since in some cases pertinent data can be transferred remotely from the structure to an offsite location for analysis.

2.5.2. Assurances of a structure's strength and serviceability

Assurances of a structure's strength and serviceability can be particularly important for long-span bridges, where visual inspections are, in many cases, impossible or inadequate for determining a bridge's safety (Pines and Aktan, 2002). In addition, SHM can be used where data is needed to provide confidence in a new building material or an innovative construction technique. In the case of a structure nearing the end of its service life, SHM may permit its continued use for a time, by providing confidence of its satisfactory performance.

2.5.3. Reduction in down time

Down time during structural repair or upgrade works is one of the major costs that must be considered in assessing the whole-life cost-effectiveness of our infrastructure systems. While costs due to down time can be extremely difficult to quantify, since they include costs to society due to loss of productivity and economic growth, inconvenience costs, and energy costs, it is now widely accepted that these costs must be considered when examining various rehabilitation and upgrading schemes, particularly for highway bridges. Early damage detection and an improved understanding of

structural behavior result in a reduction in down time for structures which may require repair or strengthening.

2.5.4. Improved maintenance and management strategies for better allocation of resources

SHM systems reduce the requirement for field inspection and enable the development of large-scale infrastructure condition databases which can be automatically updated. Decision makers can formulate better strategies to effectively deal with infrastructure deterioration and allocate shrinking budgets and scarce resources more efficiently.

2.6 Bridge SHM Technologies

SHM techniques include both the wired and the unwired systems, as presented in the next sections.

2.6.1 Wireless smart sensors

With the advancement in the electrical circuits, Micro electromechanical systems (MEMS) and network technology, wireless smart sensor network (WSSN) has shown significant potential for replacing existing wired SHM systems due to their cost effectiveness and versatility. Wireless smart sensors (WSSs) offer a solution for long-term, scalable SHM of civil infrastructure by providing easier installation and efficient data management at a lower cost than traditional wired monitoring systems. Specifically, the wireless sensor unit (IMOTE 2 and Sensor board) possesses multiple sensor channels and costs less than $500 (Sushil, 2013). As far as installation time and effort is concerned, it is less than the wired sensor network installation. The on-board computation capacity of WSS helps to mitigate the problem of data inundation that is intrinsic to densely instrumented structures (Jang et al., 2010). Moreover, the on-board microprocessor present on each sensor can be used for digital signal processing, self-diagnosis, self-calibration, self-identification and self-adaptation functions (Spencer and Cho 2011).

Fibre Optic Sensor (FOS), Micro Electro Mechanical Systems (MEMS), optical distance measurement techniques, acoustic emission and different types of lasers and radars are now available on the market (Enckell 2013). Remote sensing is the technology of obtaining reliable information on

a given object or area either wireless, or elsewhere without physical or intimate contact with the object. Any form of non-contact observation can be regarded as remote sensing. Microwave Interferometry and photogrammetry are good examples of remote sensing. Nearly any preferred parameter can be measured nowadays and existing systems also perform automatic data processing and analysis in real time and with remote access. New challenges are faced when working with emerging technologies but, with correct procedures, it is possible to accomplish sustainable SHM. People working with new and emerging technologies need to be open for new ideas, ways of thinking and need to have an idea about the future development in order to find flexible, adaptable solutions that will meet the requirement not only now but also in the future. Some emerging technologies and areas that are relevant for bridges and other civil engineering structures are presented in the following sections.

2.6.2 Interferometric radar

This is a remote sensing technology for obtaining reliable information on a given object or area either wirelessly, or elsewhere without physical or intimate contact with the object. The monitoring devices may be mounted inside or outside the structural members.

Interferometric radar is a pioneering ground-breaking technology in the domain of geodetic measurements that is now spreading out to the civil engineering field. The measurement device is coherent radar. Gentile (2010) describe their image by interferometric survey (IBIS-S) sensor that is based on both wideband and interferometric techniques and was developed to measure the deflection of several points on a structure at a sensitivity of better than 0.02 mm, a goal which was achieved and made the system the most accurate, stand-off sensor system for the remote monitoring of displacement and deflection in civil engineering structures.

Interferometric survey is a coherent radar system, meaning it preserves the phase information of received signals. The central frequency is 16.75 GHz and the antenna can be rotated in any direction. The bandwidth scanning rates are as high as 200 Hz and the sampling interval is 0.005 s. These characteristics make the system suitable for dynamic monitoring and waveform definition of acquired signals (Gentile 2010). The instrument generates, transmits and receives the electromagnetic signals to be processed to provide movement and deformation measurements (Gentile 2010). Both static and dynamic measurements of structures can be performed. This non-contact method to measure objects

distanced up to kilometres is convenient for many applications like stay cables and main cables in bridges. No instrumentation is needed, traffic can continue and the method saves time, money and resources. Interferometric Radar was used on the Manhattan Bridge, shown in Figures 2.3. Manhattan Bridge was built in 1909 and suffered of fatigue cracks concrete decks and piers. Monitoring of the vertical and torsional displacements of the mid-span using Interferometric Radar and GPS can be seen in Mayer et al. (2010).

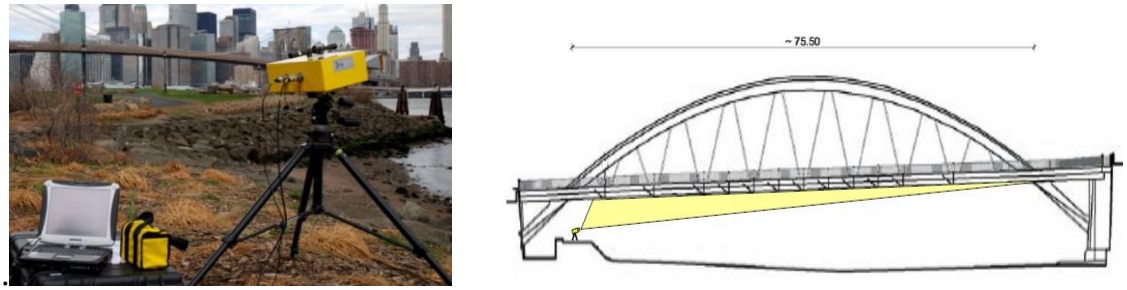

(a) (b)

Figure 2.3 Interferometric Radar Equipment IBIS-FS in front of the Manhattan Bridge (Courtesy of Ingegneria Dei Sistemi S.p.A, IDS, 2014)

2.6.3 Electro-Optical Imagery and Photogrammetry

Electro-optical (EO) sensors are those electronic sensors which are sensitive to electromagnetic radiation in the visible spectrum. Charge-coupled devices (CCDs) are the most common electro-optical sensors and this section considers the contribution of even these simple digital camera components to structural health monitoring of bridges. Photogrammetry refers simply to the practice of making measurements from photographs and would currently include measurements made from both film photography and electro-optical (digital) photography. Digital photogrammetry has been demonstrated as a viable technique for generating 3D models of structures and structural elements such as medieval bridges and has also been shown to contribute specifically to damage monitoring of such (Arias et al. 2007).

Aerial photography has long been studied as a method of SHM as it was the first remote sensing method to be developed for any application. Bridge inspection demands a higher resolution from aerial photography than is normally obtained for most applications. Though most aerial photography

missions are flown at 5,000m above sea level and higher, lower altitudes are necessary to achieve the higher resolution (and consequently smaller area imaged) that is required (Liu et al. 2010). This technique is called small-format aerial photography (SFAP). While aerial photography is also usually orthorectified (intentionally distorted to more accurately represent ground coordinates with respect to topography), at such low altitudes (e.g. 300m), SFAP imagery does not need such post-processing (Rice et al. 2010). This technique is often useful only as a qualitative assessment of cracking, corrosion, deflection, or displacement. While feature recognition and qualitative assessment are viable using FSAP, attempts at more rigorous application of the technique have demonstrated its limitations, such as its coarse resolution (e.g. 1.2 cm) which prevent it from being useful for many SHM applications (Liu et al. 2010).

2.6.4 Fibre Optic Sensor technology

Fibre Optic Sensors (FOSs) operate over a range of wavelengths but the 1550 nanometre wavelength is standard for minimal losses. They are generally divided into two kinds; single mode and multimode. Many applications for FOSs use single mode fibres with the core diameter of 5 to 10 micrometers. Optical connectors are normally used in sensor applications to connect the sensors to transmitting cables, interrogators or to each other. The market is full of various types of connectors but many commercial sensor manufacturers generally use E-2000 and FC/APC connectors. Many fibre optic sensors are ready for installation and are delivered with transmission cables connecting to the data acquisition units, connectors and connector protection. However, when working with large and complicated applications, as well as problem localization and repairing; it is necessary to have both knowledge and practical experience about related tools and equipment. A special laser pointer or a laser pen is a simple and useful tool to control the function of sensors and cables. The pen sends light into the system and the sensors and cables can be visually checked for light losses and eventual fibre breakages. Figure 2.4 shows a typical fibre breakage in an installed tape.

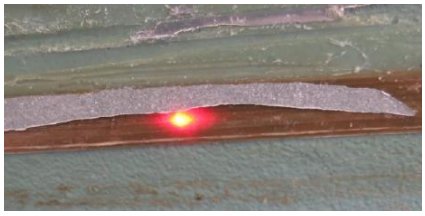

Figure 2.4 A luminous spot indicating a fibre breakage in an installed tape sensor (Song 2012)

An Optical Time-Domain Reflectometer (OTDR) is an optoelectronic instrument that is used to characterise an optical fibre. An OTDR inserts a series of optical pulses into the fibre during testing and extracts back scattered light from points in the fibre where the index of refraction changes. The strength of the return pulses is measured and integrated as a function of time. An OTDR allows measuring fibre length, attenuation and optical return losses and also helps to localize breakages. Figure 2.5 shows an OTDR system.

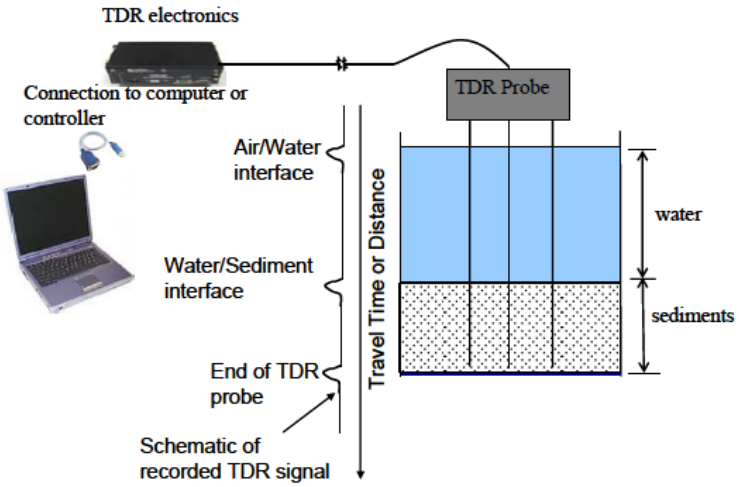

Figure 2.5 Optical Time-Domain Reflectometer (Song 2012)

There are numerous different techniques and various kinds of sensors that also can be modified for unique monitoring needs for a particular structure [Udd 1991, 1995, 2006]. FOS allow for measurements that have been unpractical or too costly with the traditional sensor technology. Hundreds of measuring points along the same fibre, as well as distributed sensing, versatility, insensitivity for electromagnetic fields, operability under extreme climate conditions and also the fact that there is no need for protection against lightning are some of the advantages over the electrical-based counterparts (Ross and Matthews 1995).

The core serves to guide the light along the length of the optical fibre and it is surrounded by cladding with slightly lower index of refraction than the core. Cladding minimise the losses as the light propagates in the fibre but also physically supports the core region. Optical fibres for FOS are usually made of very pure glass i.e. fused silica but Plastic Optical Fibres (POFs) also exist. Silica based optical fibres transmit light over large distances with very little losses while POF suffer from attenuation and distortion characteristics. Fibre optic sensors are either intrinsic or extrinsic: optical

fibre itself can be an intrinsic sensor, part of the optical fibre can be an intrinsic sensor or the optical fibre can be used to connect a non-fibre optic extrinsic sensor to a measurement system. Different parts of the optical fibre can also be used to measure different parameters e. g. strain and temperature. If the sensors are divided by the transduction mechanism affecting the property of light, the categories are the following; intensiometric, interferometric, polarimetric, modalmetric and spectrometric (Measures 2001). FOSs used in civil engineering applications are in common spectrometric and interferometric. Fibre Bragg Gratings (FBG), sensors based on Brillouin, Raman and Rayleigh scatterings are spectrometric and Fabry-Perot, Michelson and Mach-Zehnder Interferometer sensors are interferometric (Inaudi 1997). Figure 2.6 shows a typical single mode of optical fibre.

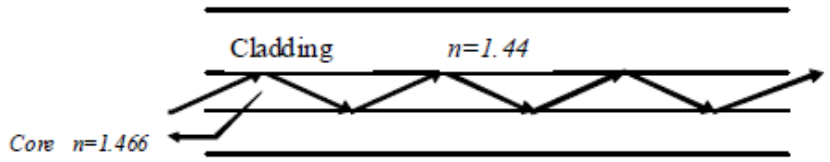

Figure 2.6 A typical single mode of optical fibre (Ansari, 1997)

The monitoring of the structure can be either local, concentrating on the material behavior or global, concentrating on the whole structural performance. Fibre optic technologies offer a wide variety of sensors for short gauge (SG) length, long gauge (LG) length as well as distributed and environmental parameter monitoring. FOSs in civil engineering can be used to measure strains, structural displacements, vibration frequencies, acceleration, spatial modes, pressure, temperature, humidity and so on. The list is long and the techniques are innovative and in the explosive stage of development. FOS can be measured and tested in many ways. The simplest way of checking is by connecting a laser pen to the sensor coupler and to see if the light travels through the sensor. Demodulators for LG sensors are the Optical Time Domain Reflectometer (OTDR).

2.6.4.1 Fibre Bragg Grating

A Fibre Bragg Grating (FBG) sensor consists of a single mode optical fibre that contains a region of periodic variation in the index of the fibre core, the so called “grating”. When intense light is exposed to the core of the optical fibre, this light wave propagates within the fibre. The wavelength corresponding to the grating field will be reflected and all the other wavelengths will pass by the grating uninterrupted. The reflected light is lead back and the analysis of the spectrum is performed

and converted into engineering units. FBG sensors for strain measurements exists both in SG and LG versions and both static and dynamic monitoring is possible. Most FBG sensors nowadays are also provided with temperature compensation. The versatility of FBGs is dominating compared to other fibre optic sensors and a lot of qualified products are already available commercially.

2.6.4.2 Distributed sensors

A Distributed sensor can replace a large number of discrete sensors, as a single cable is sensitive at every point along its length. Distributed sensor conveys measurements at discrete points that are spaced along the fibre by a constant value, called the sampling interval. Only a single connection cable to transmit the data to the interrogator is required. Various techniques for distributed sensing with FOSs exist and are based on FBG and Raman, Brillouin and Rayleigh scattering in optical fibres. These sensors can use thousands of discrete FBG points in same fibre or simply a standard single mode optical fibre. The advantage with sensors based on FBG is that they can perform dynamic measurements while other techniques measure the static behavior of the structure. The disadvantage with sensors based on FBG is the short measuring length, up to 70 meters while other distributed techniques can measure up to tens of kilometres.

Distributed systems based with discrete FBG point sensors use OFDR technique with swept-wavelength interferometry to spectrally and simultaneously interrogate thousands of sensors in a single fibre. This system can perform static measurements to distances up to 70 meters and dynamic measurements up to 7 metres.

Another distributed sensing system uses a standard single mode optical fibre and the Optical Backscatter Reflectometer (OBR) (Lanticq V et al., (2009). An OBR with swept-wavelength interferometry measures the Rayleigh backscatter as a function of the length of optical fibre. An OBR is able to interrogate thousands of points in a single fibre; it simply transforms a standard telecom fibre into a strain and temperature sensor. These two systems provide distributed measurements of temperature or strain with up to 10 millimetre spatial resolution along the length of the fibre. Resolution of ± 0.1°C, ±1 microstrain over the spatial resolution of 10 millimetres is also achieved.

Distributed sensing based on Brillouin scattering (Measures, 2001,) commonly consists of a single optical fibre which can be used to measure either strain and temperature or both along the fibre, for

distances up to tens of kilometres. Brillouin scattering takes place due to interaction of light with phonons in optical fibres. The phonons will shift the frequency of the light in order to the acoustic velocity of the phonons. The acoustic velocity consecutively is dependent on the density of the glass and material temperature. As the Brillouin frequency varies linearly with applied strain and temperature, it makes it possible to measure both parameters simultaneously along an optical fibre. The scattering phenomenon can be either spontaneous or stimulated. Raman scattering is the result of a non-linear interaction of the light travelling in the silica fibre core and based on the change in amplitude of Raman scattered light which is dependent only on temperature. Therefore, distributed sensing based on Raman scattering is used for temperature measurements. Insensitivity to strain is actually a benefit since no particular packaging of the sensor is needed. Typical spatial resolution of Raman systems is 1 m, and typical resolution is better than 1C Raman based systems are used for leakage monitoring in large structures like leakage of pipelines, dykes and dams.

2.6.4.3 Fabry-Perot sensors

There are three types of Fabry-Perot sensors; intrinsic, extrinsic and in-line fibre etalon versions (Measures, 2001). Chen et al. (2006) describes micro-air-gap based intrinsic Fabry-Perot sensors as well as their recent progress. The extrinsic Fabry-Perot sensor is easy to build; it consists of two optical fibres with a cavity, an air-gap of a few microns or tens of microns and can be seen in Figure 2.7 (Geib et al, 2003). The mirror-tipped optical fibres are supported within a micro capillary alignment tube. The sensor needs to be carefully calibrated in order to determine the gauge length of the sensor. Fabry-Perot sensors are able to measure a number of parameters; strain, displacement, pressure and temperature. Many sensors are also temperature compensated. They can be manufactured as strain rosettes meaning a sensor with several measuring points near each other; often in different directions like traditional strain rosettes based on strain gauge technology.

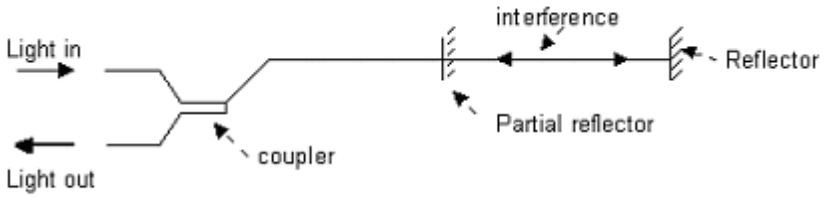

Figure 2.7 Fabry Perot sensors (yon tao dong 2010)

2.6.4.4 Michelson and Mach Zehnder interferometers

Michelson and Mach Zehnder interferometers are easy to understand and manufacture. The Michelson interferometer is more widely used. The sensor consists of two single mode optical fibres and has chemical mirrors in end parts; first fibre, the sensing fibre, is fixed in definite points and the other fibre, the reference fibre, is loose in order to keep a zero strain level (Measures, 2001). This loose fibre compensates thermal influences to the sensor. Data acquisition system sends the optical signal through a coupler to the sensor, mirrors placed at the end of each fibre reflect the signal back to the data acquisition unit that convert the measurement into engineering units. Since the sensor is pre-tensioned, it is possible to measure both elongation and compression.

A well proven Michelson interferometer is called SOFO (French acronym for Structural Monitoring using FOS) (Inaudi, 1997). The standard SOFO sensor is composed of two zones, the active zone which measures the deformations, and the passive zone transmitting data between the active zone and the interrogator. The SOFO sensor is a true LG sensor, with a typical gauge length between 20 centimetres and 10 meters. Large number of projects are installed with SOFO sensors and their long-term performance is good (Enckell, et al .2006). Figure 2.8 shows Mach Zender and Michelson interferometry sensors

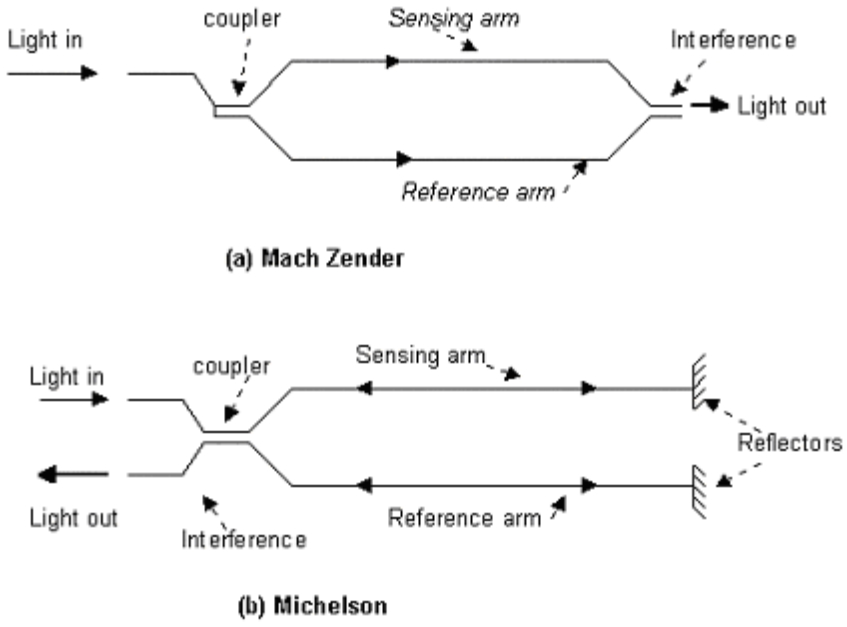

Figure 2.8. Mach Zender and Michelson interferometry sensors (yon tao 2010)

2.6.5 Accelerometers and Velocimeters

This is an in-situ monitoring technique, accelerometers are relatively simple devices that compare the acceleration they experience to the acceleration due to gravity and are commonly provided as micro electro-mechanical systems (MEMS)—tiny machines with computing power. Velocimeters typically work through the same principles as interferometry. In SHM, both are primarily used for measuring displacement—through the integration of acceleration or velocity measurements—of structural members they are attached to. As the second derivative of displacement, however, acceleration can never provide information about the absolute position of the structure making it useless for detecting differential settlements, leaning, or any permanent offsets (Kijewski.2005). GPS may provide absolute positioning, but even when it is used to inform accelerometer measurements, the second integral of acceleration provides larger relative displacements than those provided by GPS due to scale factor errors and sensor biases. In addition, the signal noise of an accelerometer is device-specific and all have a band-pass frequency response including significantly poor performance at vibration frequencies lower than 0.2 Hz which prohibits their application to long-span bridges (Meng et al. 2007).

Accelerometers have been used for their ability to detect higher-frequency vibrations, particularly those that cannot be monitored by GPS. These vibrations are either the result of ambient or forced bridge loading. Ambient movements are those which abound during the everyday life of the bridge; the results of traffic, wind, and water. Forced movements are specific loads applied to the bridge as tests for the purpose of measuring its response. Due to the cost of forced movement on long-span bridges and because it is virtually identical to the ambient movement of long-span bridges, it is generally not practiced (Meng et al. 2007).

Accelerometers have been used to monitor rigidly bolted joints for damage (Tanner et al. 2003) and could be used more generally to monitor the 3D displacement of large structural elements due to wind or load variance in real time. Accelerometers are also used in conjunction with innovative signal processing and time-series analysis for global SHM—the assessment of whether or not a structure has been damaged (Lynch et al. 2006). They are currently the convention for dynamic testing or monitoring of large structures and have also been recognized for their efficacy in studies comparing new SHM methods against them (Lynch et al. 2006). The ubiquity of accelerometers in SHM is shown by their use in studies examining more general aspects of SHM, in particular the shift from

wired to wireless sensor arrays, such as in Whelan et al. (2007).They can obtain accuracies in acceleration measurements on the order of milligrams of loading (Lee et al. 2005). Figure 2.9 shows a Schematic diagram of Piezoelectric Accelerometer

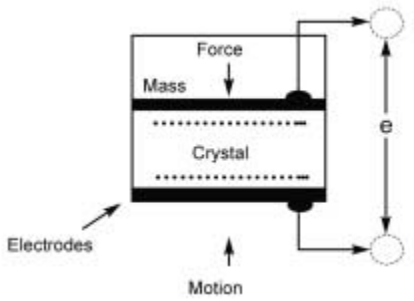

Figure 2.9 Schematic diagram of Piezoelectric Accelerometer (yon tao 2010)

2.6.6 Electromechanical Impedance

Electromechanical impedance (EMI) typically takes advantage of piezoelectric materials, which produce an electric field when subjected to mechanical stress. The effect also works in reverse in that piezoelectric materials will produce stress and/or strain when in the presence of an electric field. Obviously, this makes such materials extremely valuable for the detection and monitoring of strain in structures as a single piezoelectric device can act as both source and receiver. What is particularly innovative about the use of piezoelectric materials is that the electrical impedance measured in the circuit is directly related to the mechanical impedance of the host structure (Park et al. 2007), which makes absolute measurement possible. Mechanical impedance is directly related to the fundamental characteristics of structures such as mass, stiffness, and damping; changes in values are indicators of structural damage (Lynch 2005)

A common EMI sensor is the piezoelectric wafer (patch), typically composed of piezoelectric-ceramic lead-zirconate-titanate (PZT), which is bonded to a structure or structural element to be monitored. By applying a voltage sweep signal—commonly in the kilohertz range—the PZT patch

will induce vibrations in the structure. With an impedance analyzer connected to the wafer and controlling the voltage sweep signal, defects or deformations of the structure that are manifested as the electrical response of the PZT patch can be analyzed. By comparing conductance to frequency, a unique vibration signature of the structure is discovered which reveals structural characteristics like inherent stiffness, damping, and distribution of mass (Sohn 2004).

Damage to the structure is especially apparent as changes in the structural stiffness and/or damping, so continuous monitoring that captures the dynamic behavior of the structure is most desirable. Such monitoring in real time can be achieved with the PZT wafer and numerous studies show how this sensor is successfully employed in permanent SHM networks (Lynch 2005). This method has been employed with great success and some studies have reported that it enabled the detection of cracks in concrete before they became visible, making this technique a clear improvement over standard, visual inspection methods.

2.6.7 Emerging Technologies

The market of sensory technologies as well as data acquisition system is in accelerating change.

Emerging technologies are science based innovations that have the potential to create a new

Industry or transform an existing one (Day et al. 2000, 2008).

2.6.7.1 Acoustic emission

A structure starts to deform elastically when it is subjected to a loading; either by internal pressure or by external mechanical loading. In this manner, the stress distribution and storage of elastic strain energy in the structure changes. Acoustic Emission (AE) (Jaffrey, 1982) technology was born in the early 1960s when it was recognized that growing cracks and discontinuities in fibre reinforced plastic tanks and pressure vessels could be detected by monitoring their acoustic emission signals. AE is a naturally occurring phenomenon that takes place and generates elastic waves with these before mentioned loading conditions that relate to rapid release of energy. Acoustic emission monitors electronically ultra-high frequency sounds that stressed materials release and it is classified as a passive non-destructive testing method.

Acoustic Emission tests can be used to evaluate the structural integrity of a component or a structure, structural damage diagnosis, life-time assessment and SHM. AE monitoring detects and locates defects in real time while the phenomenon is taking place and following features can be monitored with AE: corrosion, occurrence and extension of fatigue cracks, fibre breakages in composite materials or fibre breakages in bridge main cables, stay cables or prestressed cables as well as cracking in concrete or reinforced concrete members.

Acoustic Emission sensors are piezoelectric crystals that convert movement (a variation of pressure) into an electrical voltage. The sensors must all have an identical response and they should be calibrated regularly. They are normally held in place using metallic clamps for steel structures or bonded to concrete. These are connected to the AE system using coaxial cables with shielding to prevent electro-magnetic interference. A resonant frequency of 30-100 kHz is typical for concrete applications; whereas 100 and 200 kHz is used for metallic structures. Higher frequency sensors can be used in high noise environments but only for local monitoring due to the higher attenuation at these frequencies.

A typical AE system comprises a high speed Digital Signal Processor (DSP), AE processing boards with individual processing channels for each sensor (i.e. a non-multiplexing system) and the ability to program the settings for signal thresholds and frequency range to enable the AE signal to be filtered. It should also have software for source location in both one two and three dimensions, feature extraction capability to allow characterization of the signals and stable software for long-term monitoring. Numerous codes, standards and recommended practice are already present for Acoustic Emission Monitoring. Figure 2.10 illustrates Principle of acoustic emission process.

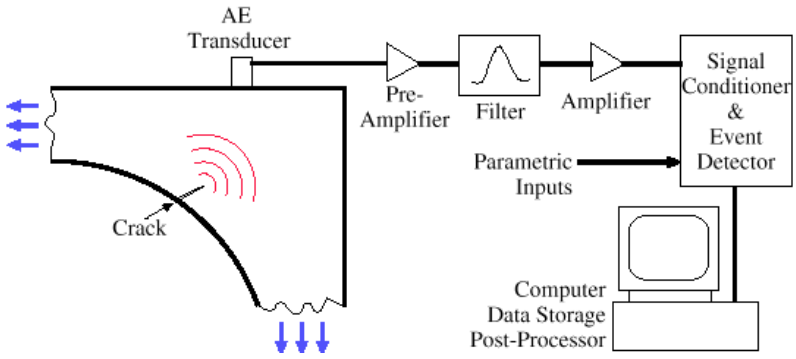

Fig. 2.10 Principle of acoustic emission process (Huang et al. 2008)

2.6.7.2 Radar technology

Radio detection and ranging (RADAR) is a well-established technique for measuring the range (distance to), altitude, direction, and speed of moving or stationary objects. This is achieved through the illumination and, commonly, the reflection off of an object with electromagnetic (EM) waves. Reflected EM waves are detected at the transmitter, making it both source and receiver. Otherwise, separate transmitting and receiving probes are used in *through-transmission* techniques. In most civil engineering applications, the reflective technique is used as it requires only one surface be accessible (Bungey 2009). Microwave, millimeter, and radio wave inspection techniques typically operate at frequencies ranging from 300 MHz to 300 GHz in dielectric (electrically insulating) materials (Chang and Liu 2009). In order to achieve 3D displacement measurements, radar measurements from independent directions must be made, as radar can only measure displacement in the range direction, parallel to transmission (Pieraccini et al. 2013). In the case of a fixed-position radar antenna, multiple targets at the same distance from the receiver (in the same *range resolution cell*) cannot be distinguished and are marked by one reflection for that *range bin.* Many of the principles discussed in this section hold true for all radar applications. Ground-penetrating radar (GPR) is discussed in Section 2.6.7 b whilst Interferometric synthetic aperture radar (IfSAR) is discussed in Section 2.6.7d.

2.6.7.3 Ground-penetrating radar

Ground Penetrating Radar (GPR) is one of the most inclusive archaeological geophysical methods. GPR uses electromagnetic waves to collects large amounts of reflection data to map the spatial extent of near-surface objects, interfaces or changes in soil media and produces massive 3D databases as well as images of those attributes. A surface antenna of a GPR propagates radar waves in distinct pulses that are reflected off buried objects in the ground, and detected back at the source by a receiving antenna. When radar pulses are being transmitted through various materials on their way to the buried object, their velocity changes, depending on the physical and chemical properties of the material through which they are travelling. If the travel times of the energy pulses are measured and velocity through the ground is known, distance can be correctly measured and a 3D data set can be produced. Various equipment are commercially available in the market [Conyers, 2002] and numerous areas are e.g. non-destructive surveys of structures and buildings, utility detection and

mapping, geology, geophysics, geotechnics and environment, archaeological and cultural heritage, forensic and security.

In the GPR method, radar antennas are moved along the ground in transects, and two dimensional profiles of a large number of periodic reflections are created. The following is a list of some applications of GPR for structural concrete: thickness estimation from one surface, the location of reinforcing bars or other metallic objects, estimation of the depth of buried objects, location of moisture variations, location of voids, the dimensions of such voids, location of honeycombing or cracking, and an estimation of the size of reinforcing bars. Advantages of GPR are that it can rapidly and effectively investigate a large swath of one surface, it requires no coupling medium, it is continuous, results have a high potential to be improved through signal processing, and there are no special safety precautions required. Disadvantages include the requirement of highly specialized equipment, the need for calibration or ground truth ‘corroboration, the expense of equipment and signal processing, and the inability to penetrate metal features (Bungey 2004). Figure2.11 shows application on road pavements.

Figure 2.11 Equipment for bridge pavement measurements (Bungey 2004).

2.6.7.4 Interferometric synthetic aperture radar

Interferometric synthetic aperture rada (IfSAR sometimes InSAR) compares pixel-by-pixel differences in phase between two synthetic aperture radar (SAR) images in order to determine changes in surface deformation or ground topography during the time interval that occurred between

the two images. Microwave differential interferometry is a very similar technique for mapping displacement phenomena.

Though many sophisticated SAR instrumentation is installed on Earth-orbiting satellites, many of these instruments are not practical for monitoring structures on Earth for despite their sufficient accuracy, they generally lack the resolution or imaging time required for SHM. Consequently, the techniques described here are ground-based (Pieraccini et al. 2013). Generating two SAR images for this purpose requires having two side-looking antennae, separated by a known baseline, ready to receive backscattered signals from a transmitting antenna. This enables the target to be scanned from two different antenna positions. The phase and amplitude of the backscattered signal is stored in each pixel, but it is the phase that reveals the most significant information for terrestrial scanning and SHM applications because it enables the generation of a digital surface model (DSM) or other 3D model (Baran 2009).

2.6.7.5 Weigh-In-Motion systems

Weigh-In-Motion or Weighing In Motion (WIM) devices capture detailed data for each individual vehicle as vehicles drive over a measurement location: dynamic weights of all axles, gross vehicle weights, axle spacing, vehicles distance and speed, vehicle classification according to various schemes and statistic representations for all types of traffic parameters. Modern WIM systems are efficient as they are capable of measuring at normal traffic speeds. Many heavy vehicles are weighty and legal limits are exceeded. Severe damage can be caused to roads and bridges and accurate information about vehicle axle loads is important in order to make prognoses for traffic development as well as in construction and maintenance planning (Quilligan, 2003).

Bridge weigh-in-motion (B-WIM) is the process by which axle and gross vehicle weights of trucks travelling at highway speeds can be determined from instrumented bridges. Strain transducers are installed to the soffit of a bridge for detecting axles in order to provide information on vehicle velocity, axle spacing and position of each vehicle. B-WIM system and a wide range of field trials have been completed in recent years. These systems are becoming gradually more accurate and they are remarkably durable as no contact with tires is required (Obrien et al. 2008).. Railway Weigh-In-Motion (R-WIM) market is under development. Though emerging, in-line wheel load weighing systems are already available and can detect overloaded wagons as well as damaged wheels and flat spots. Railroad companies check the operational safety and identify possible unsafe wagons with R-WIM.as a system that has minimal impact on the railways and there is no need to lower down the speed.

2.6.7.6 Infrared thermography

An interesting and safe non-contact and remote measurement method that can be used on both still standing and moving objects is called infrared thermography or thermal imaging. It is an example of infrared imaging science and allows fast scanning of objects and produces immediate images in real time. Thermal images produced by infrared thermography are visual displays of the amount of infrared energy emitted, transmitted, and reflected by an object. Camera and software technology improvements have made this technology common and areas of usage are; construction industry, condition monitoring and predictive maintenance industry. Detection of hidden structures, deterioration, moisture, and heat losses can be investigated quickly, remotely and cost effectively.

Emitted invisible infrared energy from an object is processed and images of that radiation, called thermograms with variations in temperature, can be produced and plotted.

2.6.7.7 Eddy Current

Eddy detection is conducted by the use of a probe coil which may have either an empty, air core or a magnetic ferrite core that induces electromagnetic currents in conducting materials. These currents nominally radiate from the coil in circular patterns (eddies). In the presence of a flaw in the material, however, these current patterns are disturbed at the site of the flaw, such as a crack. Although widely used in the inspection of surface and subsurface cracks as, this technique requires the use of a differential probe when applied to weld metal due to the wide variation in magnetic material properties. The technique remains effective even when applied to surfaces with non-conductive coatings such as zinc-based primers and lead paint (Chang and Liu 2003).

The meandering winding magnetometer (MWM) is a special type of eddy current sensor that features a meandering primary coil for induction and numerous fully parallel, secondary coils for sensing. They are typically deployed in scanning arrays but are also used for a wide variety of applications in permanently-mounted arrays. MWM arrays are particularly well-suited for fatigue monitoring. In such an array, a drive winding, made up of linear drive segments, is stimulated by a current at anywhere from 1 kHz to 40 MHz to produce a time-varying magnetic field capable of inducing eddy currents in the pattern of the drive winding. MWM arrays achieve high resolution, usually down to 1 mm by 1 mm surface areas, with the use of numerous, tiny sensing coils (Zilberstein et al. 2003). Usually, these are adhered to a substrate allowing for the production of thin and flexible chips that serve as sensors. Their size and flexibility allows them to be permanently attached to or embedded in the element to be monitored under real load conditions. Micromachining enables the production of these chips so they are cheap and identical to one another.

Zilbertstein et al. (2003) describe the processing of MWM array data by inversion of the measurement grid, which converts sensor impedance magnitude and phase response into material properties such as electrical conductivity or magnetic permeability. They ran several cyclic loading tests on plain shot-peened plates and combination shot-peened-cadmium plates, letting some of the fatigue tests run to failure while others were terminated according to when the MWM array measurements of magnetic permeability indicated the onset of failure. Fatigue and cracks were identified using

scanning electron microscopy (SEM). They concluded that gradual increases in magnetic permeability corresponded with fatigue damage prior to the formation of cracks that are much shorter than the grain size. They were able to detect the formation of cracks of the order of 250 μm or less, in length. This capability has been previously demonstrated on aluminum alloys.

2.7 Recent Application of SHM technologies to Civil Structures

Application of structural health monitoring technologies described in the previous section may be global or local . Global methods attempt to simultaneously assess the condition of the whole structure, whereas local methods focus non-destructive evaluation (NDE) tools on specific structural components. Any of the methods may be applied as response or model based. The model-based method assumes that a detailed numerical model of the structure is available for damage identification; while the response-based method depends only on experimental response data from structures, Fan (2011). Among the numerous considerations which influence the choice and effectiveness of a suitable health monitoring method are: (1) the level of damage and deterioration concern, (2) the types of sensors used, (3) the degree of measurement noise pollution, and (4) the degree of a priori information about the condition of the structure, etc., Nakamura et al. (1998). Periodic inspection of structures is essential in most cases. Structures are generally rated and monitored once a year or once in several years according to the importance and the age of the structure, Uomoto (2000-a).

2.7.1 Response Based and model based SHM

A typical procedure for response-based SHM method involves the modal and/or static tests of the structural system from which the responses due to external excitations are measured. Since the dynamic and static responses of a structural system are functions of the structural parameters, these parameters may be identified by using the changes in dynamic and/or static characteristics. One of the consequences of the development of damage is the decrease in local stiffness, which in turn results in changes in some of the responses. It is therefore, necessary that the dynamic and/or static characteristics of the structure be monitored for damage detection and safety assessment. On the other hand, in model-based damage detection method, one makes use of general framework of Finite element model refinement (FEMR), Zimmerman and Kaouk (2004). Thus, the damage detection problem is considered as a particular case of the general model-updating problem, where the aim of

FEMR is to seek a refined model with its modal parameters in agreement with those obtained from the experiment.

Model-based methods are generally capable of estimating existence, location, and absolute severity of the damage. However, response-based methods are typically limited to the existence and location of the damage when applied to civil engineering structure, since an unsupervised learning mode has to be used, Guan and Karbhari (2008). It is worth to mention that it is not mandatory to use only one of the above methods in SHM. Some researchers have combined both modal and static responses for damage identification (Lee et al. (2010). Other researchers have combined both modal response and model-based method for more effective SHM, Guan and Karbhari (2008).

2.7.1.1 Application of FOSs as a state of the art method of SHM for large civil structures

Health monitoring has expanded because of the advances in data processing, computational power, and economy of microprocessors. Also, this expansion is attributed to the advances in mechanical static/dynamic measurements such as transducers, and introduction of LASER, (light amplification by stimulated emission of radiation), in sensing and gauging applications. LASER can be used directly as in scanning laser doppler vibrometer (SLDV), or indirectly as in the fiber optic sensors (FOSs), Abdo (2002).

When compared with traditional electrical strain gauges used for strain monitoring of large composite or concrete structures, FOSs have several distinguishing advantages, Yu and Yin (2002), including:

- A much better invulnerability to electromagnetic interference, including storms, and the potential capability of surviving in harsh environments.
- A much less intrusive size (typically 125μm in diameter - the ideal size for embedding into composites without introducing any significant perturbation to the characteristics of the structure).
- Greater resistance to corrosion when used in open structures, such as bridges and dams.
- A greater capacity of multiplexing a large number of sensors for strain mapping along a single fiber link, unlike strain gauges, which need a huge amount of wiring.
- A higher temperature capacity with a widely selectable range.

- A longer lifetime, which could probably be used throughout the working lifetime of the structure (e.g., >25 years) as optical fibers are reliable for long-term operation over periods greater than 25 years without degradation in performance.

These features have made FOSs very attractive and suitable for quality control during construction and health monitoring after building large structures. Thus, in addition to the laboratory studies described above, FOSs have been used to measure strain and vibration in a number of newly constructed structures. They have also been attached to existing structures for non-destructive evaluation of structural health, such as crack growth, and monitoring use, e.g., traffic load on roadways. A state of the art of application of FOSs in concrete structures as well as in advanced fiber reinforced composites is given by Grattan and Meggitt (1999).

2.7.1.2 Demonstration of FOSs for SHM of Mechanical properties for Bridges and Dams

Yu and Yin (2002) demonstrated applications of FOSs to large civil structures; bridges and dams. For bridges, they showed the advantages and disadvantages of different FOSs for measuring temperature, static strain, and transient strain of both steel and concrete bridges. They stated that the choice of sensors is vital for the accuracy of different response measurements. Since dams are probably the biggest structures in civil engineering, hence it is vital to monitor their mechanical properties during and/or after construction in order to ensure the construction quality, longevity, and safety of the dam. They used a Brillouin-based distributed sensor to monitor temperature distribution in a concrete slab with dimensions of: 15m length, 10m width, and 3m height. These concrete slabs are used for raising the height of the dam in order to increase the power capability of the associated hydroelectric plant. They showed that the embedded fiber cable which is installed during the concrete pouring could give two-dimensional temperature distribution of the whole slab area at different times after concreting. They also showed that FOSs can be used in monitoring load and displacement changes in underground excavations of mines and tunnels.

2.7.1.3 Application of FOSs for monitoring of Strain & Temperature on Gas pipe line and Dams

Inaudi and Glisic (2006) used distributed FOSs for the monitoring of civil and industrial structures. The strain and temperature of two dams as well as an old gas pipeline are successfully monitored.

They used sensors based on Raman and Brillouin scattering which are able to measure strain or temperature variations of fibers with length up to 50 km with spatial resolution down in the meter range. Using a single optical fiber with a length of tens of kilometers they could obtain dense information on the structure‟s strain and temperature distribution. They showed that using an appropriate sensor design, it is possible to successfully install distributed sensors on large or elongated structures; such as dams, large bridges and pipelines and obtain useful data for the evaluation and management of the monitored structures.

2.7.1.4 Application of fiber Bragg gratings for monitoring of deformations

Xu et al. (1994) developed a new bending gauge, using a pair of surface mounted fiber Bragg gratings with excellent agreement with the expected strain sensitivity. Djordjevich and Boskovic (1996) proposed a new fiber-optic gauge, which is sensitive to the deformation curvature of structures. Using such sensors, they could measure deformation curvatures with a diameter approaching 5 km. The advantage of these sensors is that curvatures can be measured anywhere, including along the neutral axis of the cross section where there is no strain in Bending. Djordjevich (1998) extended the application of curvature gauge to include torsional and axial loading situations. Djordjevich et al. (2000) applied the curvature gauge to measure the mode shapes. The number of gauges required equals the number of dominant vibration modes of interest. The analytical mechanism of using curvature gauges to measure curvature directly is given by Kovacevic et al., (2008). Application of the advances in FOSs in the field of damage detection and system identification will make it more reliable and applicable in near future. Mohamed (2014)

2.7.1.5 Application of vibration-based SHM

The modal approach can be considered as the main stimulus for the growth of the field of vibration-based structural health monitoring and damage detection. The attractiveness of this approach can be attributed to the fact that dynamic characterization of the structure is in many cases easier to perform in the field than static characterization. Due to the advances in sensor technology, low input energy levels are usually sufficient to produce sets of measurable dynamic response. Hence ambient sources can be used as the excitation for structures eliminating the need for expensive excitation devices. Relatively accurate results of natural frequencies, mode shapes, and modal damping can be extracted

from vibration based measurements due to advances in response measurements, Guan and Karbhari (2008).

Detecting structural distresses throughout the changes in dynamic characteristics has many advantageous features. Among those advantages are:

- Damage can be located and sized without solving a system of equations,
- Rely only on the measured data without any prior theoretical model,
- Only lower mode shapes are needed for the analysis, and
- Damage can be located and sized using few modes.

A typical procedure for response-based structural health monitoring involves the modal and/or static test of the structural system from which the responses due to external excitations are measured. Since the dynamic and/or static responses of a structural system are functions of the structural parameters, these parameters may be identified by using the changes in dynamic and/or static characteristics. One of the consequences of the development of damage is the decrease in local Stiffness, which in turn results in changes in some of the responses. It is therefore, necessary that the responses of the structure be monitored for damage detection and safety assessment, Abe (2008). In fact, understanding of the relationships between the damage and the corresponding changes in the dynamic properties is the key point to detect damage in a structure.

2.7.2 Physical Model-Based Method

When a finite element model of the structure is utilized in the damage identification process, such physical model-based methods are sometimes also referred to as finite element model updating (FEMU) based methods. The process of finding a model from data is called system identification. General system identification is a research branch of electrical engineering. An authoritative reference regarding system identification is the book of Ljung (1999).

Caesar (1986) has given a very comprehensive review on the optimal matrix update approach. An excellent textbook discussing the finite element model updating techniques and their applications is due to Friswell and Mottershead (1995). Lim and Kashangaki (1994) compared the best achievable

eigenvectors with the measured modes to detect the damage in a space truss. Ruotolo and Surace (1997) fit a mathematical model to the modal parameters of the lower modes for damage detection and sizing of cracks in a steel beam. Also, Kosmatka and Ricles (1999) could detect the damages inflicted to a space truss using analytical model that is correlated to the experimental baseline data. Abozeid et al. (2006) used the experimental modal testing of the Suez-Canal cable-stayed bridge to obtain the dynamic characteristics of the bridge. He could extract mode shapes and corresponding natural frequencies which were very near to those extracted theoretically using finite element analysis. Thus, regular updating can be used to assess the status of the bridge.

2.8 Views of previous researchers on finite element modelling for SHM

Previous researchers have shown that FEMU can be an extremely useful technique for SHM under certain conditions. But it should also be noted that some difficulties still exist when implementing FEMU technique in a vibration-based structural health monitoring system. It is not always an easy task to guarantee the accuracy and validity of a finite element model. Some of the current challenges involve the non-uniqueness of the solution, ill-conditioning of the identification problem, and numerical convergence problems of the optimization algorithm. Firstly, due to the fact that only a small number of degree-of-freedoms can be measured experimentally and there exist a large number of uncertain parameters to be updated, the updating problem is usually ill-conditioned. This directly leads to the second problem of numerical convergence difficulties. A small amount of noise in the measured structural response can sometime corrupt the result to a great extent. That is the reason that some researchers state that this approach is expensive and time consuming, Abdel-Wahab and De Roeck (1999).

2.8.1 Suggestions to Improve FEMU for SHM

Although some of the above challenges are inherent to the inverse identification problem to which the FEMU problem belongs, others can be solved or alleviated through the use of appropriate techniques. Indeed, the choice of proper structural parameters to update is one of the main difficulties of FEMU. Careless choice of parameters usually leads to ill-conditioned identification problem. It is suggested that the ill-conditioning of the FEMU problem can be greatly alleviated by using the

information about the damage location. Such information can be obtained from damage localization procedures such as the modal curvature techniques or element strain energy damage indices. Also, dense sensor networks could be used to improve the spatial dimension of the measured data, thus reducing the ill-conditioning of the problem. Dynamic properties other than mode shapes and frequencies could also be used to provide higher sensitivity to structural changes. Globally, robust optimization algorithms can be adopted to alleviate the convergence problem, Guan and Karbhari (2012). Again, model-based SHM methods are capable of estimating both the location and absolute severity of the damage and provide at least level III of structural damage identification.

2.9 Future of SHM

Based on the review of the existing literature, it can be concluded that combined methods and long-term vibration-based health monitoring of civil structures is still in its infancy. This can be clearly seen from the rarity of successful real world applications. Current health monitoring systems e.g., (Abe et al. (2010), Lee et al. (2010), Miyashita and Nagai (2008), and Hoult et al. (2010)) place more emphasis on monitoring of local structural behavior such as strain, stress, force and temperature rather than the global dynamic response of the structure. Although local structural behavior can be a useful indicator of the health condition of the structure, such monitoring system provides no information about the global behavior of the structure and will face difficulty in accomplishing tasks of estimating the remaining capacity and usable life. Furthermore, among the large number of papers in the literature on the topic of SHM, few papers if not none have dealt with a combination of Global and Local based method of SHM. The majority are limited to the modest goal of discovering the occurrence and the location of the damage. Thus, new approaches with improved performance under real world situations are needed hence the further motivation for under taking this research.

Each method has its advantages and disadvantages; this is why engineers should combine two or more methods for structural evaluation. In addition, these NDE techniques have some limitations such as: (1) the quality of the process is often dependent on the inspection personnel experience and knowledge, (2) results from one (local) area of a structure does not necessarily represent conditions at another area, and (3) as a result, it would be necessary to make measurements at a large number of points so as to have a good representation of the global structural condition. These constraints imply that NDE techniques, which are commonly used for localized evaluation of large structures, fail when used for complete evaluation of the global and local performance of the structure. The need for

additional global damage detection methods that can be applied to complex structures is the motivation to the development of methods that examine changes in the dynamic/static characteristics of structures via monitoring their dynamic and/or static responses. The response-based techniques have the potential to evaluate the whole structure due to its simple setup and potential automation of data acquisition, data processing, and defect detection (Aktan and Grimmelsman, 2006).

2.10 Summary

In view of the pre-mentioned limitations of visual and localized experimental methods of SHM, a better approach is one that uses global indices. Global damage identification techniques, either response-based or model-based. The response-based method depends only on experimental response data from structures; while the model-based method assumes that a detailed numerical model of the structure is available for damage identification, Fan (2011). On a broader scale, the current approaches to the SHM problem can be divided into two distinct areas: (1) using structure-dynamic properties to detect structural changes at global level, and (2) using local NDE methods to locate and quantify damages in local components. Both approaches have their own advantages and limitations. Neither alone can satisfy all the stringent requirements from the end users. A new multi-level structural health monitoring system integrating global and local-level diagnostics needs to be developed (Mohamed and abdo 2014). Global-level techniques can be used to provide rapid condition screening, locate the proximities of the anomalies and evaluate their influence on global structural behavior, while local Sensor/NDE techniques can be applied to the identified distressed region in order to better define the location and severity of the damage and its effect on local components (Mohamed and abdo 2014). This was the motivation of conducting a combined (Global and Local) method of structural Health monitoring on Zambian Highway bridges, by the use of a combination of finite element modelling and sensor technology.

CHAPTER 3: METHODOLOGY

3.1 introduction

This Chapter outlines the methodology adopted to carry out the research presented in this thesis. It begins with a review of the methodological considerations that led to the formulation of the mixed method (qualitative and quantitative) used in this study. The application of a global and local structural health monitoring for effective results as recommended by other researchers. The Chapter also explains how the stated problem was investigated and describes the combination of tools used in carrying a successful SHM. An effective SHM system should be capable of providing information on demand about the condition of a structure as well as warnings regarding any significant damage that has been detected. Clearly, the development of such a system involves the use of expertise/knowledge in many disciplines, such as structures, materials, damage detection, sensors, data management and intelligent processing, computers, and communication (Bisby 2006).The chapter further discusses the stages that were applied in conducting a successful periodic bridge structural health monitoring by use of sensor technology carried out on Nansenga Bridge in Lusaka province of Zambia.

3.2 Research scheme

The flow chart in figure 3.1 presents the methodology in stages for this research

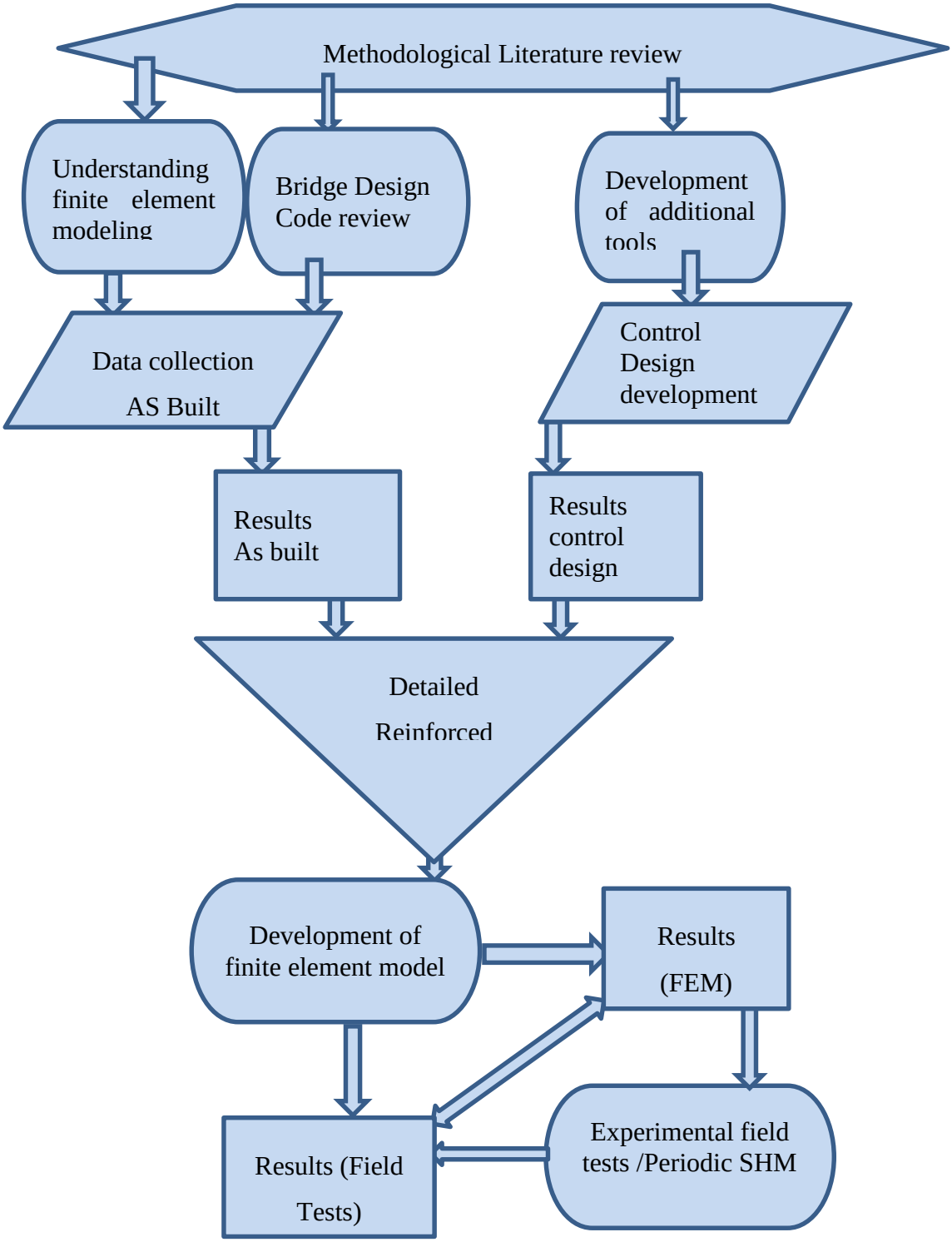

Figure 3.1 Research methodology flow chart

3.2.1 Methodological Literature

3.2.1.1 Method of SHM by other researchers

In recent years, research has categorized Structural health monitoring (SHM) of bridges in to two classes. The first category consists of FE or analytical modeling of bridges and/or bridge–vehicles interaction, which was carried out to perform moving load analysis and evaluation of bridge decks (Yin el at 2010). Recent developments in electronic data storage and computer data acquisition reviewed in chapter 2 make up the second category (Mohamed and abdo 2014). . Experimental methods such as wired or wireless sensors network systems were utilized mostly on superstructure to use in SHM (Farhey 2006; Wang et al). It was very necessary to have an understanding of finite element modelling, bridge design and force and moment distribution

Experimental tests are generally performed to get realistic data, to observe the possible behavior of members in real life and to identify the risks for a specific member under various loading conditions. Another way of testing members and getting realistic data is via the use of sophisticated finite element software. A researcher can perform numerical analysis by modeling a member that was already tested experimentally by other researchers. Same boundary conditions, load magnitude, and location, material properties, member imperfections and all the relevant experimental parameters should be used to achieve accurate results. This approach is known as verification of experimental results. A structural Health monitoring process is said to be successful if the results (e.g. displacements, stresses, etc.) obtained from Finite Element modelling reasonably agree with the ones obtained from experimental tests within a certain period.

3.2.1.2 Concrete Bridge Design with FEM

This sub chapter explains design methods as well as, force and moment distribution in bridge structures. The underlying theory of FE modeling and FE modeling of bridges is explained in more details. Design methods for analysis of bridge structures is often performed using FE analysis. The analysis is mainly done with 2D or 3D beam or 3D shell elements. The analysis is usually linear elastic. Nonlinear analyses and analysis with continuum elements are seldom used due to massive work efforts (Davidson, 2003).

3.2.1.3 Applicable Bridge Design code

According to Both BS5400 and Eurocode2-1-2, CEN (2001) there are four approaches to determine the force distribution in a structure:

• Linear elastic analysis

• Linear elastic analysis with limited redistribution

• Plastic analysis

• Non-linear analysis

For design in serviceability limit state (SLS), linear elastic analysis or non-linear analysis should be used. Eurocode 2, CEN (2001 part 2) state that the geometry and the properties of each part of the structure should be taken into account in the design the same is applicable for BS5400. According to Engström (2007) cracking can have significant effects on the structure in the service state and can only be analyzed by non-linear analysis. A linear elastic analysis is valid if the concrete structure is un-cracked or in ultimate limit state (ULS) when the assumed moment distribution is reached after plastic redistribution, Engström (2007). It is however not valid for analysis of a cracked section in service state. A common assumption according to Engström (2007) is that the difference between the real moment distribution in SLS and the distribution from linear elastic analysis is neglectable. Nevertheless, for a continuous beam an underestimation of 25 % of the negative moment at interior support can occur. Hence, non-linear analysis gives the most reliable analysis of concrete structures, which allow for the possibility to follow the redistribution in service state as well as in ultimate state, Engström (2007).

3.2.1.4 Reinforced Concrete Bridge Designs

Most of the existing bridges in Zambia today have been designed using 2D frame analysis. According to earlier British design codes, bridges should be designed according to elastic force and moment distribution, except for accident loads where the lower bound theory of plasticity could be used. The main reason for this is to avoid choices of moment and force distributions that require too large plastic redistribution. The elastic theoretical distribution is considered sufficient for design of reinforcement

and to avoid too large cracks. A distribution using strictly linear elastic analysis gives an uneconomical solution and is sometimes a practical impossible.

Solution basis for reinforcement design. For concentrated loads and values extracted over supports, the result can give high peak values which has to be interpreted, Davidson (2003). It is a requirement that design of bridge structures in Zambia should be carried out according to SATCC which makes reference to BS5400. According to TK Bro, a manual for bridge design in Sweden, many similarities apart from partial safety factors exist between the Eurocode 2-1-2 and British code in analysis of bridge structures CEN (2001 part 2).

"The structural model for system analysis shall with respect to loads, geometry and deformation properties describe the overall response of the structure". In this TR Bro is further interpreted as: "A global three dimensional structural model can be considered to describe the overall response of the structures. Two-dimensional structural models do not meet this criterion, except for a structure that with respect to geometry, loads and design conditions have a clear two-dimensional response." Furthermore" A structural model consisting of three-dimensional beam or truss members cannot be expected to give a good representation of a structure in which the essential elements consist of slabs and walls." This has by the Swedish structural engineers designing bridges been interpreted as, more or less, a requirement to perform a 3D shell FEM analysis for basically all bridges, since slab elements occur in almost all bridges .

3.2.1.5 Force and moment distribution in concrete bridge structures

Force and moment distributions in a concrete beams, over the supports and in the span, are dependent on the variations of stiffness across and between cross-sections. A common assumption is that the influence of reinforcement in the uncracked state is small but according to Engström (2007) more than a 20 % increase of stiffness of the section can be gained from the reinforcement for concrete structures. This means that the reinforcement cannot always be disregarded (Engström 2007). A stiffer region attracts moments and forces and, due to this, it will crack before the less stiff regions. When the region cracks it loses stiffness and the forces and moments will be redistributed to stiffer regions (Engström 2007). The stiffness of a cracked concrete section is mainly dependent on the amount of reinforcement in the section, Davidson (2003). In cracked reinforced concrete, the local effects at the crack result in a drastically decreased stiffness. The local cracks also affect the global

distribution of forces and moments as one or some critical sections can affect the stiffness of the whole section. This means that a fully cracked structure can behave differently compared to an un-cracked structure (Engström 2007). In SLS, the design load is often significantly higher than the crack load and the whole section is often regarded as cracked in bending. Since the position of critical section of the structure depends on the force and moment distribution, the reinforcement distribution is of great importance. In linear elastic analysis, the moment and force distribution is only dependent on the concrete cross section.

These analyses disregard the redistribution due to cracking and reinforcement (Engström 2003). During further increase of the load up to the ULS, the material response will become non-linear for concrete in compression and yielding will start in the reinforcement. The stiffer, heavily reinforced areas start to yield before the ultimate limit state is reached. On the other hand, the less stiff sections attracts less of the forces and moments and will therefore start to yield later. The load can still be increased since the reinforcement yields, which leads to increase of deformation. In other words, a plastic redistribution takes place with yielding reinforcement and eventually crushing of concrete. The plastic redistribution continues until the ultimate limit state is reached and the structure collapses. In the ultimate limit state, the force and moment distribution will become equivalent to the linear elastic distribution. This is due to the fact that the moment in a cross-section does not exceed the posted capacity and that it was designed for the same linear distribution, Engström (2003).

According to these facts, reinforced concrete bridge deck structures have a plastic redistribution both in transverse and longitudinal direction even if it is designed for a linear elastic distribution. Design of reinforcement is done in linear elastic analysis with regard to plastic theory principles. In other words, the force and moment distribution are calculated with elastic theory, but, the reinforcement is designed taking into account the plastic material behavior. This requires that the critical cross sections are not over reinforced. It is important that the reinforcement can handle the forces and moment from a simplified calculation method, Engström (2003). As earlier stated, concrete structural behavior varies with increasing load due to cracking of concrete, yielding of reinforcement and other non-linear material response. However, the concrete structures will also be affected by other factors than then the external load. For example prestressing, creep, shrinkage, temperature and support settlements will influence the moment and force distribution, Engström (2007).

3.2.1.6 Finite element modeling and analysis

When performing modeling and analysis with the finite element method (FEM) it is essential to understand the underlying theory, Blaauwendraad (2010). In order to comprehend the examinations and comparisons made in this thesis, it is necessary to have a general understanding of FEM and how it can be used for bridge structural Health monitoring. This section gives an overview of this area and describes the FEM modeling process in more details

a) Background to FEM

The finite element method (FEM) is a numerical method which can be used to solve virtually all physical problems. The advantage with FEM is that it allows systematical and accurate calculations on all types of structures. In recent years structural engineers have to a greater extent started using linear elastic FE analysis for structural analysis of bridges. Shell elements are mainly used, if necessary in combination with beam elements. In other industries, shell and volume elements has been used for decades and has dramatically changed the design and product development process. (Chalmer 2012)

3D FE analysis gives a more detailed and geometrically more correct distribution of forces and moment in comparison to the traditional 2D frame analysis, Davidson (2003). However, to be able to benefit from the advantages of the third dimension, an accurate analysis is required. The analysis demands knowledge and the results need to be properly evaluated. Rombach (2004) states that today, graphical input user-friendly software makes it fairly straightforward to produce three-dimensional finite element models with several thousand degrees of freedom. Furthermore, huge structures can be analyzed with a simple computer. This has led to an increased use of finite element analysis. Nevertheless, incorrect application of the method has also increased. It occurs that engineers believe that expensive computer software is free from errors, but this is more or less never the case. It should also be kept in mind that the finite element method is a numerical method based on numerous assumptions and simplifications. Reinforced concrete is a complex nonlinear material and is very time consuming to analyze in a nonlinear method. This is one of the main reasons why elastic analysis is often chosen for the material modeling. The model disregards the reduction and redistribution of stiffness as a result of cracking of the concrete and yielding of the reinforcement. However, an engineer does not have the time or the experimental data to verify a complicated non-linear analysis.

Furthermore, the aim of the engineer is often not to find the correct response of the structure; it is rather to find a safe and economical design for the structure, Rombach (2004).

b) The FE modeling process

In this subchapter, the FE modeling and analysis process is divided into six basic theoretical steps. The section describes the accuracy and restrictions for each step. In Figure 3.2 the description of FE modeling process below is mainly based on Samuelsson & Wiberg (1998).

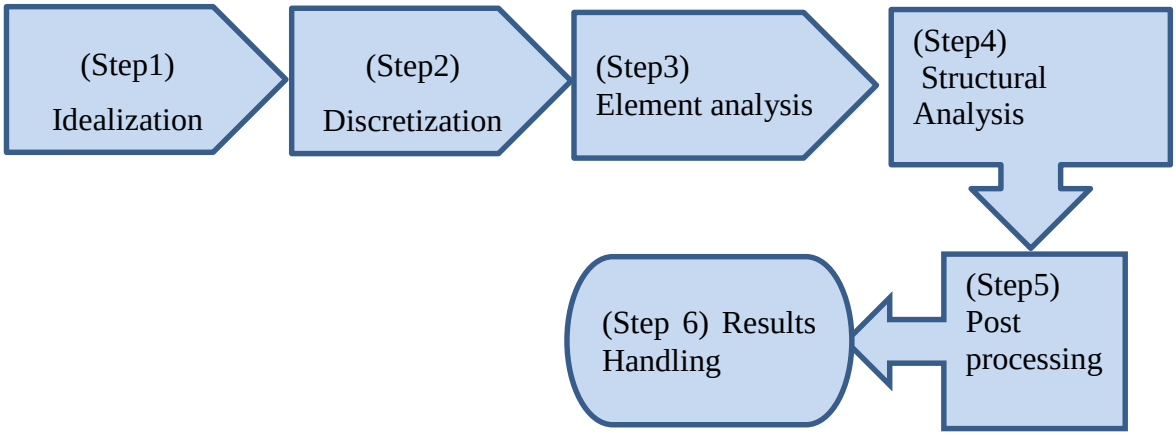

Figure 3.2 Illustration of different steps on how to obtain a FE model. Samuelsson & Wiberg (1998).

i) Idealization step 1

In the first step of FE analysis an idealization and simplification of the real structure is done by representing it with a structural model, for example by a 3D Shell model. The model includes geometry, boundary conditions, loads etc. In design of concrete structures it is commonly assumed that the material is linear elastic. Boundary conditions at supports are often simplified as being 100% fixed or not fixed at all even though in reality it is somewhere in-between. In some situations it is important to include the support stiffness to give a good interpretation of reality, Rombach (2004). The designer should have in mind that the interpretation of the reality gives rise to a variety of choices and selections. This puts high demands on the structural engineer since wrong assumptions have a large impact on the resulting outcome. Two theories that are often used for analyzing linear plates are the Kirchhoff-Germain and the Reissner-Mindlin theories. Both theories can be used for moderate thin plates, where the deflection is less than half of the plate's thickness. According to Blaauwendraad

(2010), thin plates should preferably be calculated with Kirchhoff theory. Similar result can be achieved with Mindlin theory but a much finer mesh is required. The required element size in case of Krichhoff theory should not be larger than approximately the plate thickness. However, for very thick plates, the Mindlin theory must be used. For the Mindlin theory, the width of the edge zone is comparable to the thickness of the plate; in this edge area a sufficiently fine mesh should be applied, Blaauwendraad (2010). In slab structures modeled with linear plates, discontinuity regions may appear under point loads and at pin supports. According to plate theory a point load is acting in a single point in which the shear force and bending moment approaches infinity, Rombach (2004). One way to overcome this is to include the load or support pressure distribution in the model.

ii) Discretization (Step 2)

In the second step, the structural model is divided into finite elements. The results, primarily in integration points, depend on the element size, the type and shape, and how the load is applied. Consequently a denser element mesh and less distorted elements lead to a more correct answer. Higher order elements often lead to a more correct result, Ottosen & Petersson (1992). However, quadric shell and plate elements can lead to a large variation in sectional forces at point loads and pin supports. Shell elements differ from plate element due to that shell element can be curved and can carry both membrzane and bending forces, Michigan Tech (2011). Shell element needs larger computer capacity. A lower order element can in this case be favorable, even if the element size need to be smaller.

iii) Element Analysis (Step 3)

Element approximation and element stiffness is calculated in this step. The internal element stiffness in the element analysis is approximated with a base function. In FE analysis, a numerical integration is used to get an accurate integration over the chosen integration points in the elements. This integration is an approximation even if a sufficient amount of integration points is used, due to the fact that integration of rational functions does not give exact solutions, Rombach (2004).

iv) Structural Analysis (Step 4)

A calculation of the stiffness matrix is done by paring the single elements´ stiffness matrix with equilibrium conditions and geometry conditions. The equation system can be solved for the whole

structure. The computer can only use a certain amount of significant numbers; thereby rounding errors can arise in this step.

v) Post Processing (Step 5)

In this step, the calculations of stress components in all the elements are performed. The stress is calculated in the integration points. These points are generally not situated in the elements nodes, but are situated a distance into the element with for example Gauss integration. The values in the integration points are the most exact results from the FE analysis. Nevertheless, the results are often showed in the element nodes. The integration point results are extrapolated to the nodes with the element base functions. Generally an element with high order produces a better approximation for a linear elastic analysis, Ottosen & Petersson (1992). Every node is in general connected to more than one element. Due to this, the node result is calculated as a mean value from the single elements contributions. In other words all elements connected to the same node have an effect on the node value. Hence, the results from the post processing as mentioned above are not exact and contains rounding.

vi) Result Handling (Step 6)

The results from the FE-analysis has to be further analyzed. This leads to large uncertainties due to considerations of the structure`s real behavior. The analysis is dependent on choices made in Step 1. For 2D frame analysis the output data is manageable for large models. Due to the increased complexity with 3D shell analysis, it is very hard and sometimes practically impossible to analyze all output data. The use of reviewing all the output from the analysis can also be questioned. Instead a combination of words, numbers and iso colour plots gives a good description of the results, Davidson (2003).

3.3 Research tools

Tools and equipment used in the research included the following:

i). NDT/E equipment both (wireless and wired)
ii). Data loggers
iii). ICT facilities

iv). Transport (Motor vehicle)

v). Miscellaneous tools and facilities such as ladders, PPE and Camera

vi). Ultrasonic pulse velocity detector

vii). Micro crack detector

3.3.1 Development of a Bridge Control Design to BS5400.

After methodological literature review, it was established that additional tools are required for monitoring and verifying results obtained by Nondestructive testing equipments for error elimination in raw data to validate the finite element model, this lead to a creation of a control systems design of the bridge to BS5400.Before that, interviews were conducted with residents living near by the bridge in order to estimate age of the bridge as RDA does not have data about this bridge.it was found that the bridge was built just after the British colonial rule. Hence the BS5400 design code was adopted.

A control design of Nansenga Bridge to BS5400 of 1978 parts 2 & 4 was developed in order to compare with as built bridge structural parameters obtained by Nondestructive testing and evaluation equipment. Physical measurements of the bridge were conducted to obtain geometrical parameters. Both serviceability and ultimate limit state design was considered with their respective partial safety factors provided for in the code. Serviceability Limit State ensures that crack widths do not exceed values specified for different environmental conditions, and also ensures that concrete and reinforcement stresses are maintained below a safe limit. Ultimate Limit State ensures that the structure will not collapse. Load combinations C1 (permanent Plus HB loads and C3 were considered. Table 3.1 summarizes design consideration as per BS 5400 code of practice.

3.3.1.1 Design load considerations in accordance with BS 5400 part 2 (1978)

Table 3.1 Design load considerations in accordance with BS 5400 part 2 (1978)

Load	Type		SLS		ULS	
Load combinations			**C1**	**C3**	**C1**	**C3**
			Partial Safety factors			
Dead load	Concrete		1.0	1.0	1.15	1.15
Super imposed dead load	Surface		1.2	1.2	1.75	1.75

Live Load	HA	1.0	1.0	1.5	1.25
	HB	1.1	1.0	1.3	1.1
Temperature Difference			0.8		1.3

From the geometry of the bridge figure 4.4, grillage analysis was employed and the girder with extreme loading was adopted for reinforcement design considerations.

3.3.1.2 Highway Bridge Loadings

a) HA loading

HA loading is a formula loading which is intended to represent normal actual vehicle loading. The **HA** loading consists of either a uniformly distributed load plus a knife edge load (KEL) or a single wheel load. Impact loads are inclusive in this load. Uniformly distributed load (UDL), HA loading is 30 kN per linear metre of notional lane for loaded lengths (L) up to 30 m and is given by equation (3.1) .

HA UDL=151 (l/L)$^{0•0475}$ *kN* per linear metre of notional lane (equation 3.1)

For longer lengths, but not less than 9 kN per linear metre. KEL is taken as 120kN per notional lane. The magnitude of the Uniformly Distributed Load is dependent on the loaded length as determined from the influence line for the member under consideration.

The loading covers the following

a) Impact load (caused when wheels 'bounce' i.e. when striking potholes or uneven expansion joints).
b) Overloading
c) Lateral bunching (more than one vehicle occupying the width of a lane)

a) HB Loading

HB loading is intended to represent an abnormally heavy vehicle. The nominal loading consists of a single vehicle with 16 wheels arranged on four axle as shown in Figure 3.3.

Figure 3.3 shows the plan and axle arrangement for one unit of nominal HB loading.

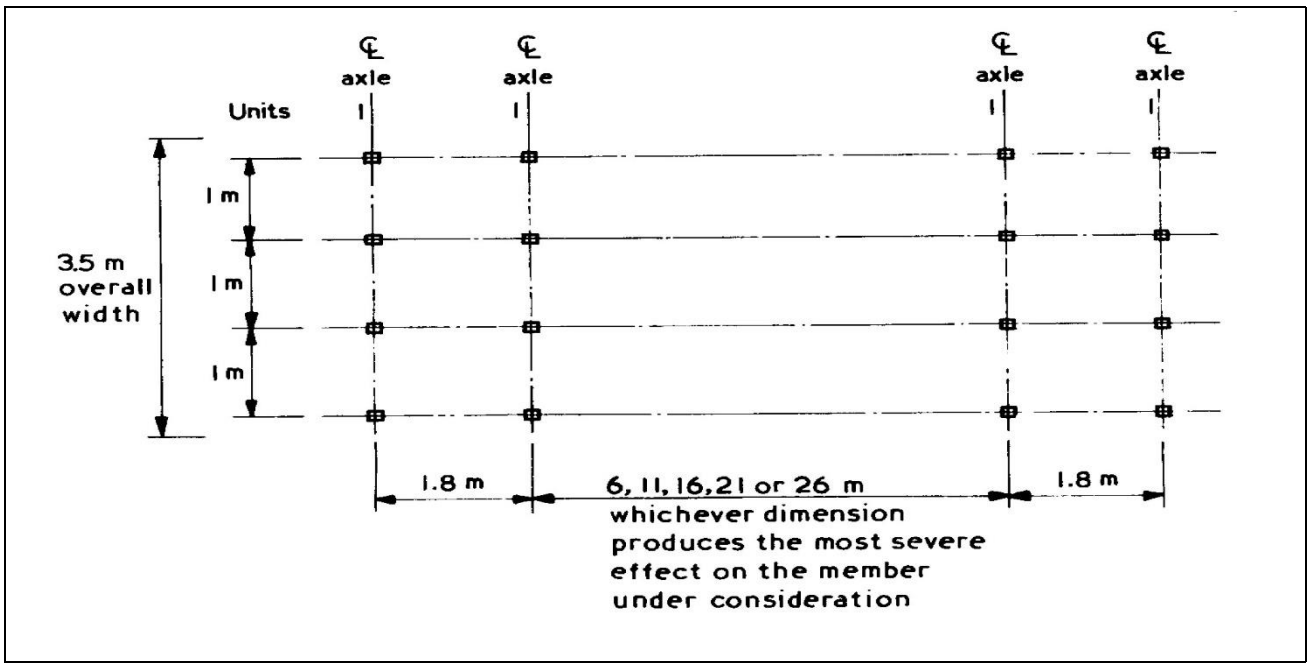

Figure 3.3 plan and axle arrangement for one unit of nominal HB loading (BS5400 of 1978 parts 1&2)

Where HA loading is coexistent with HB loading (6.4.2) $_{fL}$, as specified in **6.3.4**, shall be applied to HA loading.

Type HB loading. For all public highway bridges the minimum number of units of type HB loading that shall normally be considered is 25units, and 45units for all bridges on Trunk roads

(6.3.1) ***Nominal HB loading.*** Figure 3.3 shows the plan and axle arrangement for one unit of nominal HB loading. One unit shall be taken as equal to 10 kN per axle.

The overall length of the HB vehicle shall be taken as 10, 15, 20, 25 or 30 m for inner axle spacing of 6, 11, 16, 21 or 26 m respectively, and the effects of the most severe of these cases shall be adopted. Only one HB vehicle is considered to load any one superstructure. The vehicle is positioned within one notional lane or straddles two notional lanes in order to obtain the worst effect on the member. HA loading is placed in any remaining lane not occupied by the HB vehicle. Also, if the deck is long enough, the HA UDL only is placed in the lanes occupied by

the HB vehicle, but is omitted from the length of lane within 25m from the front and back of the HB vehicle

3.3.2 As-built Data acquisition of Nansenga Bridge

Due to lack of design data and as built drawings on the bridge of study and most old bridges it was a requirement to collect real time data of the bridge without causing or inducing any damage to the structure for the purpose of simulating the true behavior of the bridge in the finite element analysis.

Nondestructive testing and evaluation equipment were employed to determine the real time conditions of materials on bridge structural elements and collect as built bridge structural details. Ground penetration radar technology was used to scan concrete elements for rebar diameter and cover to reinforcement. Ultrasonic pulse velocity was used to determine strength of concrete members on beams, piers and deck slab.

3.3.2.1 Ultrasonic Pulse Velocity for concrete strength determination

As stated earlier this is one of the most popular techniques used for the detection of flaws in a concrete. The ultrasonic pulse is generated by an electro acoustical transducer. Now since ultrasonic waves do not travel through air or vacuum, a couplant like grease is used to get the transducer in contact with the member surface. When the pulse is induced into the concrete from a transducer, it undergoes multiple reflections at the boundaries of the different material phases within the concrete. A complex system of stress waves is developed which includes longitudinal (compressional), shear (transverse) and surface (Rayleigh) waves. The receiving transducer detects the onset of the longitudinal waves, which is the fastest. The material without any defects results in a higher velocity than that of the damaged ones. Using a combination of sound and velocity the modern UPV equipment automatically calculates the mean strength of structural concrete. Data was stored and processed within its hard drive that was later transferred to computer software via Wi-Fi, Bluetooth and USB drive for final processing.

The transducers where set in opposite direct surfaces on piers and beams as shown in option (A), on bridge deck option (C) was used Figure 3.4.

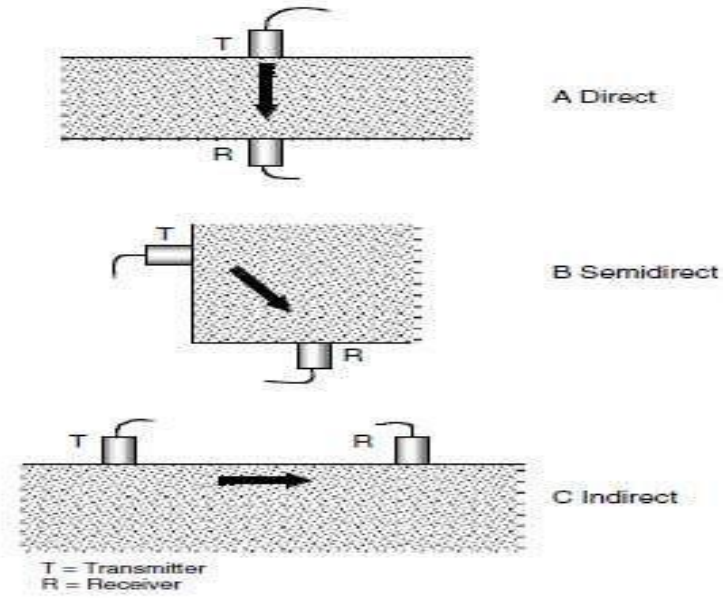

Figure 3.4 shows transducer positioning

3.3.2.2 Ground penetration radar (GPR) rebar scanning

The bridge structural concrete members, piers, girders and deck were scanned using Ground penetration radar in order to determine rebar sizes, placement, spacing and cover to reinforcement.an integrated rebar scanner was used that was able to store and process data. The equipment was able to penetrate concrete medium up to a depth of 300mm.both grid scan and imagery scan was conducted on bridge components. Bluetooth and USB facilities where used to transfer data from the equipment to the data processing software installed on a laptop computer for further processing. A Grid scan was employed for both transverse and longitudinal reinforcement detection. Shear, compression and tensile reinforcement were both investigated.

3.3.3 Finite Element Modelling.

A full 3D finite element model was developed using a finite element package software FEM Design 17. A 2/3/4 finite element analysis was used and the model consisted of 49419 nodes, 12594 surface shell elements and 13016 line connection elements. The model comprised of the bridge deck, girders and piers. Hinged connections between girders and piers where formed to represent elastomeric bearings. Fixed line connections were used between the deck and girders. The bridge was modelled

as an integral structure with beams, columns and the deck. A crack analysis, linear, dynamic and linear static analysis were performed

As the crack analysis is a non-linear calculation, the principle of superposition is valid. By this fact the crack analysis is not applicable for load groups and the calculation was executed for every single combination. (Ferenc Nemeth 2015)

Applied Theory and Design - Analysis calculations

The linear static analysis is the solution of the equation:

K u = Q … *equation (3.2)*

Linear, inhomogeneous equation system with constant coefficients, which is derived from the displacement method, where:

K is the coefficient matrix of the system

Q is matrix of the load vectors, derived from the loads of every load cases,

U is matrix of the displacement of node

Linear dynamic

If the loads acting on a structure vary quickly, the node displacements of the structure also vary as a function of time. In this case the outer loads-according to the d'Alambert theorem-should be extended by the distributed inertial forces which are proportional to the acceleration of the points of the structures. This results in the following basic equation, if the damping of the structure is ignored:

K u = Q - M u"……*equation (3.3)*

where: M is the diagonal mass matrix of the structure and u" is the matrix of the node acceleration (second derivative of the node displacements and rotations).If the structure is unloaded, i.e. the free oscillation is analyzed, all points of a structure with statically determined supports move periodically, according to the following equation: equation (3.4)

u = A sin (ωt). *equation* (3.4)

If Q = 0, it results in the following eigenvalue problem:[K - ω2M] A = where:ω is the eigen angular frequency and A is the matching vibration shapes, or amplitude distribution.

stiffness matrix of the system is a linear function of the normal internal forces in plane plates and membrane. Based on this principle equation 3.5.

[K + KG (N)] u = Q..*equation (3.5)*

Where K is the original (linear) stiffness matrix, u is the matrix of the node dis-placement, Q is the matrix calculated from the loads, and KG is the geometrical stiffness matrix. N in the argument means the distribution of the normal internal stresses within the membrane.

3.3.4 Periodic Monitoring and Experimental field Tests

Periodic monitoring was conducted monthly for a period of three months. An integrated microscopic crack width detector was used to identify cracks upon scanning and provided self-automated crack width measurements within its band width. Microwaves where projected at distressed member points with a high resolution Probe Cam that sends measured cracks to a screen/Tablet via Bluetooth and Wi-Fi. This is a remote sensing technique which can be done within a radius of 30m.

An ultrasonic detector was used to determine depths of cracks. Testing was conducted on highly distressed areas obtained from the finite element model. These nondestructive tests were conducted in intervals of 30days.Figures show tests conducted on the four Girders at support ends.

3.4 Summary

Apart from methodological literature review the chapter further presented methodology infour categorize. Global and local method of structural Health monitoring was used in this study as recommended by most researchers through the literature reviewed. The first part involved acquisition of data as per built details of the bridge by using GPR system and Ultrasonic Pulse Velocity Detector. The second part involved redesigning and development of a control design of the bridge to BS 5400 Part 2 & 4 of 1978 aimed at verifying field data. The third part comprised development of a Finite Element analytical model of the bridge with an HB moving truck load. The FEM was validated by use of SHM field data. Part four involved the use of integrated wireless micro crack detectors, GPR

system and Ultrasonic pulse velocity tester to measure and quantify experimental conditions of highly distressed areas indicted by linear and dynamic FE analysis. It was found necessary to adopt the mixed research method due to combination of data collection and analysis strategies employed in the research.

CHAPTER 4: RESULTS AND ANALYISIS

4.1. Introduction

The previous Chapter outlined the methodology and tools for carrying out this research and the four stages introduced in this study that helped achieve desired results of a successful structural health monitoring process. This chapter therefore presents analysis of obtained results.

4.2 As built Data Acquisition Results.

Acquisition of current state data of the bridge while in use was achieved by use of nondestructive testing equipments and ultrasonic pulse velocity detector. Measurements and testing the strength of materials for bridge members were done and results are presented Table 4.1 and 4.2. Scanning of bridge components was done using a ground penetration radar in order to determine rebar sizes, placement and cover to reinforcement as presented in Table 4.3. Detailed general arrangement of As-Built drawings where developed using Prokon 3.0 as shown in Figure 4.1c and 4.1d
Figures 4.1a and 4.1b show scanning of the bridge girders.

Table 4.1 Bridge Geometrical Parameters

Length of deck (mm)	**Spans(mm)**	**Carriageway width(mm)**	**Deck depth (mm)**	**Foot/cycle path width(mm)**
33100	7000,18300,7000	6800	200mm	1200
Parapets	**Girder**	**No# Notional lane**	**Piers**	**Abutments**
Open	Hunched Beam (1350x850)	2No. (3.4m wide each)	2No.	Non- Integral
Foundations	**Material Type**	**Bearings**	**Bearing location**	
Reinforced Concrete	Reinforced concrete	Elastomeric	Pier	

(a)

(b)

Figure 4.1 scanning of the bridge girders (2017)

4.2.1 Geometry and Structural Characteristics of Nansenga Bridge

The Bridge is a reinforced concrete three span balanced cantilever along the Kafue –Livingstone road (T1) with high traffic flow. Figures 4.2 shows a truck traversing the bridges while Figure 4.3 shows the bridge geometry and Table 4.1 summarizes details of the bridge.

Figure 4.2 Nansenga Bridge

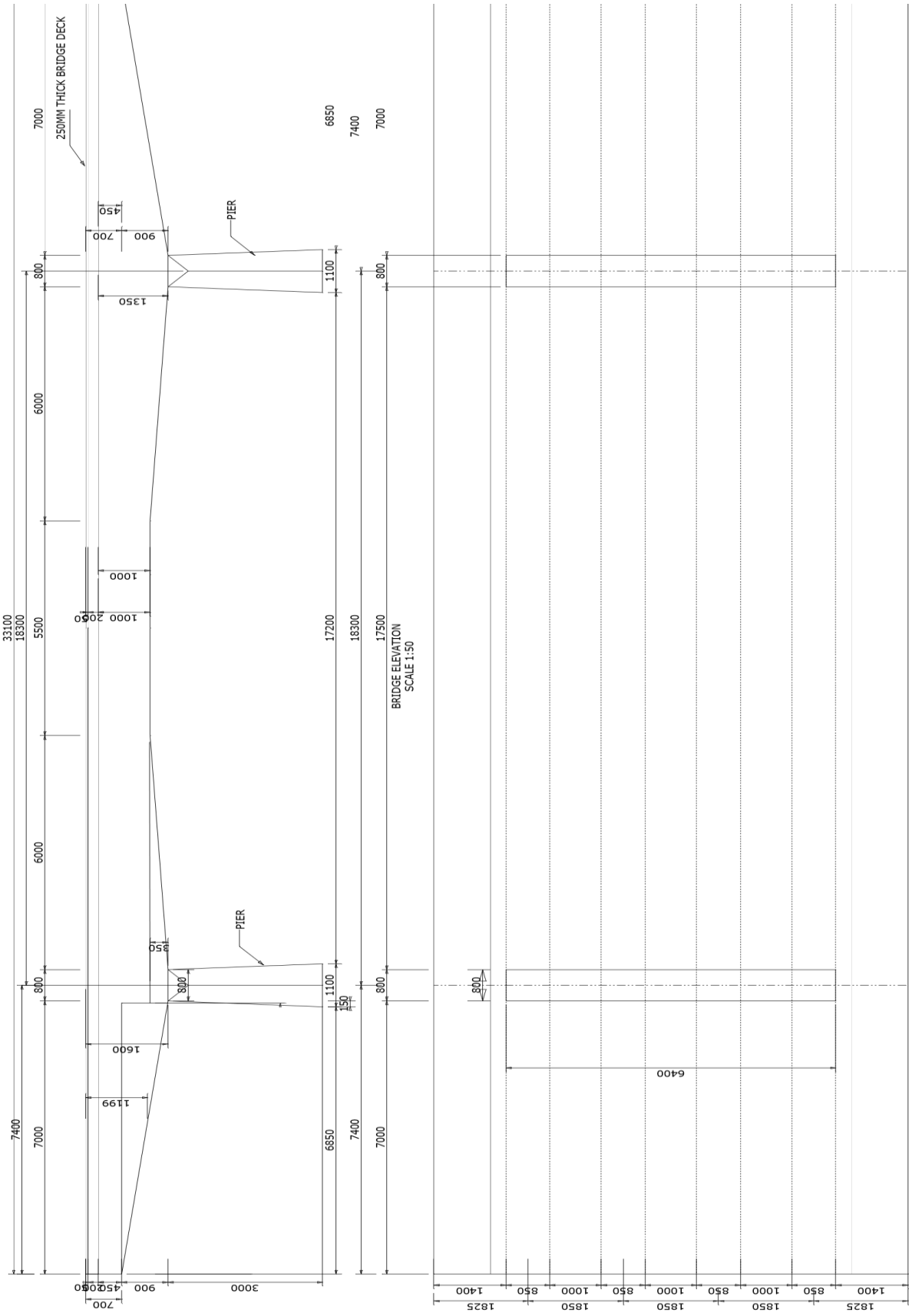

Figure 4.3 Bridge layout and elevation (as built measurements during control design**)**

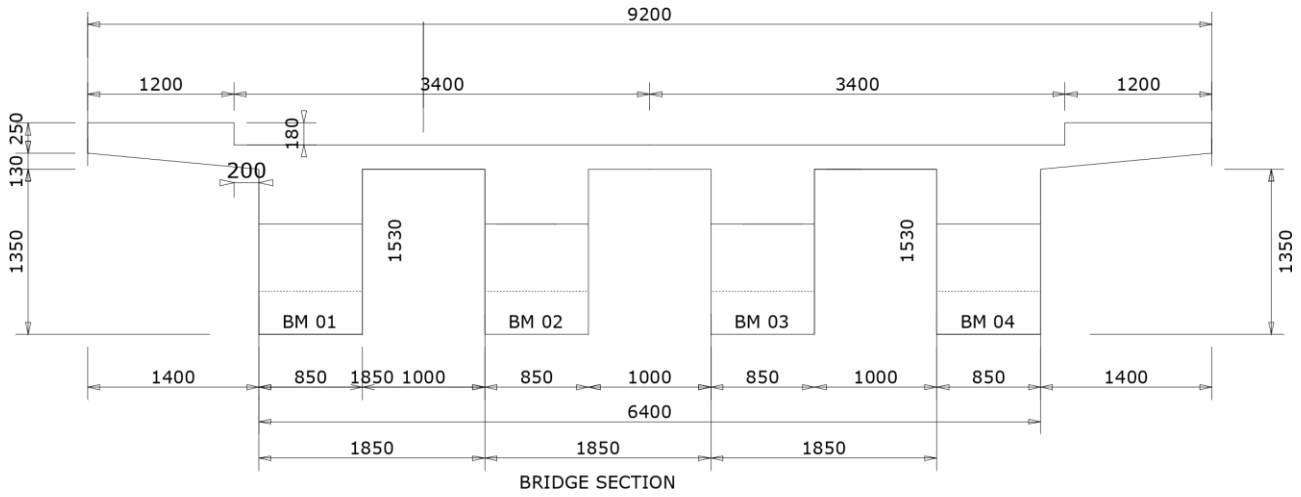

Figure 4.4 Bridge Deck Crosss-Section (as built measurements during control design)

4.2.2 Concrete compressive strength results

Ultrasonic pulse velocity tests were conducted by applying both opposite and surface methods. In the opposite method, transducers (receiver and transmitter) were placed in opposite directions at zero degrees while in the surface method transducers were placed adjacent to one other on the same face at 180 degrees. The opposite method is known to be the most accurate and was used on most tests. Transducer frequency was set to 50 kHz Results are presented in Table 4.2.

Table 4.2 Test results of bridge support members

Component Name	Distance (mm)	Time (µ)	Velocity km/s	Test points	Transducer frequency	UT method/test angle	Average compressive strength (Mpa)
Beam 01	850	167	4.84	3	50kHZ	Opposite/0	43.7
Beam 02	850	224	3.79	3	50kHZ	Opposite/0	35.9
Beam 03	850	219	4.20	3	50kHZ	Opposite/0	36.9
Beam 04	850	185	4.24	3	50kHZ	Opposite/0	36.2
Column 01	900	180	4.62	3	50kHZ	Opposite/0	40.9
Column 02	900	199	4.42	3	50kHZ	Opposite/0	39.1
Deck slab	200	77	3.59	3	50kHZ	surface/180	28.5
Deck slab	200	54	3.79	3	50kHZ	surface/180	30.1

Figure 4.5a and b show concrete compressive strength wave forms for beams and columns produced by ultrasonic detector during data collection. The consistency in weaker interface signals indicates minor defects in concrete tested with quality ranging from (excellent - good – normal) as evidenced by the velocities in table 4.2.

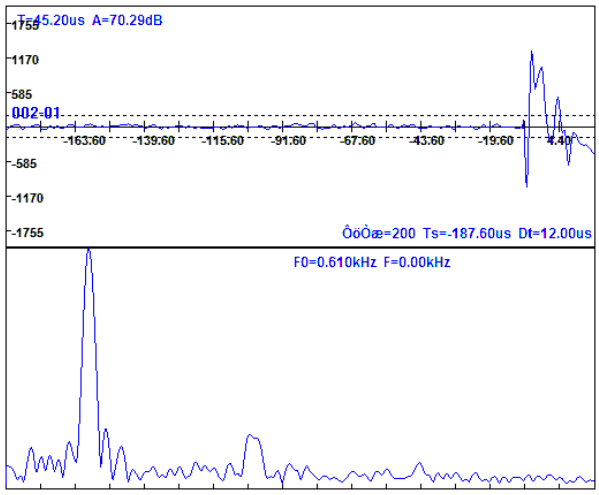

(a) Compressive strength wave form columns. produced by ultrasonic detector during data collection

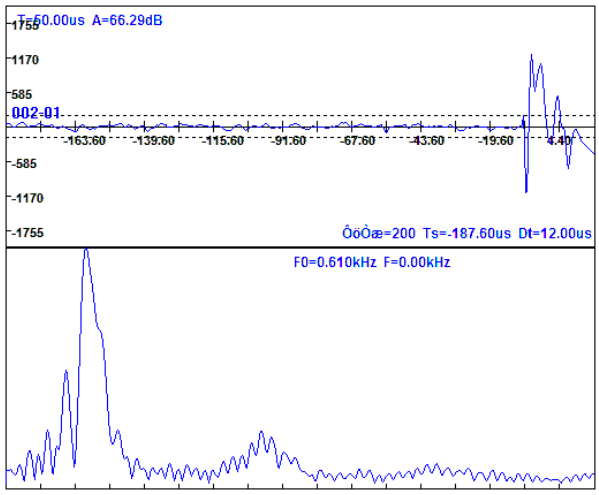

(b) Compressive strength wave form Beams. produced by ultrasonic detector during data collection

Figure 4.5 Compressive strength wave form for columns and beams

4.2.3 GPR scanned results of reinforcement details

Results of Ground penetration radar scanning of bridge components for rebar size detection, spacing of top and bottom reinforcement and measurement of cover to reinforcement are presented in Table 4.3. Beam 01 is located at the edge of the deck while Beam 02 is at the center. Results of the two beams where adopted for the other beams as they had similar load distribution. Both 3D image and grid scans where employed for Longitudinal and transverse reinforcement detection. Figures 4.6a to d show GPR Grid scan output of beams and piers.

Table 4.3 GPR scanned Results for reinforcement details

Element	Beam 01 cantilever	Beam 02 cantilever	Beam 01 Mid span	Beam 02 Mid span	Deck slab
Average Cover	72mm	67mm	59mm	55mm	41mm
Tensile reinforcement	8Y32 top	8Y32 top	8Y25 bottom	8y25bottom	Y10@240
Compression reinforcement	6Y25 bottom	6Y25 bottom	6Y20 top	6Y20 top	-
Stirrups	R10@(100, 200mm)	Stirrups R10@ (100,200m)	Stirrups R10@ (100,200m)	Stirrups R10@ (100,200m)	-
Punching Shear Reinforcement	Present (Y25) top	Present(Y25) top	-	-	-
Flexural Reinforcement	Present 6Y20	Present (6Y20)	-	-	-
Crack control reinforcements	Y20@185	Y20@200	Y20@200	Y20@200	Y10@250
Flange Transverse	Y10@240	Y10@250	Y20@200	Y20@200	Y10@250
Flange longitudinal	Y10@260	Y10@250	Y10@260	Y10@250	Y10@250

Figures 4.6a, b, c and d show GPR Grid scanning of beams and piers for detection of rebar spacing,cover to reinforcement and rebar diameter and general reinforcemet placement.

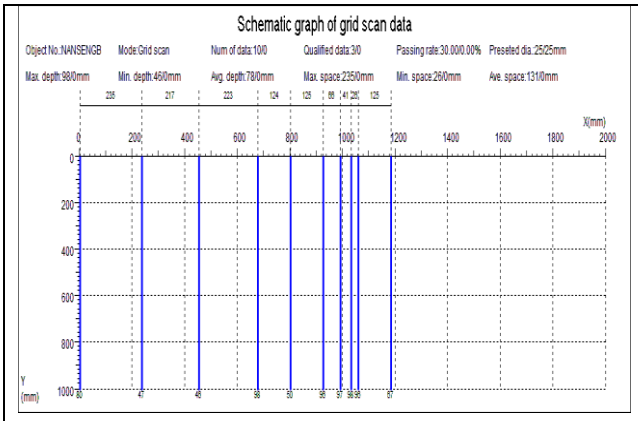

(a) Grid scan data for rebar diameter, rebar spacing and cover detection

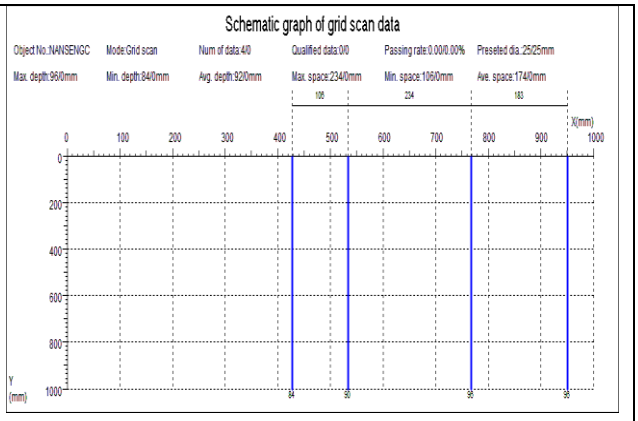

(b) Grid scan data for rebar diameter, rebar spacing and cover detection

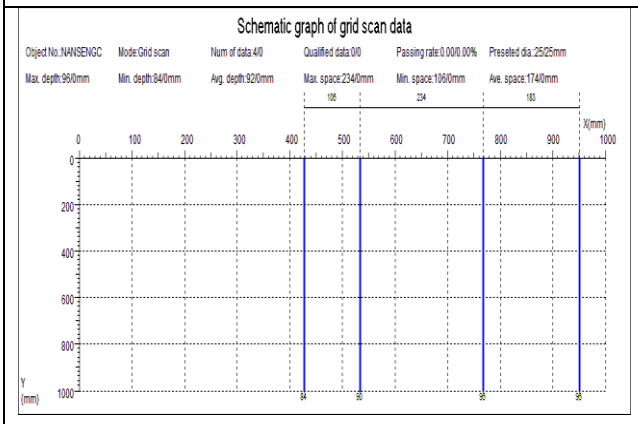

(c) Grid scan data for rebar diameter, rebar spacing and cover detection

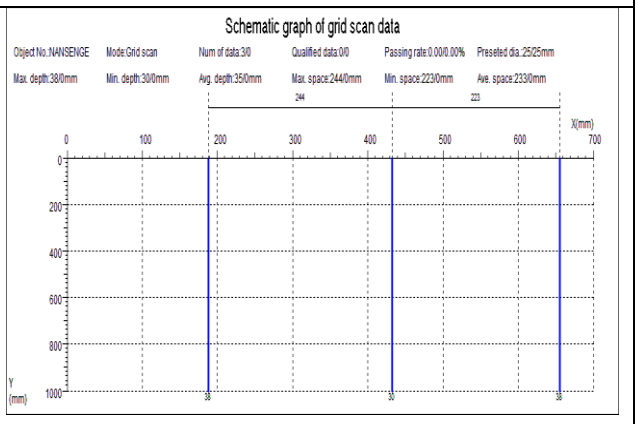

(d) Grid scan data for rebar diameter, rebar spacing and cover detection

Figure 4.6 show GPR Grid scanning of beams and piers.

4.3 Bridge Control Design Results

As stated in Chapter 3, Literature review of the applicable design code was done and a control design to BS5400 part 2 of 1978 was developed as the SATCC code of practice was not applicable by then. It was estimated that the bridge was built in the late 1960s just after Zambia got its independence from the British colonial rule. This estimate was achieved by conducting interviews of old people living near by the bridge. From section 4.2.1, the bridge geometry was established and the general arrangement was known. Therefore this sub chapter presents results of load considerations and

structural analysis of Nansenga Bridge under BS5400 part 2 of 1978. FEM design 17 software was used and was customized to suit the British Code BS5400.

4.3.1 Determination of Beam with extreme (HA +UDL) on loaded length using Grillage Analysis.

The loaded length referred to above is the length of the base of the positive or negative portion of the influence line for a particular effect at the design point under consideration.

i). Carriageway width =6.8m

ii). Number of notional lanes (3.2.9.3.1) =2

iii). Notional Lane width=6.8/2=3.4m

iv). Temperature difference of Group 4 loadings were considered in the software FEM design. Max 37^o C and Min 9^oC (5.4.3)

v). HA UDL Loaded length $25.7m > 30m$ therefore load intensity is 30kN/m (6.2.1)

vi). Load intensity HA UDL = $30/3.4 = 8.82kN/m^2$

a. $= 1.55x8.82 = 13.67kN/m$ Beam 01

b. $= 1.85x8.82 = 16.32kN/m$ Beam 02

vii). HA KEL (knife edge load) = $120/3.4 = 35.29kN/m$ (6.4.1)

a. HA KEL on BEAM 01=$= 1.55x35.29 = 54.7kN$ (grillage) (6.4.1.4)

b. HA KEL on BEAM 02= $1.85x35.29 = 62.29kN$ (grillage)

viii). Super imposed dead load Beam 01 (SIDL) = $= 0.05x22x1.55 = 1.71kN/m$

ix). Super imposed dead load Beam 02 (SIDL) =$= 0.05x22 = 2.04kN/m$

x). Dead load $= 0.378x24 = 9.1kN/m$ Beam 01

xi). Pedestrian= $5.0KN/m^2x1.2m = 6kN/m$ Beam 01 (6.5.1)

xii). Total UDL (*HA+DL+SIDL+PL*) on BEAM 01=29.48KN/m

xiii). Total UDL (*HA+DL+SIDL+PL*) on BEAM 02=18.36KN/m

a. Result Comment: $\underline{Beam\ 01\ UDL > Beam\ 02UDL}$

xiv). Max moment on Beam 01=2894KN.m >2714 kN. m Max moment on Beam 02,

a. Therefore Beam 01 controls the design.

Figures 4.7a and 4.7b show Maximum Bending moment under Load Combination C3.

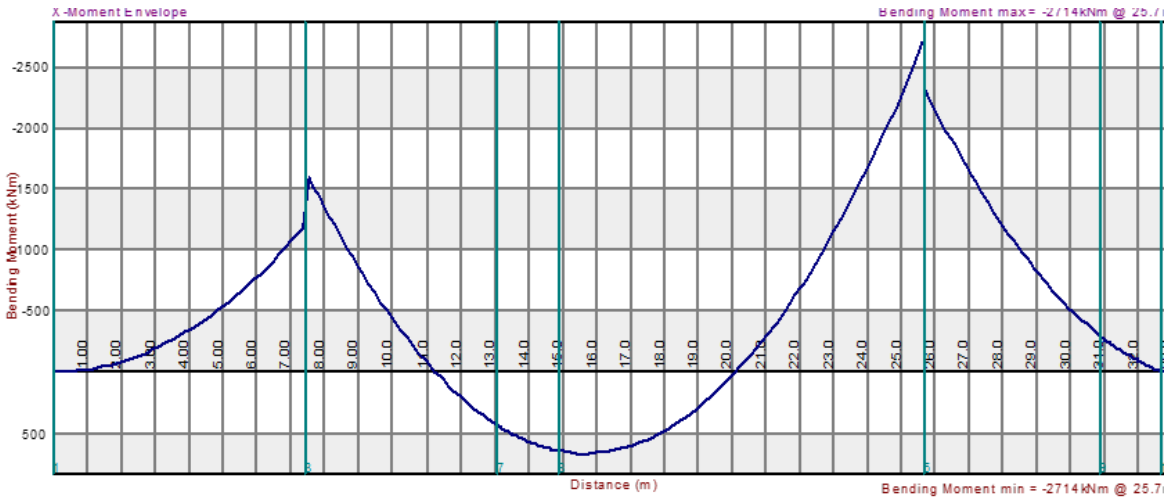

(a) –Ve Maximum Bending moment Beam 02=-2714 kN-m

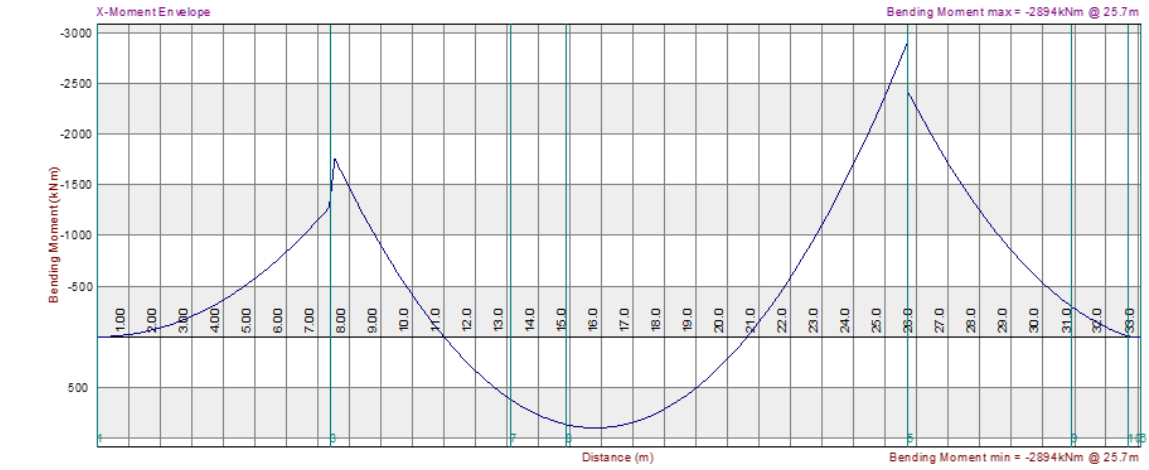

(b) Maximum Bending moment Beam 01=-2894 kN-m

Figures 4.7 show Maximum Bending moment under Load Combination C3

4.3.2 Determination of extreme position for member design

HA KEL loads are initially proportioned to the adjacent members and joints then the worst effects will always be achieved by positioning the KEL directly above a transverse member. Two positions of the KEL to give the worst effect will be checked along the loaded Length. From the influence line the following positions are checked to determine the extreme position for member design.

i). 1st position is KEL@ 9.15m of the second span of the bridge

ii). 2nd position is KEL @ is at 7.0 m of the cantilever

4.3.2.1 Results of Extreme loading position analysis for HA KEL

Table 4.4 Results of Extreme loading position analysis for HA KEL

Load combinations	**C1**	**C3**	**Location**	**HA KEL (position)**
+ve max bending moments	1838kN.m	1121kN.m	16.52m mid span	9.15m mid span
-ve max bending moments	2488kN.m	2715kN.m	25.7m @ cantilever second support	9.15m mid span
+ve max bending moments	1433kN.m	777.1kN.m	15.93m mid span	7.0m 3rd span cantilever
-ve max bending moments	2812kN.m	2984kN.m	25.7m @ cantilever second support	7.0m 3rd span cantilever.0m

Figures 4.8a and 4.8b shows +Ve and -Ve Maximum bending moment under Load combination C1.

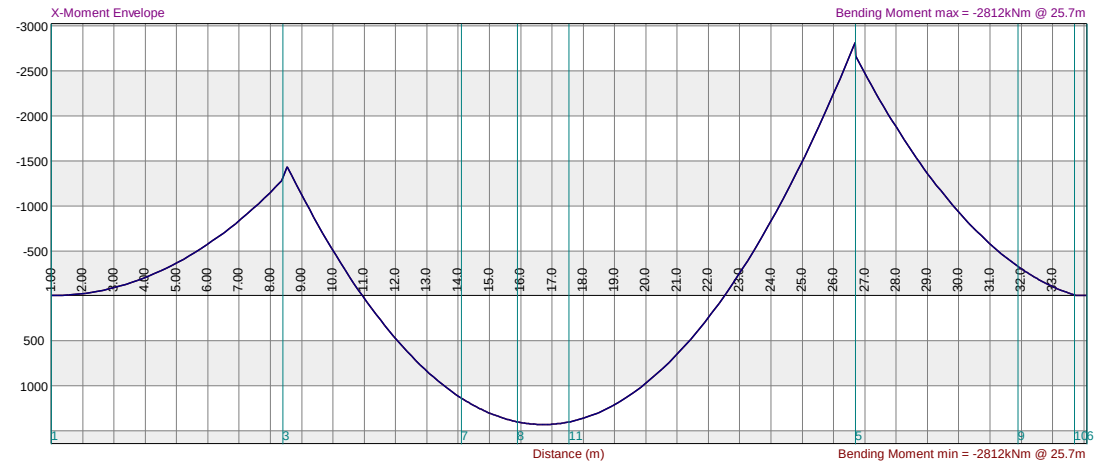

(a)-Ve Maximum Bending moment Beam 02=-2812 kN.m for Load combination C1

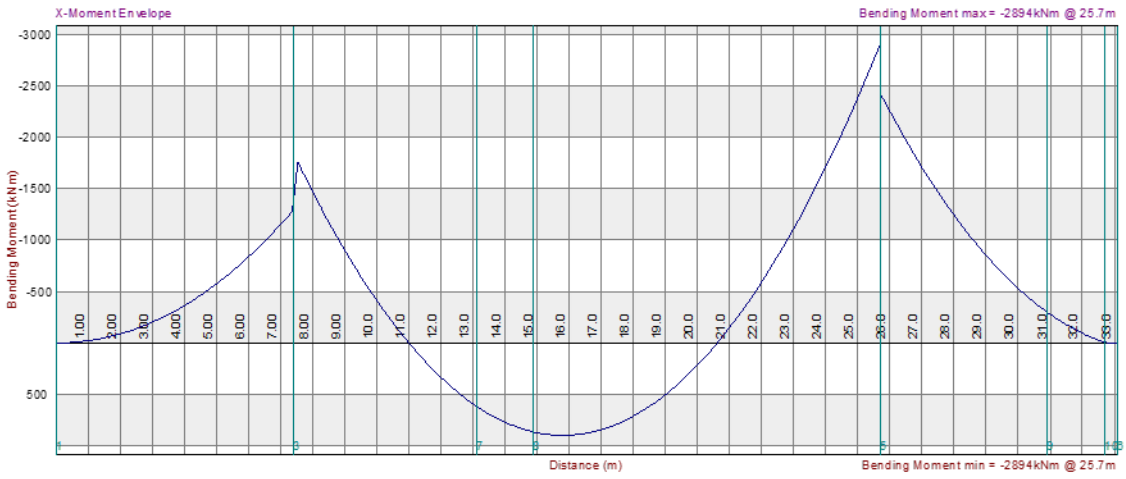

(b) -Ve Maximum Bending moment Beam 01=-2894KN.m for Load combination C1

Figure 4.8 -Ve Maximum Bending moment Load combination C1

From the above analysis, HA KEL produces a higher moment when it's positioned at 7.0m of cantilevered span 3.Therefore this position is adopted for extreme design load conditions of the girder.It is therefore useful to separate the HA UDL and HA KEL into different load cases to avoid repeating the calculation for the effects of the UDL. The UDL and various positions of the KEL can be added together in different combination cases.

4.3.3 Determination of extreme HB Loading.

The HB vehicle consists of four axles with four wheels on each axle and is applied to the grillage as a series of point loads. Clause 6.3.2 and 6.3.3 allow the wheel loads to be applied as patch loads however there is little to be gained in a global analysis by applying this refinement and point loads will be a suitable representation for the wheel loads.

A check is performed from the five variations of the inner axle spacing for the HB vehicle that can produce critical loading for member design moments and shear forces. Using FEM design a moving point load indicates the positions of critical HB loading to achieve the design moments and shears.it is usual to design all internal beams for the critical loading condition for vehicles on the carriageway.

i). Inner axle spacing of 6 and 26 are eliminated as they will only produce moments in one direction of the loaded length.

ii). The loaded length is 25.7m inner axle spacing of 26m is eliminated.

iii). Checking for HB vehicle with inner axle spacing of 11m, 16m and 21m on the loaded length.

4.3.3.1 Results of Extreme loading position analysis for HB axle spacing (11m, 16m, and 21m)

Table 4.5 shows a summarized results of Extreme loading position analysis for HB axle spacing of (11m, 16m, and 21m).

Figure 4.9 to 4.10 show loading and graphical representation of HB loading at axle spacing of 11m. For graphical representation of axle spacing of 16m and 21m refer to Appendix A2

Table 4.5 Results of Extreme loading position analysis for HB axle spacing (11m, 16m, and 21m)

Load combinations	**C1**	**C3**	**Location**	**HB Vehicle** **Axle spacing**
+ve max bending moments	1148kN.m	1469kN.m	17m mid span	11m
-ve max bending moments	3069kN.m	3267kN.m	25.7m @ cantilever second support	11m
Shear force	789kN	746kN	25.7m @ cantilever second support	11m
+ve max bending moments	1377kN.m	794kN.m	14.91m mid span	16m
-ve max bending moments	3069kN.m	3245kN.m	25.7m @ cantilever second support	16m
Shear force	706.5kN	676.6kN	25.7m @ cantilever second support	16m
-ve max bending moments	3068kN.m	3083kN.m	25.7m @ cantilever second support	21m
+ve max bending moments	713kN.m	228.5kN.m	14.56m mid span	21m
Shear Force Max	682.7kN	655,2kN	25.7m @ cantilever second support	21m

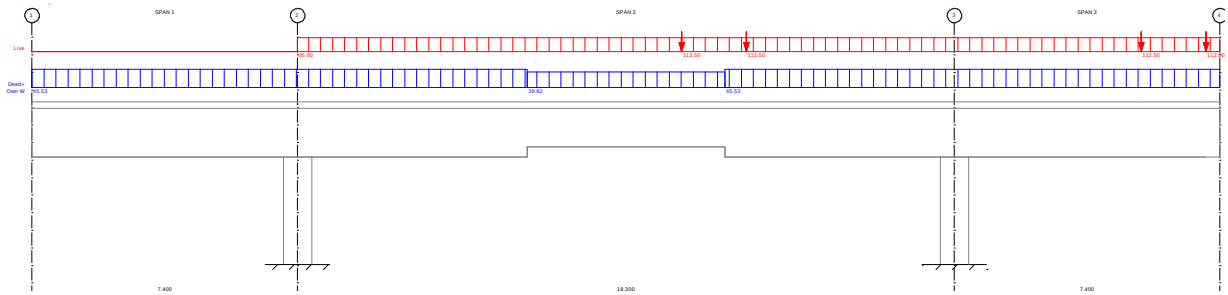

(a) HB loading @ axle spacing of 11m with temperature loads

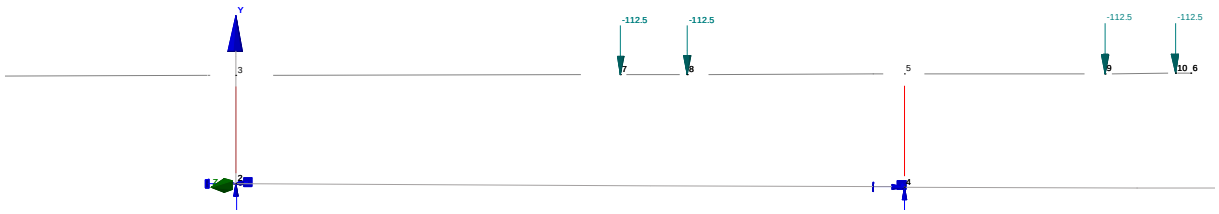

(b) Analysis for HB vehicle with 11m axles spacing moving

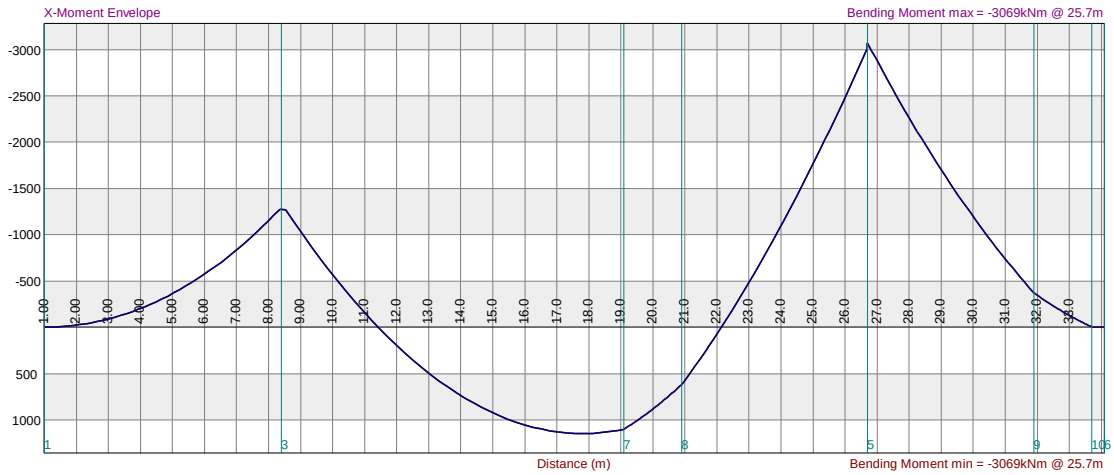

(c) -ve maximum Bending moment 3069kN.m @HB AXLE SPACING 11m L C1

Figure 4.9 Analysis for HB Vehicle with 11m axles spacing

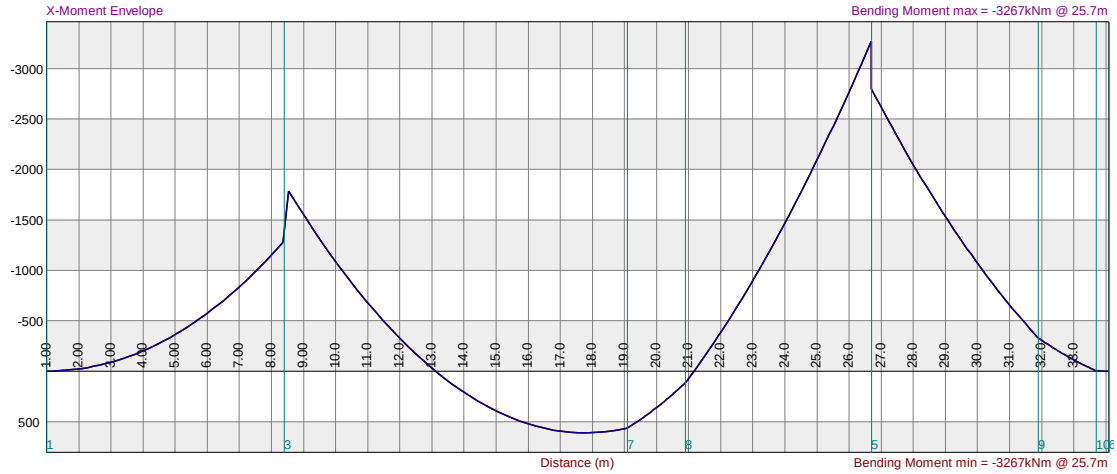

(a) -Ve Maximum Bending moment 3267KN.m @HB AXLE SPACING 11m L C3

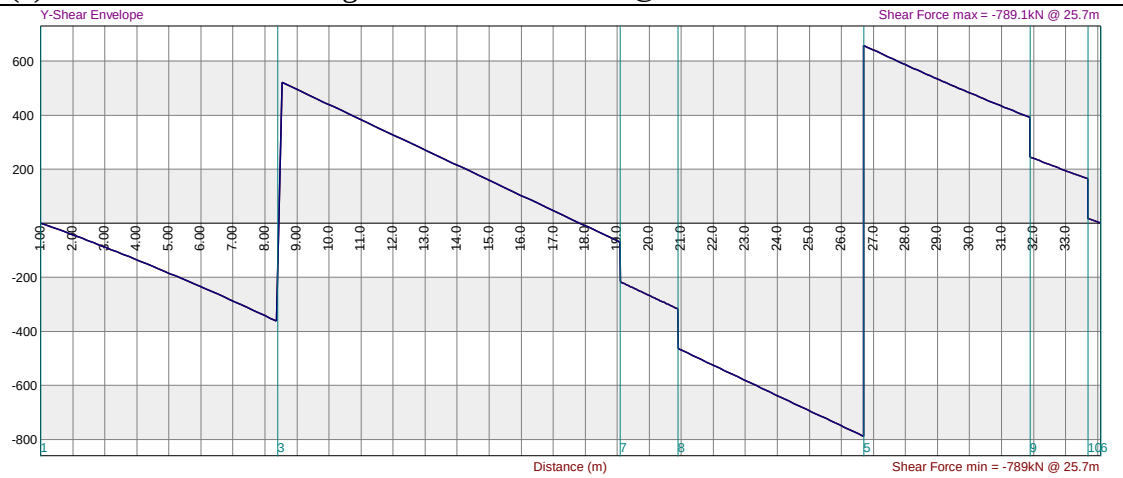

(b) Shear Force Max=789kN @HB AXLE SPACING 11m L C1

Figure 4.10 Analysis for HB Vehicle with 11m axles spacing

4.3.4 Results and analysis of extreme Load combinations

HB vehicle with axle spacing of 11m produces extreme loading conditions with a total Max moment of **3267kN.m** in combination C3.Therefore HB vehicle with axles spacing of 11m is adopted for design considerations in both ultimate and serviceability limit state.

HA UDL +KEL total max **moment 2982kN.m < 3267kN.m** HB vehicle total max moment. Therefore HB loading is Critical

In this case HB loading controls the design since it produces extreme loadings. From Table 4.5 load combinations C3 and C1.

i). Load combination C1

HB total max moment = (C1)**3069kN.m (ULS +SLS)**

ii). Load combination C3

HB total maximum moment= (C3) **3267kN.m (ULS+SLS)**

HB (LC3)>HB (LC1)

Hence load combination **C3** is critical for both ultimate and serviceability limit state design.

4.3.5 Design of reinforced concrete girders

i) SECTION TYPE 1 (1530x850)) REINFORCED CONCRETE BEAM SECTION AT END SPAN

The beam under consideration comprises of two 2 sections,` a 1530mmx850mm and a 1250mmx850mm section, figure 4.11 shows beam section while table 4.6 show parameters of the beam under consideration.

A	mm^2	1.4805E6
Ixx	mm^4	326.22E9
Iyy	mm^4	164.06E9
Ixy	mm^4	0.0000
Iuu	mm^4	326.22E9
Ivv	mm^4	164.06E9
Ir	mm^4	490.29E9
Ang	deg	0.0000°
Zxx(T)	mm^3	477.68E6
Zxx(B)	mm^3	385.12E6
Zyy(L)	mm^3	177.37E6
Zyy(R)	mm^3	177.37E6
Zuu	mm^3	385.12E6
Zvv	mm^3	177.37E6
Zplx	mm^3	609.30E6
Zply	mm^3	397.86E6
Yc	mm	847.07
Xc	mm	925.00
rx	mm	469.41
ry	mm	332.89
ru	mm	469.41
rv	mm	332.89
Xpl	mm	925.00
Ypl	mm	870.71
Perim.	mm	6.7600E3
J	mm^4	207.49E9
Zt	mm^3	268.78E6
Cw	mm^6	14.160E15
A-shear	mm^2	1.0257E6
Bx		247.97
Vr		476.95E-3
Γ		380.90E-3

Table 4.6 and 4.6b sectional properties

Code	X/Radius	Y/Angle
+		
	0	-180
	500	0
	0	-1350
	850	0
	0	1350
	500	0
	0	180
	-1850	0

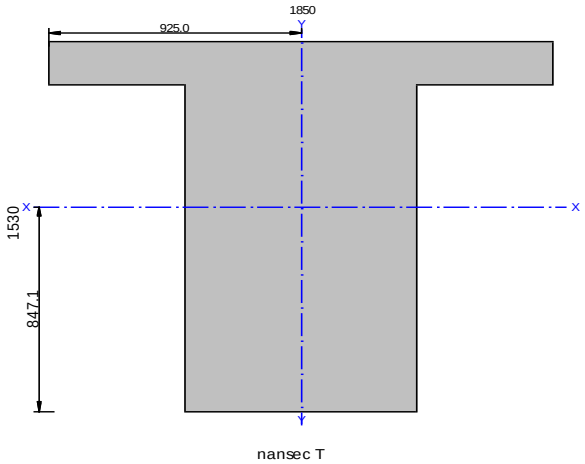

Figure 4.11 (1530x850) Beam section

ii) Pure Torsion:

J = 207E9 mm4 Zt = 269E6 mm^3

iii) Shear Centre:

X = 925 mm Y = 1.00E3 mm

iv) Warping Torsion:

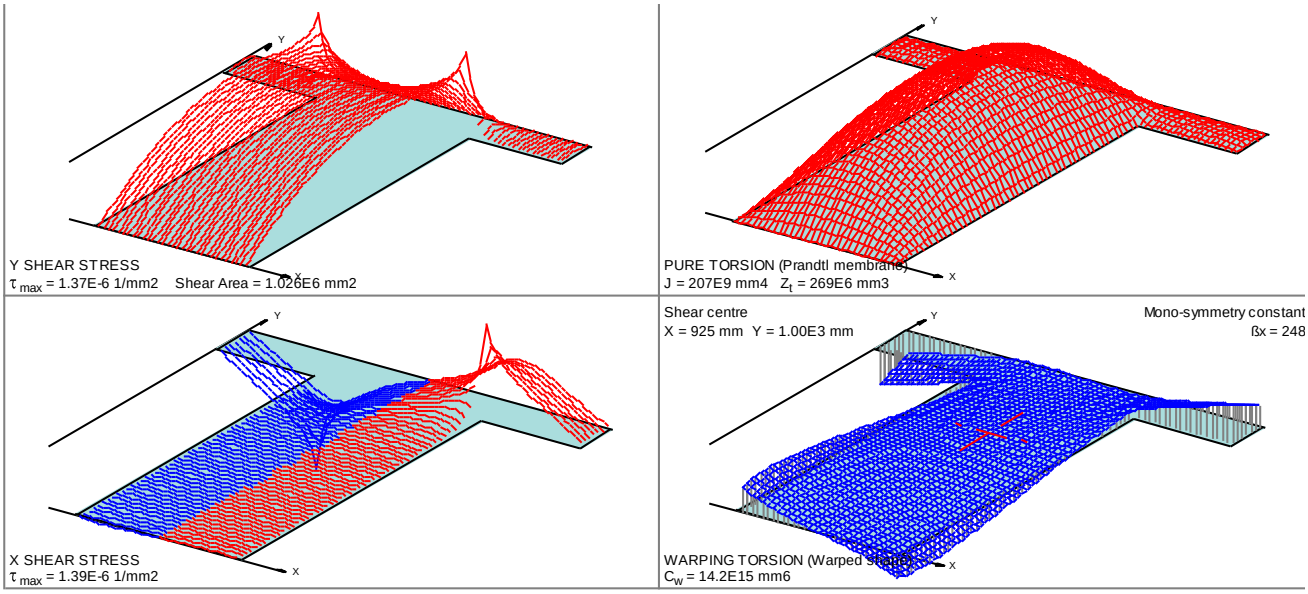

Cw = 14.2E15 mm^6,k

Figure 4.12 Graphical shear stress and torsion distribution of 1530x850 section

4.3.5.1 Flexural capacity design and reinforcement calculations

Table 4.7 shows a summary of design calculations for Beam Section 1

Ultimate applied moment $M_d = 3267kN.m$ (Hogging)

f_y=460mpa,*cover*=50mm,d=*1480mm*,b_w=*850mm*,h_f=*180mm*,*bf=1850mm*,f_{cu}=*35*

Table 4.7 summary of design calculations for Beam Section 1

Item No.	***Description***	***Result***	***Comment***
1	*Maximum compressive stress* $f_{st} = 0.87\text{fy} \ldots eq(4.1)$	400.2MPa	
2	*Rectangular stress block properties* *β=0.9,α=0.67,ϕ=0.67*		
3	*Steel strains* $S_{st} = \frac{f_{st}}{200000} \ldots eq(4.2)$	0.002	
4	*Balanced Neutral Axis* $x_{ml} = \frac{d}{\left(1 + \frac{S_{st}}{0.035}\right)} \ldots eq(4.3)$	941.82mm	
5	*Neutral Axis limitation* *With 10% redistribution* *(0.9-0.4)d*	*740mm*	
6	Depth of rectangular stress block	*666mm*	*$> (h_f)$ extends beyond flange width*
7	$F_{hf} = 0.45 f_{cu} \alpha \phi h_f \left(d - \frac{h_f}{2}\right) \ldots eq(4.4)$	3.9kN.m/mm	
8	Moment of resistance on full flange width $M_f = 0.45 f_{cu} b_f h_f \left(d - \frac{h_f}{2}\right) \ldots eq(4.5)$	$7290kN.m$	$M_f > M$ ok
9	Flange moment of resistance without web $(1850 - 850)x3.9 \ldots eq(4.6)$	$3900kN.m$	

Table 4.7 continues…..

10	Moment of resistance of concrete $M_c = \left(3900 + \beta x_{ml} f_{cu} b_w \phi\alpha \left(d - \frac{\beta x_{ml}}{2}\right)\right)\llbracket \quad \rrbracket x10^{-6} \ldots eq(4.7)$	$14100kN.m$ (M) < M_c	Adopt rectangular beam design properties
11	Concrete moment capacity $M_u = \left(f_{cu} b_w \phi\alpha \left(d - \frac{a}{2}\right)\right) x10\rrbracket^{-6} \ldots eq(4.8)$	22203kN. m	M_c > M No compression reinforcement required
12	Lever Arm $Z = d[0.5 + \sqrt{0.25 - \frac{M}{2f_{cu} b_w \phi\alpha d^2}} \quad \ldots eq(4.9)$	1440mm	$Z = 0.95d$
13	Tensile Reinforcement $A_s = \frac{3267x10^{-6}}{0.87\text{fyz}} \quad \ldots eq(4.11)$	$5806mm^2$<0.04A_c	provide 8y32 top
14	Moment of resistance in steel $M_r = 0.87 f_y A_s \left(d - \frac{h_f}{2}\right) \ldots eq(4.12)$	$3579kN.m$	>3267kN.m OK
15	Nominal flexural reinforcement $\frac{b_w}{b_f} = \frac{850}{1850} = 0.46 > 0.4 \ldots eq(4.13)$	$1690mm^2$	6y20 bot
16	Shear reinforcement ratio $V_c = {f_1}^{0.3333} x {f_2}^{0.25} \quad \left(\frac{0.79}{1.25}\right) \ldots eq(4.14)$	0.49	
17	Actual shear stress $V_{sh} = \frac{V}{A_{sh}} \ldots eq(4.15)$	$0.627MPa$	
18	Shear reinforcement $V_{sh} = \frac{(V - V_c)b}{0.87 f_y} \ldots eq(4.16)$	1.563	R10@200 links

ii) SECTION TYPE 2 (1250x850) REINFORCED CONCRETE BEAM AT MID SPAN

Figure 4.13a shows beam type 2 section while figure 4.13b shows graphical shear stress and torsion distributions

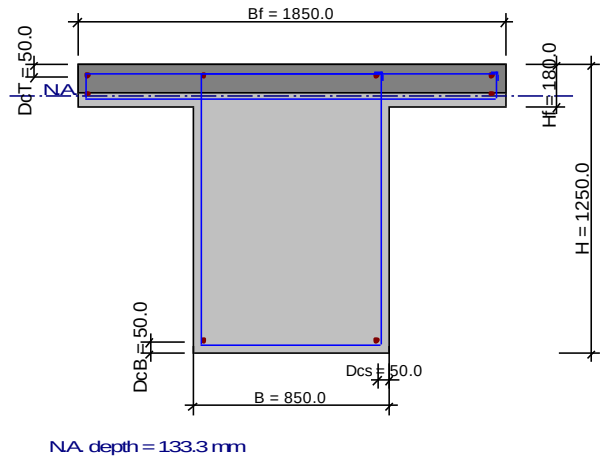

(a) (1250x850 beam section)

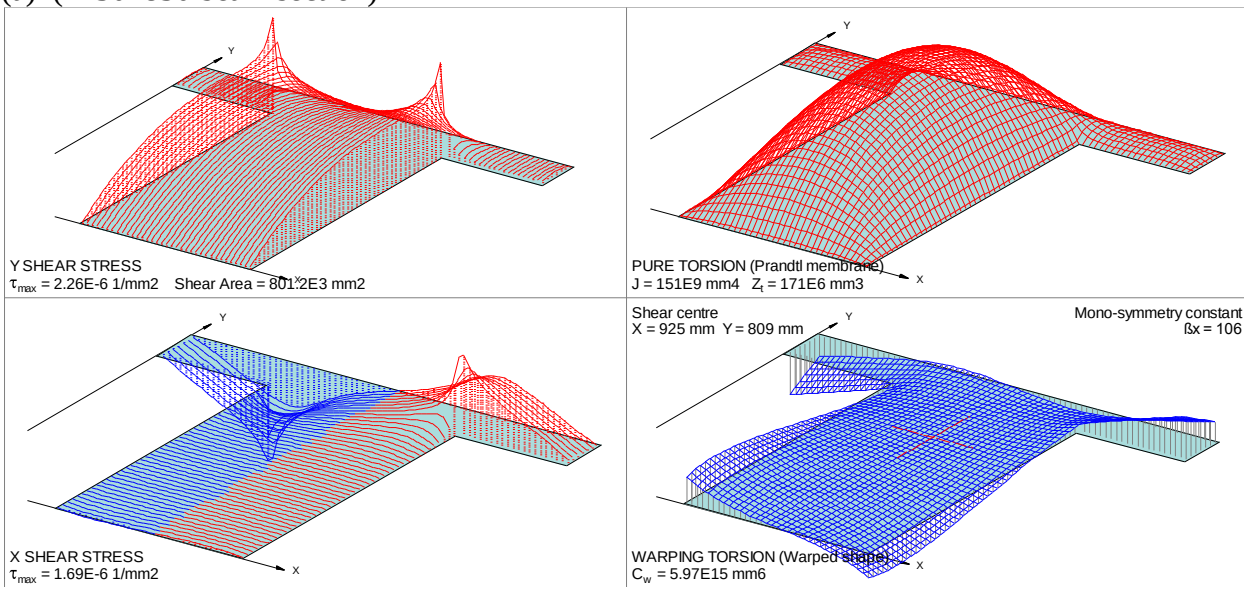

(b) Shows Graphical shear stresses and torsion distribution of 1250x850 section

Figure 4.13 Graphical shear stresses, torsion distribution and 1250x850 beam section

4.3.5.2 Flexural capacity design and reinforcement calculations for beam section 2

Table 4.8 shows a summary of design calculations for Beam Section 2

$Ultimate\ applied\ moment\ M_d = 1469KN.m$ (Sagging)

f_y=460mpa,*cover*=50mm,d=*1200mm*,b_w=*850mm*,h_f=*180mm*,bf=*1850mm*,f_{cu}=*35*

Table 4.8 summary of design calculations for Beam Section 2

Item No.	***Description***	***Result***	***Comment***
1	*Maximum compressive stress* $f_{st} = 0.87\text{fy} \ldots eq(4.1)$	400.2mpa	
2	*Rectangular stress block properties* $\beta=0.9, \alpha=0.67, \phi=0.67$		
3	*Steel strains* $S_{st} = \frac{f_{st}}{200000} \ldots eq(4,2)$	0.002	
4	*Balanced Neutral Axis* $x_{ml} = \frac{d}{\left(1 + \frac{s_{st}}{0.035}\right)} \ldots eq(4.3)$	763.6mm	
5	*Neutral Axis limitation* *With 10% redistribution* *(0.9-0.4)d*	*540mm*	
6	Depth of rectangular stress block	*666mm*	$> (h_f)$ *extends beyond flange width*
7	*Moment of resistance on full flange width* $F_{hf} = 0.45 f_{cu} \alpha \phi h_f \left(d - \frac{h_f}{2}\right) \ldots eq(4.4)$	$5821kN.m$	$M_f > M$ ok
8	Moment of resistance on full flange width $M_f = 0.45 f_{cu} b_f h_f \left(d - \frac{h_f}{2}\right) \ldots eq(4.6)$		$M_f > M$ ok
9	Flange moment without web $F_{hf} = f_{cu} \alpha \phi h_f \left(d - \frac{h_f}{2}\right)(bw - h_f) \ldots eq(4.7)$	3110kN.m	

Table 4.8 continues…..

10	Moment of resistance of concrete $M_c = \left(3110 + \beta x_{ml} f_{cu} b_w \phi\alpha \left(d - \frac{\beta x_{ml}}{2}\right)\right)\llbracket \quad)x10\rrbracket^{-6} \ldots eq(4.8)$	$9600kN.m$ (M) < M_c	Adopt rectangular beam design properties
11	Concrete moment capacity $M_u = \left(f_{cu} b_w \phi\alpha \left(d - \frac{a}{2}\right) x10\right]^{-6} \ldots eq(4.9)$	14597KN. m	M_c > M No compression reinforcement required
12	Lever Arm $Z = d[0.5 + \sqrt{0.25 - \frac{M}{2f_{cu} b_w \phi\alpha d^2}} \quad \ldots eq(4.10)$	1178mm	$Z = 0.95d$
13	Tensile Reinforcement $A_s = \frac{3267x10^{-6}}{0.87\text{fyz}} \quad \ldots eq(4.11)$	$3219mm^2$	provide 5y32 bot
14	Moment of resistance in steel $M_r = 0.87 f_y A_s \left(d - \frac{h_f}{2}\right) \ldots eq(4.12)$	1785.8kN. m	>1469KN.m OK
15	Nominal flexural reinforcement $\frac{b_w}{b_f} = \frac{850}{1850} = 0.46 > 0.4 \ldots \ eq(4.13)$	$1381.3mm^2$	5y20 top
16	Shear reinforcement ratio $V_c = {f_1}^{0.3333} x {f_2}^{0.25} \quad \left(\frac{0.79}{1.25}\right) \ldots eq(4.14)$ $f_1 = 0.32$	0.432	
17	Actual shear stress $V_{sh} = \frac{V}{A_{sh}} \ldots eq(4.15)$	$0.19MPa$	
18	Shear reinforcement $V_{sh} = \frac{(V - V_c)b}{0.87 f_y}$ =0.316… $eq(4.16)$	$A_{sh} = 1.563$	R10@200 links
19	Crack control reinforcement $= \sqrt{\frac{Sb}{f_y}} \quad \ldots eq(4.17)$	19.2mm	Provie Y20@200 sides of beam
20	Transverse reinforcement. $Tr_{reinf} = 180\text{x}1000\text{x}0.0015 \ldots eq(4.18)$	270mm	Provide Y10@250

4.3.6 Production of Detailed reinforcement drawing as per BS5400 part 1&2 of 1978.

From the control design, a detailed reinforcement drawing Figure 4.14 and bending schedule Table 4.9 were produced to compare and guide correct rebar placement, cover to reinforcement and rebar diameter during finite element modelling.

Figure 4.14 shows detailed reinforcement layout to BS 5400

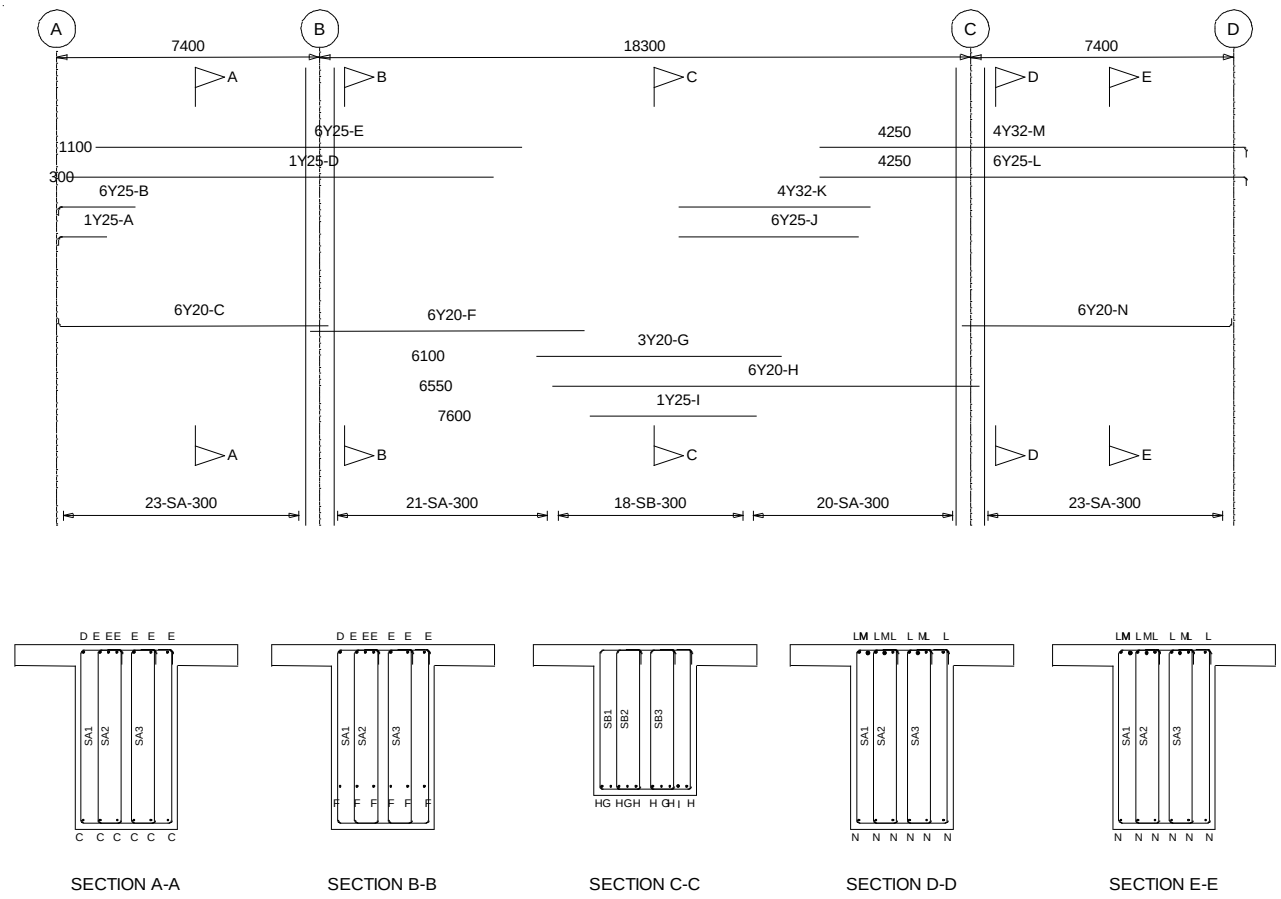

Figure 4.14 Detailed reinforcement layout to BS 5400

4.3.6.1 Bending schedule

Table 4.9 summarises the reinforcement bending schedule.

Table 4.9 Reinforcement Bending schedule

Bars	Mark	SC	Span	Offset	Length	Hook	Layer
1Y25	A	34	1	0.050	1.575	L	T
6Y25	B	34	1	0.050	2.475	L	T
6Y20	C	34	1	0.050	7.600	L	B
1Y25	D	20	1	0.500	12.000	L	T
6Y25	E	20	1	1.400	12.000	L	T
6Y20	F	20	2	-0.250	7.700	L	B
3Y20	G	20	2	6.100	6.700	L	B
6Y20	H	20	2	6.550	12.000	L	B
1Y25	I	20	2	7.800	4.400	L	B
6Y25	J	20	3	-8.500	5.375	L	T
4Y32	K	20	3	-8.500	5.690	L	T
6Y25	L	34	3	-4.250	12.000	R	T
4Y32	M	34	3	-4.250	12.000	R	T
6Y20	N	34	3	-0.250	7.600	R	B

4.3.6.2 Results GPR Scanned VS Design Control

Table 4.10 summarises bridge scanned results and design control results

Table 4.10 Results GPR Scanned VS Design Control (BS 5400 part 2)

Element	GPR Scanned	Design Control BS 5400 part 1&2 of 1978
Average Cover	72mm	50mm
Rebar(compression & tension)	8Y32 top of cantilever, 8 Y25 bottom,Y12 stirrups	8Y32 top of cantilever ,8 Y25 bottom,r12 stirrups
Rebar spacing average	Stirrups R10@(100mm, 200mm)	Stirrups R10@ (100mm,200m)
Compressive Strength	36 MPa	30-40 MPa
Punching Shear Reinforcement	Present (Y25) top	Present(Y25) top
Flexural Reinforcement	Present 6Y20	Present (6Y20)
Crack control reinforcements	Y20@185	Y20@200

Table 4.10 continues

Flange Transverse reinforcement	Y10@240	Y10@250
Flange longitudinal reinforcement	Y10@260	Y10@250

4.4 Finite Element results

Calculated values of reinforcement and scanned values were compared before developing the finite element model. From the above table 4.10 scanned values agreed with calculated reinforcement areas and were therefore used for validating the model.

4.4.1 Moving Load (Dynamic Analysis.)

45units of HB in one notional Lane was introduced as moving load on the bridge at a constant speed of 30km/hr, in order to investigate the dynamic behavior of the bridge (Figure 4.18a)

Table 4.11a Moving Loads

No.	Name	Vehicle	Return	Lock direction	Cut loads to path extent
1	HB	EC LM1 Lane 1. (Truck) [Distributed]	Yes	Yes	No
2	moving load	EC LM1 Lane 2. (Truck) [Concentrated]	Yes	Yes	No

Note: This table continues in Appendix C

4.4.1 Crack presence predictions due to load combinations

Tables 4.11a and4.11b show results of crack predictions due to load combinations with a moving load.

Table 4.11b Crack presence predictions due to load combinations

No	Type	Load combination	Non-linear elements	Plastic elements	Non-linear soil	Cracked section	2nd order	Imperfection shape
1	U	1.15*Dead load + 1.75*super imposed + HB live load	Yes	Yes	No	No	Yes	-
2	Sq	Dead load + super imposed + HB live load	Yes	Yes	No	No	No	-
3	Sf	Dead load + super imposed + HB live load	Yes	Yes	No	No	No	-
4	Sc	Dead load + super imposed + HB live load	Yes	Yes	No	Yes	No	-
5	U	1.15*Dead load + 1.75*super imposed + HB Truck moving live load	Yes	Yes	No	No	No	-
6	Sq	Dead load + super imposed + HB live load + truck moving load	Yes	Yes	No	Yes	Yes	-
8	Sc	Dead load + super imposed + HB truck moving load	Yes	Yes	No	Yes	Yes	-

Figures 4.15 show the FE model and load effects of the bridge during stages of finite element analysis

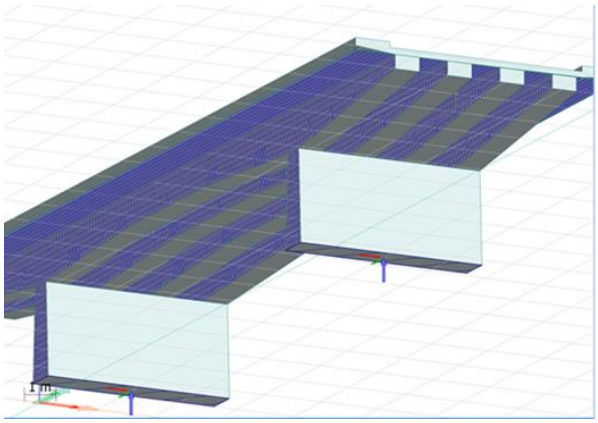

(a) Full 3D Nansenga bridge finite element model

(b) Full 3D Nansenga bridge finite element model

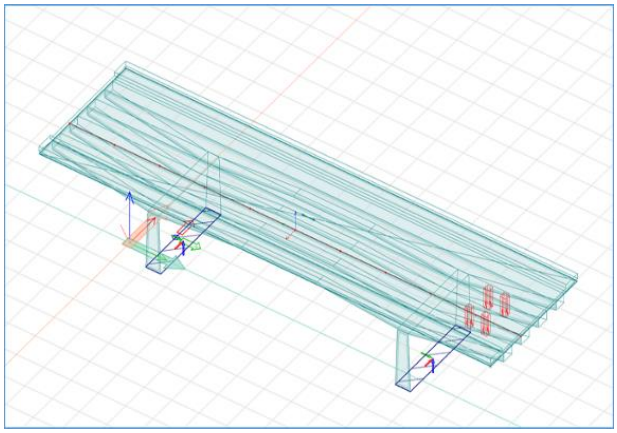

(c) HB truck moving load

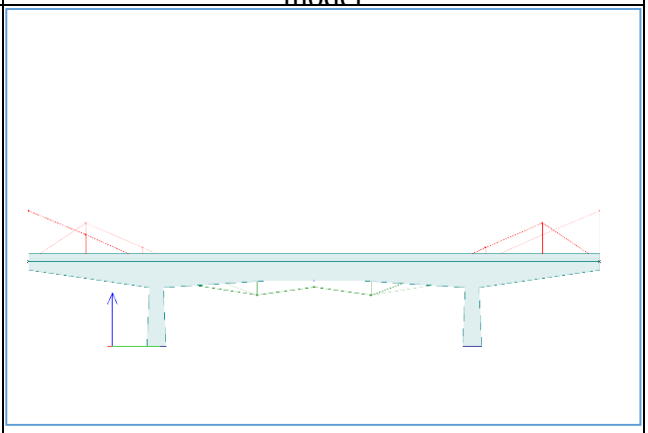

(d) Moving load max influence line

Figure 4.15 shows the FE model and load effects of the bridge during stages of finite element analysis

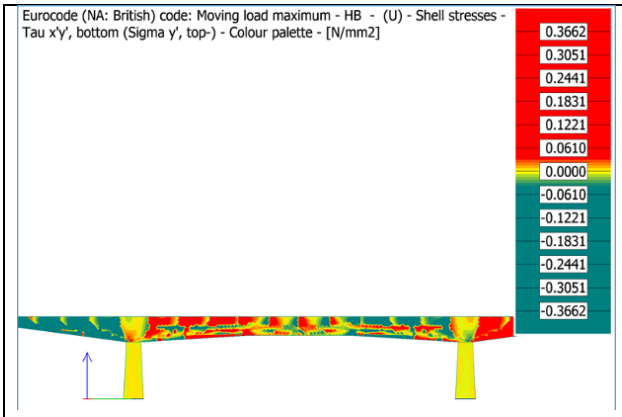

(a) ULS dead + HB Moving load maximum shell stresses

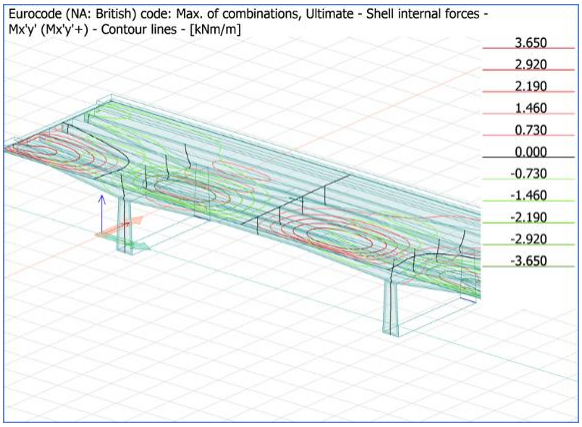

(d) maximum load combinations ultimate shell stresses

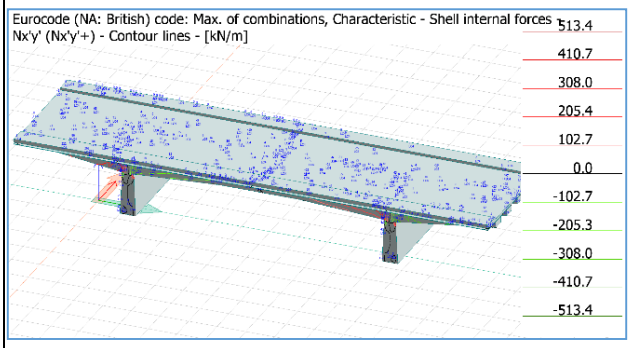

(c) Max of combination characteristics internal forces

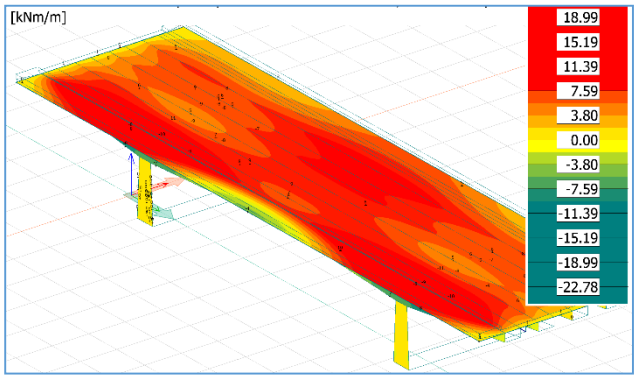

(d) 1st order load combinations max shell stresses

Figure 4.16 shows the FE model and load effects of the bridge during stages of finite element analysis

4.5 Experimental field test results and Periodic monitoring

Experimental field tests involved periodic structural health monitoring for 2 months with the stated equipments in section 3.2. Figures 4.17a and 4.17b show crack depths measurements during experimental field tests and periodic monitoring conducted on the bridge.

(a) experimental field tests/ SHM Nansenga bridge

(b) experimental field tests/ SHM Nansenga bridge

Figure 4.17 Experimental field tests/ SHM Nansenga bridge

4.5.1 Periodic Crack width detections Beam 01 and Beam 02 results

As a huge indicator of distress to structural members crack widths were measured for a period of 3months. Attention was paid to distressed regions indicated by the finite element model. Progressive crack growth was measured as shown in the Figures 4.18(a, b, c, d, e f, g, h, i).

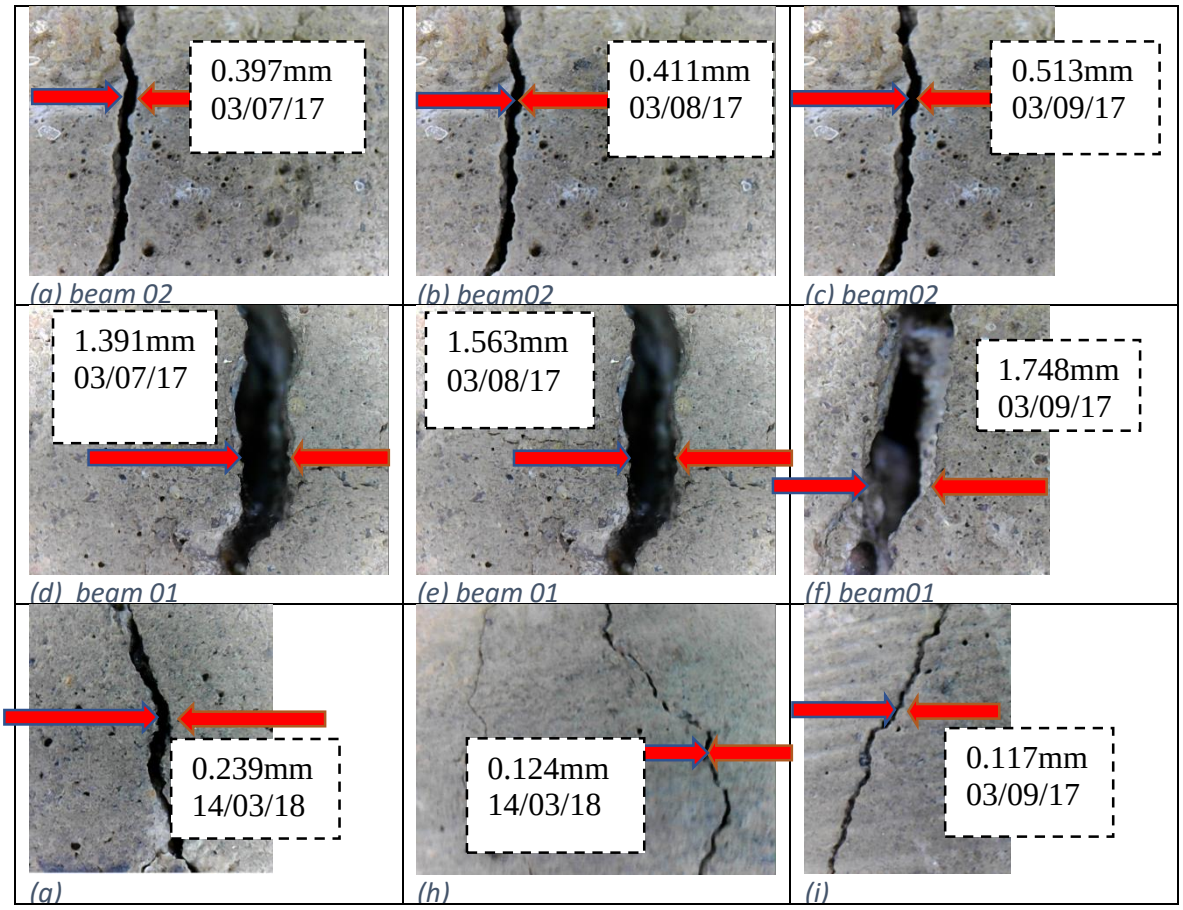

Figure 4.18 shows progresive Crack growth detections Beam 01 and Beam 02 results

4.5.2 Crack depth Detection

The depth of cracks was investigated with an ultrasonic pulse velocity with attention paid to highly distressed regions reviewed by the finite element model. Two transducers were placed at intervals of 50mm, 100mm, and 150mm on surface of each crack.4 sample tests were done on each crack the figure shows propagated wave form that corresponded to the average depth of crack detected. A maximum crack depth of 212.63mm was detected on beam 01 while 94.4mm depth in beam 02.Figure 4.19 to 4.22 show details of cracks.

i). Crack depth Beam 01

Whether crossing or not: Cross-over crack

Starting distance: 50.00mm

Distance Interval: 50.00mm

Calculation method: Auto.

Depth of Crack 1: -1.00mm

Depth of Crack 2: **212.63mm**

No.Time 1(us) Dist(mm) Depth of Crack(mm)

002-01	50.00	50.00	-1.00
002-02	143.60	100.00	85.92
002-03	222.00	150.00	237.61
002-04	222.00	200.00	212.63

Crack depth (fig 4.19&4.20) right

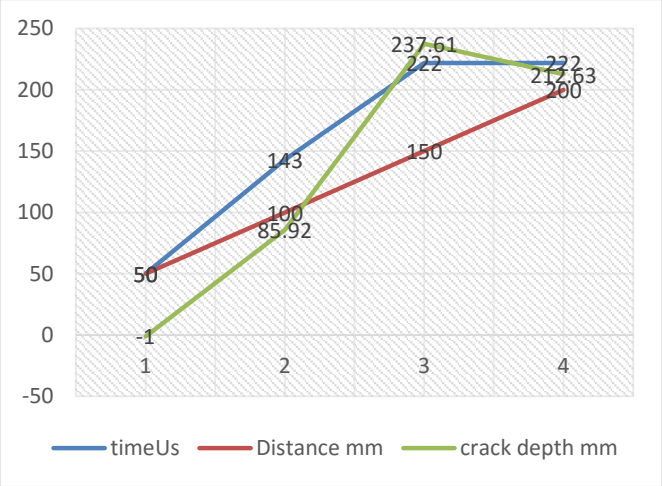

Figure 4.19 cross over crack

ii). Crack2 beam 2

Test points 5No

Whether crossing or not: Cross-over crack

Starting distance: 50.00mm

Distance Interval: 50.00mm

Calculation method: Auto.

Depth of Crack 1: -1.00mm

Depth of Crack 2: **94.44mm**

No.	Time 1(us)	D(mm)	Crack depth(mm)
01	50.00	50.00	-1.00
02	222.00	100.00	161.18
03	191.20	150.00	112.40
04	188.40	200.00	176.49

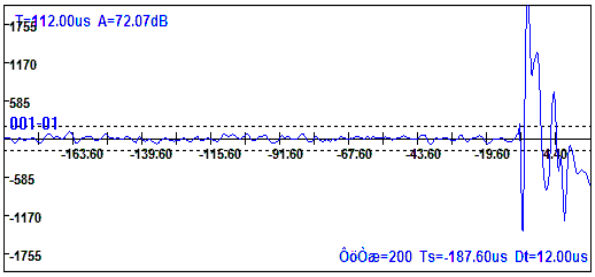

Figure 4.20 crack wave form

iii). Crack 3 Beam 03

Total Points: 3

Whether crossing or not: Cross-over crack

Starting distance: 50.00mm

Distance Interval: 50.00mm

Calculation method: Auto.

Depth of Crack 1: -1.00mm

Depth of Crack 2: 51.76mm

No.	Time 1(us)	Distance (mm)	Depth of Crack (mm)
002-01	127.60	50.00	52.30
002-02	157.60	100.00	49.05
002-03	198.00	150.00	54.47

Crack depth (fig 4.21 cross over crack)

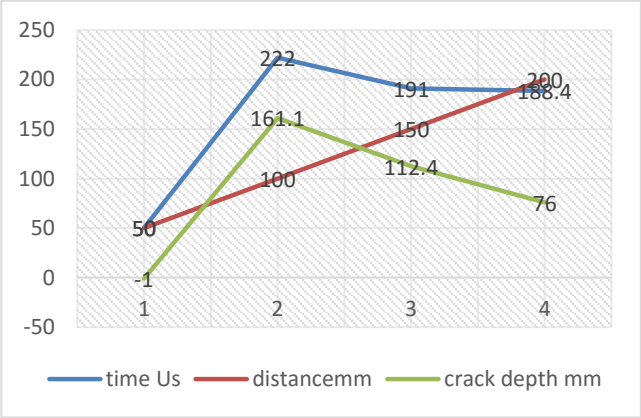

Figure 4.21 crack cross over

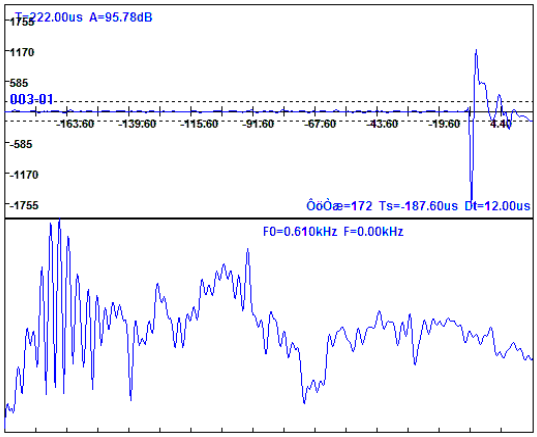

Figure 4.22 crack wave

CHAPTER 5 DISCUSSION OF RESULTS

5.1 Introduction

This chapter compares and discusses results obtained from the method applied in achieving the specific objectives of this research. The method included, review of improved and cost effective SHM technologies, development of tools that lead to the application of SHM sensor technology on Nansenga Bridge of Zambia. Numerous results obtained from the SHM technique employed in this research have been well highlighted in this chapter through the Control design, finite element modelling and periodic SHM experimental field tests with respect to true behavior of the bridge as predicted by finite element modelling. Experimental field tests conducted for 60days demonstrated a successful application of structural health monitoring technology on Zambian Highway Bridges .A proposed rationale decision making tool is further presented at the end of this chapter for adoption by road authorities and other government agencies.

5.2 Review of SHM technologies.

There is currently no structural health monitoring nor a SHM program for bridge infrastructure being applied in Zambia except on the current ongoing construction works of the Kazungula Bridge that have employed force gauges for monitoring of forces. All inspections if any, on Zambian bridges are based on adhoc, unplanned, subjective and inefficient methods of simply visualization of the outer surface of the structure. This is the general case on bridge infrastructure in southern African region as structural health monitoring is still in its infancy despite there being a lot of research in developed countries.one of the contributing factors is the huge cost associated with structural health monitoring technologies and lack of expertise.

From the literature reviewed in Chapter 2, researchers have highly recommended use of a multi-level structural health monitoring system integrating global and local-level diagnostics. Global-level techniques can be used to provide rapid condition screening, locate the proximities of the anomalies and evaluate their influence on global structural behavior, while local Sensor/NDE techniques can be applied to the identified distressed region in order to better define the location and severity of the damage and its effect on local components (Mohamed and abdo 2014).

As a recommendation by previous researchers, In this study, a combination of global and local based method was applied as illustrated in chapter 3 and chapter 4.Finite element modelling was carried out for a global based physical model response of the bridge structure and sensor/nondestructive testing equipment were used for local based diagnosis of bridge elements in distressed regions for damage location and periodic monitoring. The approach used in this study is more efficient and cost effective as it comprises of an error elimination technique via comparison of scanned values versus design control system. And does not require onsite installation of permanent sensors, and hiring a moving load in order to obtain a true behavior of the bridge, instead all these are performed through simulations within Finite Element analysis.

Among the reviewed improved and effective technologies for SHM, Fiber optic sensors where reported to be the most efficient and cost effective technology for structural health monitoring (Mohamed and Abdo 2014), with several advantages when compared with other technologies like Laser Doppler Velocity and use of strain gauges .These are explained in section 2.7 of this study. Though there is need for experienced expertise, the newly demonstrated method of structural Health monitoring in this research would be a far much cheaper technology, despite its requirement to have full understanding of finite element modeling, structural analysis and use of sensor and nondestructive testing equipment.

5.3 Control design

An efficient and effective SHM must be free from Data input errors and should have a true representation of the structural characteristics of the bridge of study in its present state. Therefore a control systems design to compare and verify NDTE collected data was a necessary tool to successfully meet the main objective with several specific objectives.

Nondestructive technique was employed to determine the strength of concrete, rebar diameter, spacing and cover to reinforcement. As built drawings/details in particular for the bridge of study (Nansenga Bridge) could not be located therefore a control design to BS5400 part 2 and 4 of 1978 was developed and was consistent with most collected/measured field data as shown in Table 4.10. The loaded length was calculated to 25.7m. Considering load combinations 1&3. The 3 span bridge was loaded with 30kN/m HA UDL + KEL in one notional lane and 45units of HB in one notional lane for both Load combinations 1and 3, respectively. HB loading combination 3 with axle spacing of 11m on one notional lane produced most severe effects as indicated by influence line with a

maximum hogging moment of 3267kN.m and maximum sagging moment 1148 kN-.m as compared with other axles spacing in Table 4.5.

Therefore HB Loading with Axle spacing of 11m combination 3 was adopted for design considerations. Loads due to temperature differences where considered in combination C3. Combination 2 was not applicable due to non-consideration of wind loads which were restricted by bridge height of less than 6m above ground level as per design code. Grillage analysis was used to design the bridge girder/beams in PROKON 3.0 considering girders as flanged beam. Table 4.10 compares results of calculated reinforcement with scanned reinforcement, prior to finite element modelling. Part 2 loadings of the design code was applied considering both ultimate limit and serviceability limit state factors Table 3.1. Figures 5.1, 5.2, 5.3 and 5.4 present bending moment distribution diagrams, shear force diagrams, Areas of reinforcement and long term elastic deflections. Areas of reinforcement are adequate as shown by calculations in chapter 5.3 and the red boundary line Figure 5.3. In Figure 5.4 long term deflections of 23.9mm on 7.4m cantilever are within range and are acceptable.

5.3.1 GPR Scanned results Vs Design Control calculated values

Table 5.1compares Scanned flexural, shear, tensile and compressive reinforcement on longitudinal beams with calculated values from the design control. Shear reinforcement was detected at beam-pier supports. Cover to reinforcement averaged 72mm, more than the 50mm allowed for in the design code.

Table 5.1 Shows GPR Scanned results Vs Design Control calculated values to (BS 5400 part 2)

Table 5.1 GPR Scanned results Vs Design Control calculated values (BS 5400 part 2)

Element	GPR Scanned	(Calculated) Design Control BS 5400 part 1&2 of 1978
Average Cover	72mm	50mm
Rebar(compression & tension)	8Y32 top of cantilever, 8 Y25 bottom,Y12 stirrups	8Y32 top of cantilever ,8 Y25 bottom,r12 stirrups
Rebar spacing average	Stirrups R10@(100mm, 200mm)	Stirrups R10@ (100mm,200m)

Table 5.1 continues…

Compressive Strength	36 MPa	30-40 MPa
Punching Shear Reinforcement	Present (Y25) top	Present(Y25) top
Flexural Reinforcement	Present 6Y20	Present (6Y20)
Crack control reinforcements	Y20@185	Y20@200
Flange Transverse reinforcement	Y10@240	Y10@250
Flange longitudinal reinforcement	Y10@260	Y10@250

5.3.2 Graphical representation of moments, shear forces and areas of reinforcement

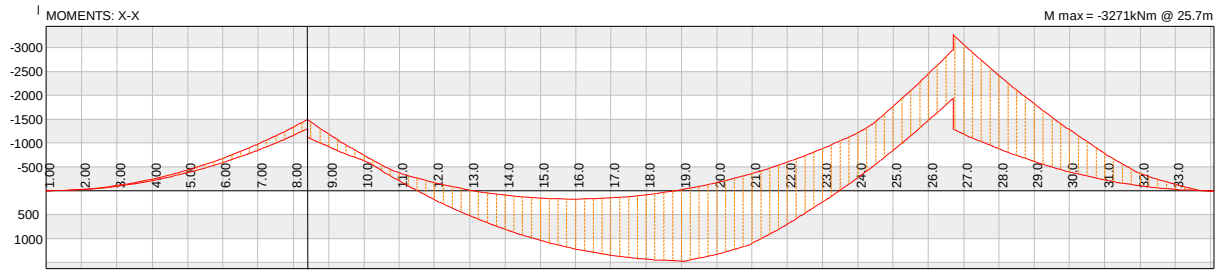

Figure 5.1 Graphical max and min moment distribution diagram LC 3

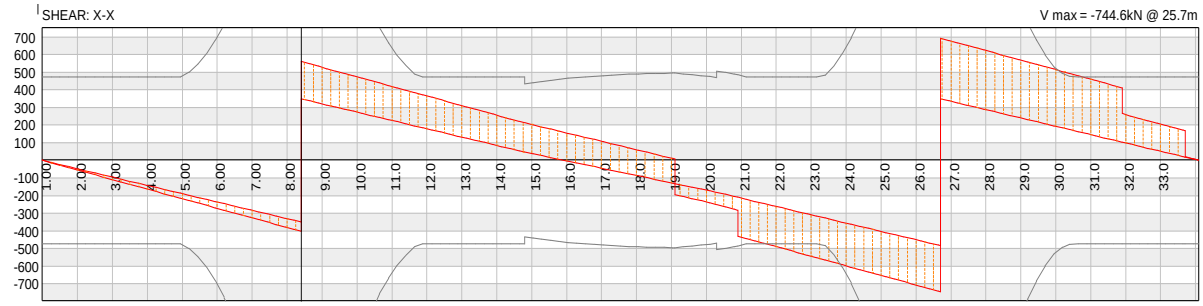

Figure 5.2 Max & min Shear force diagram LC 3

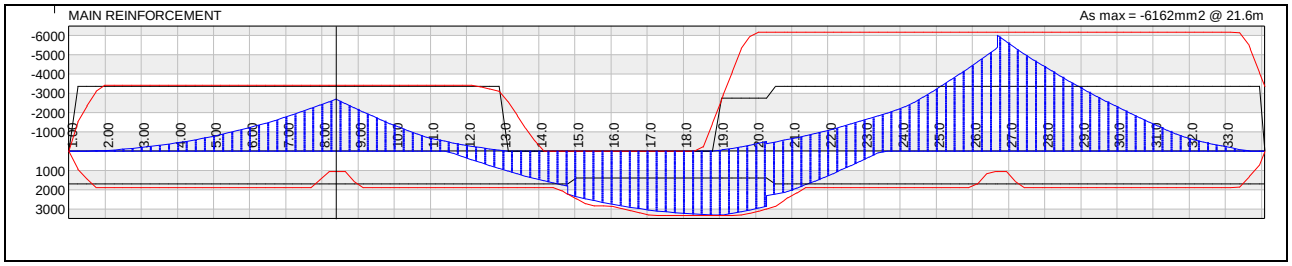

Figure 5.3 Max & Min Main reinforcement areas LC 3

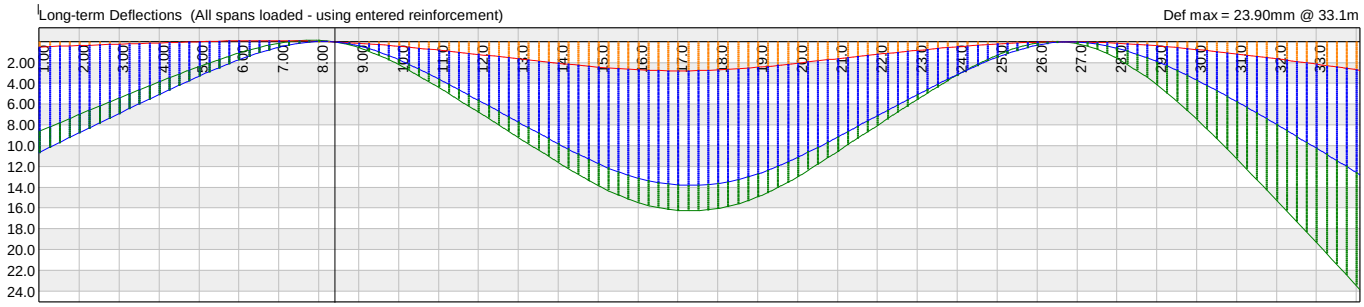

Figure 5.4 Long term deflections LC 3

5.4 Finite Element modelling

In order to meet specific objectives of the study which was to, (i) propose an efficient and effective method of structural health monitoring and (ii) highlight numerous results that could be achieved. A combination of global and local based SHM as recommended by other researchers is more efficient and effective (Muhammad and Abdo 2014), finite element modelling was developed to correctly represent global bridge behavior and accurately predict distresses. Linear, dynamic, fatigue, and thermal analyses were conducted. In this section various results achieved are well highlighted and how they matched with predicted global response of the bridge.

The finite element model was validated with the field data which was verified by the control design, Using FEM Design 17.0 the reinforced-concrete bridge investigated was modeled with triangular and quadrilateral shell elements of 4/3/2 nodes. Stresses at various points through the thickness of the elements were indicated as a moving load and uniformly distributed load was applied based on the Euro Code EC1 part 3.which was of particularly important for this study. Reinforcement was placed as per real time scanned sizes, spacing and average cover. Concrete plane plates were used to simulate typical reinforced-concrete bridge piers. FEM design 17 employs a plasticity-based constitutive model that simulates cracking, tension stiffening and shear capacity of cracked

concrete. Table 4.11 shows results of crack predictions of shell elements. Figures (4.15 to 416) in chapter 4 show the general type of behavior exhibited by the reinforced concrete bridge.

Second-order analysis of structures based on the linear theory means that the equilibrium conditions are determined according to the shape of the structure before loading. In case of larger deformations the results would be more accurate if the change of structure geometry was taken into consideration. Therefore in this research, deformations during the loading were only taken into consideration in the relationship of membrane forces and bending moments. In reinforced concrete normal forces influence the bending moments because of the deflections perpendicular to the rebar and modifies of course the deflections. Consequently, the stiffness matrix of the system is a linear function of the normal internal forces in plane plates and membrane. Based on this principle equation (7) applied.

The second order theory gave accurate results as they were verified with field measurements.

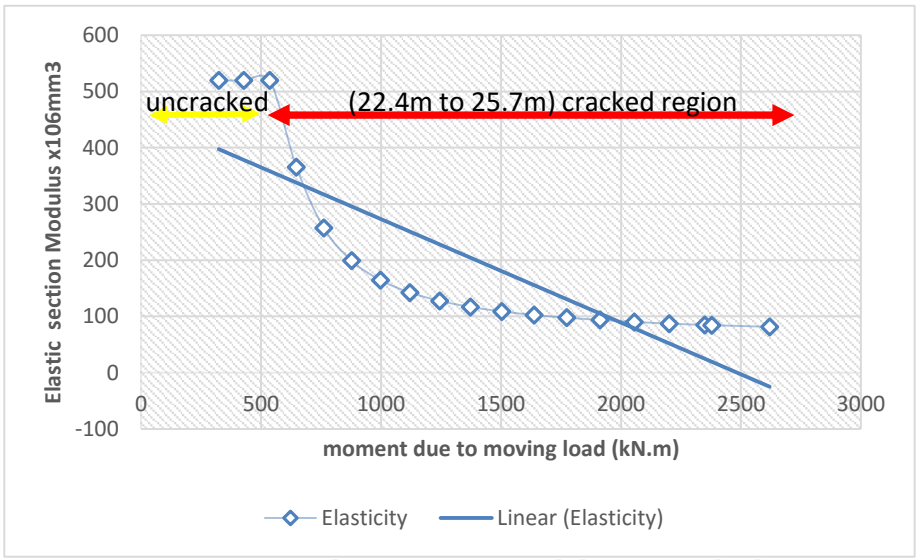

Figure 5.5 elastic section modulus Vs applied

The model revealed that flexural shear cracking was first observed as the moving load under load combination ULS (LM1) distributed (938kN/m^2) was introduced. These cracks propagated laterally in the X and Y directions as the applied load increased, with wider cracks occurring parallel with the X direction. In figure 5.5, the graph shows a decrease in modulus of elasticity as a moving load was applied during the finite element analysis. No cracking was observed at 21.0m of the span and moment of rapture of 536kN.m with section modulus of 519x10^{6}mm^3.In the region of 22.4m to 25.7m the section modulus reduced to between 365x10^{6}mm^{3}and 81x10^{6}mm^3 at 25.7m before rising back to 500x10^{6}mm^3 (Figure 5.6) at 30.15m of the span as the applied moment due to moving load exceeded the moment of rapture/crack resisting moment of 536 kN.m. A Maximum

applied moment of 2619kN.m at 25.7m where the bridge support pier is located resulted in side/top surface cracks at stresses ranging from 0.366Mpa to 1.0mpa while side /bottom surface cracks developed at stresses ranging from 1mpa to 10.4Mpa refer to appendices E.

Table 4.12 shows the analytical predictions of cracks due to high stresses at the top and bott om surfaces of the beam element. At a maximum moment of 2619kN.m Figure 5.5b as the applied moment due to a moving load reduces, the modulus of elasticity increases from $81x10^6mm^3$ at 25.7m of the span to $500x10^6mm^3$ at 30.15m of span. At a region beyond 30.15m of span3 the tensile stress is less than the modulus of rapture and the elastic modulus resists failure and retains the beam to its initial position.

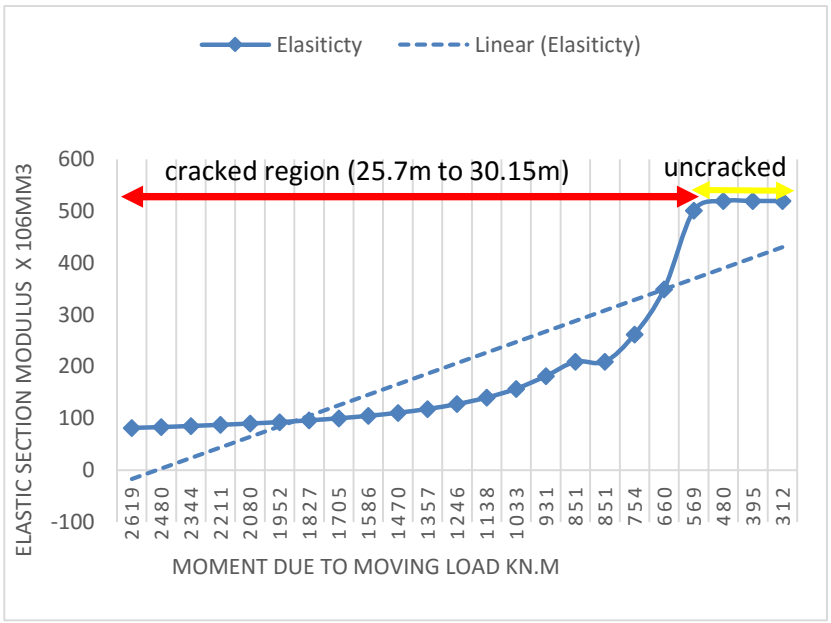

Figure 5.6 Elastic section modulus Vs applied moment right Pier.

Figure 5.7 shows the general behavior of the bridge under HB moving load, initial cracking starts after exceeding a crack resistance moment of 536 kN.m at 22.4m. As the load is increased after the modulus of rupture of the concrete is exceeded, cracks begin to develop in the (top) tensile

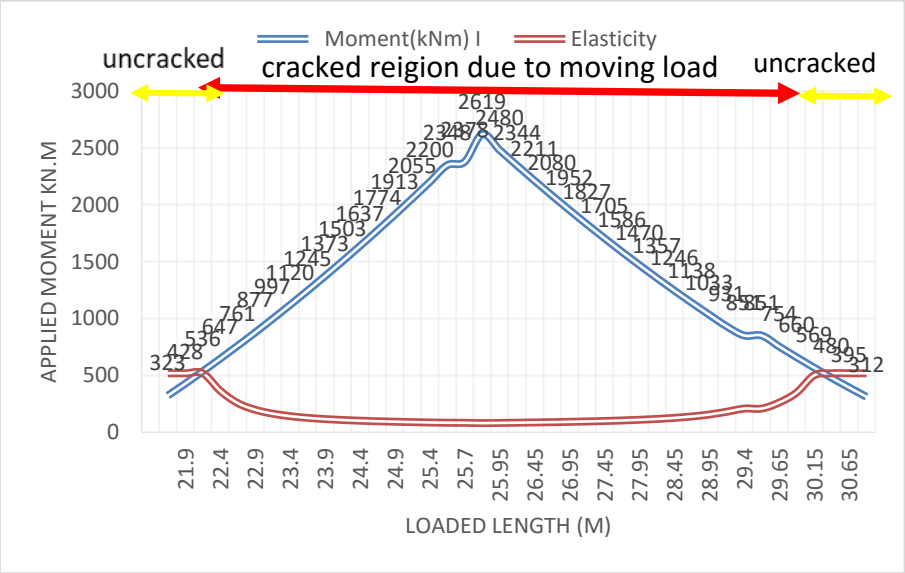

Figure 5.7 Elastic section modulus Vs applied

region of the cantilevered beam. The moment at which these cracks begin to form that is, when the tensile stress in the top of the beam equals the modulus of rupture referred to as the cracking moment, As the applied moment is further increased, these Cracks quickly spread up to the vicinity of the neutral axis, and the neutral axis begins to move upward reducing modulus of elasticity to $81x10^6mm^3$ at 25.7m. The cracks occur at those distressed point (21.9m to 30.15m) along the beam where the actual applied moment is greater than the cracking moment, as shown in Figure 5.5,5.6,5.7). Now that the bottom has cracked, another stage is present because the concrete in the cracked zone cannot resist tensile stresses the steel takes care of that. This stage will continue as long as the compression stress in the bottom is less than one half of The concrete's compression strength, and as long as the steel stress is less than its yield stress. As the moving truck drives out of the bridge, the applied moment continues to reduce together with tensile stresses to a value less than the crack resistance moment and the beam retains to its initial modulus of elasticity at 30.15m of the span. The stresses that caused cracking in the compression region ranged from 1Mpa to 10.4Mpa higher than tresses in the tensile region.

5.5 Experimental field tests and periodic monitoring

As the main objective of the research was to apply sensor technologies for SHM on Zambian Highway Bridge with a case study of Nansenga Bridge. A demonstration and application of SHM was achieved by experimental field tests carried out on the bridge for a period of 60days, with the use of high tech based nondestructive wireless equipment, attention was paid to predicated areas of

high distresses and cracking regions as analyzed above by the finite element model with an HB moving load. Figures 4.18(a, b, c, d, e, f,) Indicate tests conducted that corresponded with the finite element analysis. Table 5.2 shows a comparison between experimental SHM field tests and finite element analysis results.as explained by graphical representations in figures 5.6 and 5.7 cracks located at and near to supports on the top of the cantilevered beams where wider than the cracks on the bottom. At the midspan of the simply supported beam cracks were wider at the bottom than cracks observed on top. This is because lower values of stresses in the tensile region were required to exceed the modulus of rapture while higher values of stresses in the compression region where required to exceed the same cracking moment.

Flexural shear cracks with increasing crack widths from top to bottom on both cantilevered beams of the bridge at the supports where detected. In Figures 5.8a and b. The cracks, monitored for a period of 3months, exhibited a maximum progressive growth of 0.172mm on beam 01 whilst beam 02 had a growth of 0.102m for one month. Minimum-Maximum crack width ranged from 0.397mm to 0.513mm on beam 02. Figure 4.18 (a, b, c). 1.391mm to 1.748mm on beam 01 measured figure 4.23(d, e, f) .Experimental crack widths on top of cantilevered beams where lower than finite element values because tensile cracks tend to close with reduction in load while compression crack widths open wider with reduction load. Therefore the moving HB load caused cracks to open wider in tension regions and reduced crack width in the compression regions.

The depth of cracks was investigated with an Ultrasonic pulse velocity detector. Crack depths were measured on each crack. A maximum crack depth of 212.63mm was detected on beam 01 while on beam 02 it was 94.4mm

5.5.1 Experimental results Vs FE Analysis

Table 5.2 compares experimental field results to FE Analysis ones.

Table 5.2 Experimental field results Vs FE Analysis

element	Experimental (SHM)Tests		FE Analysis	
	Crack width(mm)	position	Crack width(mm)	position
Beam 02@support	0.397	top	0.399	top
	0.213	bottom	0.193	bottom
Beam 02@ support	0.513	top	0.671	top
	0.411	bottom	0.294	bottom
Beam 01@support	1.748	top	2.126	top
	1.39	bottom	0.726	bottom
Beam 01@support	1.563	top	1.931	top
	1.294	bottom	0.664	bottom
Beam 03@support	0.79	top	0.816	top
	0.441	bottom	0.643	bottom

Figure 5.8 (a) and (b) present Graphical representation of Experimental Field SHM tests Vs finite element analysis results

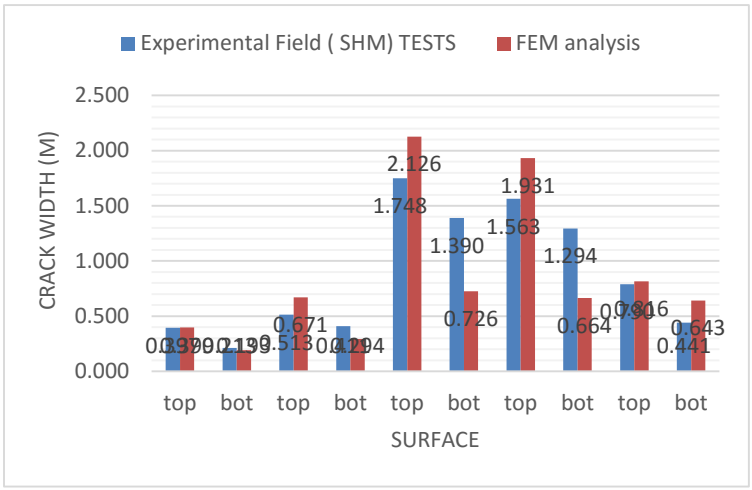

(a) Tensile and compression cracks FEM Vs Experimental values

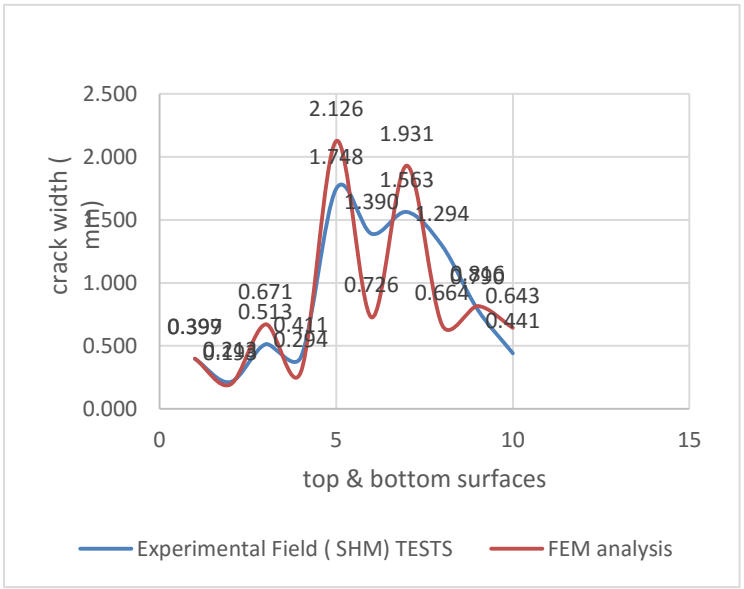

(b) compares experimental (SHM) cracks to FEM (ten sile & compression cracks)

Figure 5.8. Tensile and compression cracks FEM Vs Experimental values

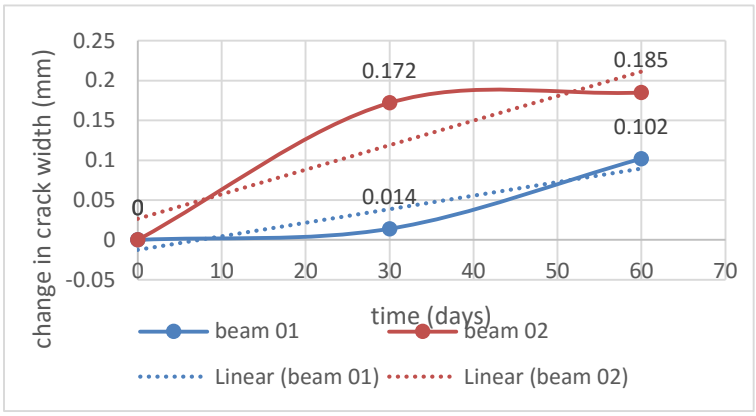

(b) shows progressive crack width growth during experimental periodic SHM of the bridge

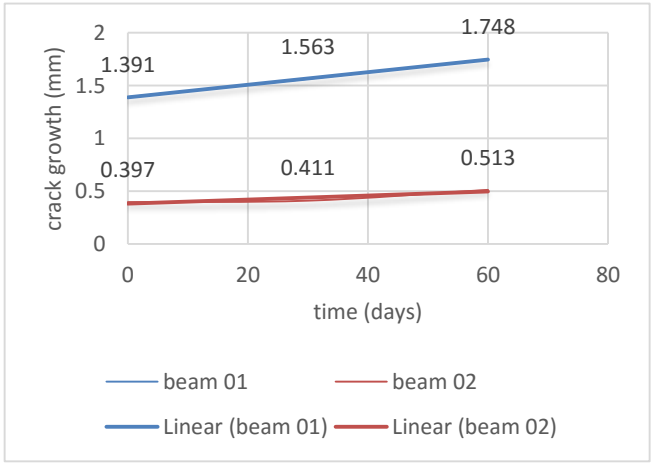

(b) Change in crack growth against time

Figure 5.9. shows progressive crack growth during experimental periodic SHM of bridge

5.6 The Proposed Decision Model

A proposed decision making model has been developed Figure 5.10 in this research which could be adopted in undertaking successful structural health monitoring projects for Zambian Highway bridges. The first step is to identify a bridge structure of interest and collect as-built data, in cases

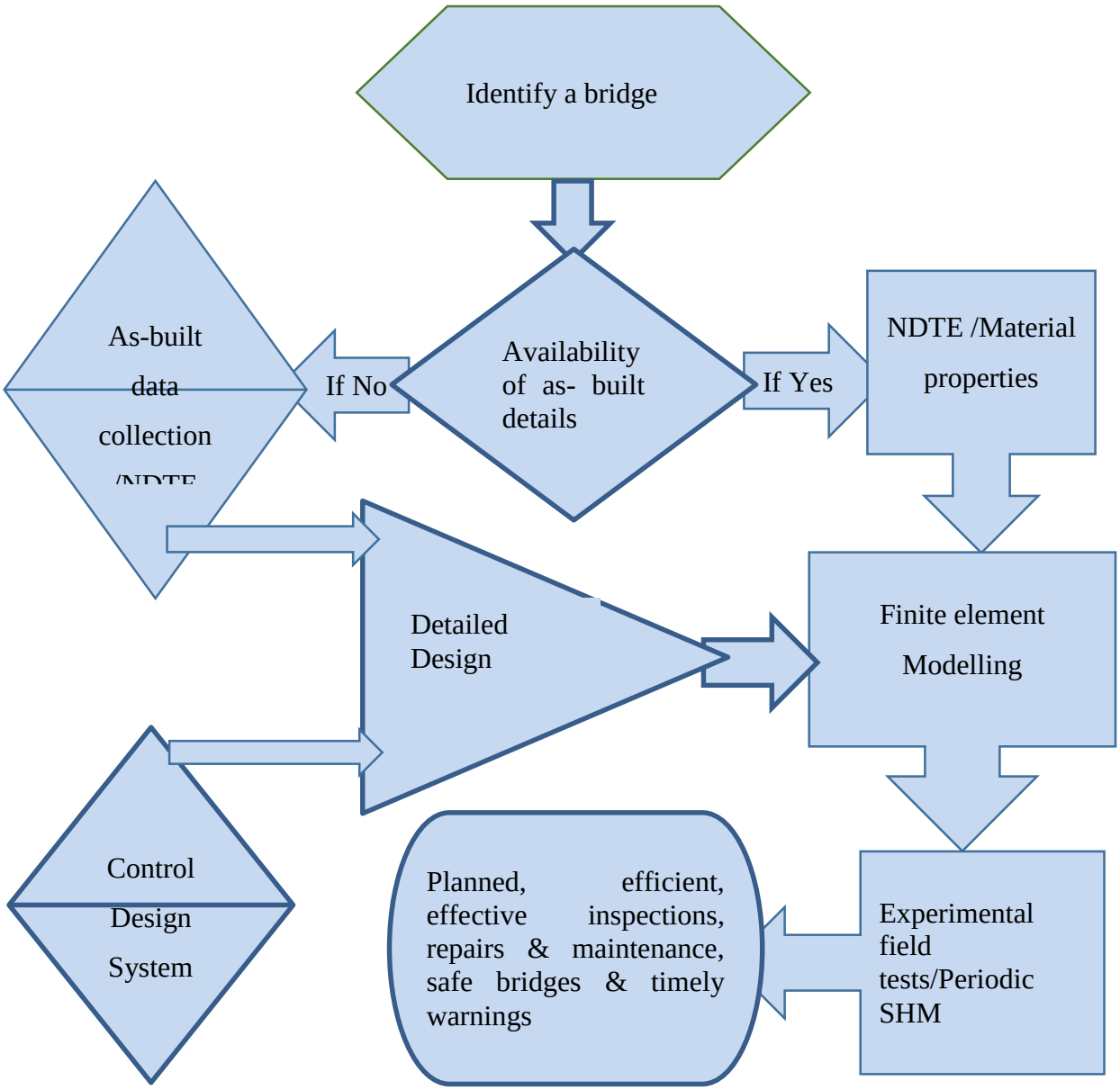

Figure 5.10 proposed rational decision model for SHM of high way bridges in Zambia

were As-built data may not be available, use of NDTE equipment could be used to collect material properties and reinforcement details while comparing this with the control system design which acts as a guide to collected data. A detailed drawing or design is later developed which is then used to

validate a finite element model. After finite element analysis with a moving load or appropriate loadings, highly distressed regions are identified and predictions of cracking regions. Later periodic monitoring is then employed by use of sensors or nondestructive testing equipment with attention paid to predicted regions of distress by the finite element model. It is important to understand that were As-built data is available, material properties/strength of existing bridge members should be obtained by NDT/E in order to validate the finite element model

CHAPTER 6 CONCLUSION AND RECOMMENDATIONS

6.1 Conclusions

From the works presented in the previous chapters of this study, the objectives of this research were all met successfully as stated in the following sections of this chapter with reference to the specific objectives.

6.1.1 Review types of Structural Health Monitoring in use in Zambia.

From the literature reviewed in chapter 1 and 2, there is currently no structural health monitoring nor SHM program being applied in Zambia. Only the new construction works of the Kazungula Bridge have employed force gauges for monitoring of forces. If there is any, all monitoring is limited to visual inspections, which are unreliable and inefficient methods of SHM. It worth to mention that not even localized methods of SHM have been and are being conducted on Zambia infrastructure, and there is currently lack of expertise in the area of structural health monitoring.

6.1.2 Review improved and cost-effective technologies on SHM of bridges that could be applied in Zambia.

Fiber optic sensors where found to be the most effective and cost effective technology for structural health monitoring, with several advantages when compared with other technologies like Laser Doppler Velocity and use of strain gauges . These are explained in section 2.7 of this study, though it requires experienced expertise. The newly demonstrated method of structural Health monitoring in this research would be a far much cheaper technology, despite its requirement to have full understanding of finite element modeling, structural analysis and use of sensor and nondestructive testing equipment.

6.1.3 Apply sensor technologies for SHM on Zambian Highway Bridge with a case study of Nansenga Bridge.

Sensor technology comprising of wireless micro crack detectors, transducers, ground penetration radar, ultrasonic pulse velocity detectors have been successfully applied on Nansenga Bridge for

structural Health monitoring. Periodic monitoring was conducted for 3months, and SHM experimental results obtained represent the true behavior of Reinforced Concrete Bridge under a moving load as confirmed by the finite element model.

6.1.4 Demonstrate the application of SHM technology in order to illustrate the salient features of the subject area and highlight the numerous results that could be achieved.

Use of sensor technology in particular NDT/E combined with finite element modelling produced accurate results for structural health monitoring of highway bridges, in the absence of as built structural details and drawings.The use of non destructive testing and evaluation equipments (GPR,UPV) to collect data provided adequate guidance during the development of a conctrol design. On the other hand, the control design guided and verified data collected by NDT equipments. This eliminated incorrect data input errors in finite element modelling.

With a damping ratio of 5%, the finite element analysis predicted a true behaviour of bridge elements (beams and deck) highlighting numerous results that could be achived when applied with SHM sensor technologies. Distressed and cracked regions were well predicted and matched with experimental field tests. This was confirmed by detection of flexural shear cracking of beams at points of maximum moments on loactions as analysed by the finite element model.

The model predicted higher values of crack widths in tensile regions which agreed with experimental field values.this is because in concrete the maximum design stress limits will ensure cracks close up once loading is removed as the moving HB truck passed the bridge.in a similar manner compresive crack widths predicted by FEM where lower than experimental field SHM crack widths.this is because,as the load is removed cracks in the compression region tend to open wider as the concrete member retains to its initial elastic modulus.This is the true behavoir of reinforced concrete under a moving load, therefore this approves applicability of the SHM technology developed and demonstrated by this research to reinforced concrete bridges in zambia and across boarders.

The width of cracks detected on girders exceeded allowable crack widths in the British and Euro codes which limits maximum crack widths to 0.3mm and 0.25mm, respectively. Crack widths of 1.748mm on top and 1.593mm on bottom of the cantilivered beam were recorded. Crack depths

of 212.63mm and 94.4mm have excessively reduced cross sectional properties, resulting in loss of stiffiness (flexural and shear capacity) which could lead to structural failure, if bridge is not attanded to urgently. This rapid detorioaration is due to increased traffic loads and high impact loads at the bridge deck-abutment interface. Further due to poor planning & maintenance, the bridge surface is potholed leading to higher impact loading. Considering the above findings it's evident that this research has presented a rational decision making tool for bridge infrastructure interventions in Zambia.

6.1.5 Highlight the general results and applicability of SHM

Other than what has been stated in section 6.1.4 other general results and SHM applicability includes, On-site current state geometric and material property measurements, modelling of bridge structure and comparison within as-built parameters established, indication of distressed regions for effective and efficient structural Health monitoring, monitoring of all reinforced concrete bridges both new and old including pre-stressed concrete bridges of any spans. Appreciation of applicable design codes and in-depth understanding of the true behavior of bridge infrastructure under a moving load.

6.1.6 Propose a rational decision making tool for bridge infrastructure interventions in Zambia, based on SHM of technology.

In chapter 5 section 5.5 a rational decision making tool has been developed for bridge infrastructure interventions. In the previous chapter, Figure 5.10 shows a proposed rational decision making tool as a flow chart with stages involved in conducting bridge infrastructure interventions that would result in properly planned, efficient, effective inspections, repairs & maintenance. Safe bridges and timely warnings of failure to mention a few advantages amongst others.

6.2 Contribution of the research

The research has added to the body of knowledge of structural engineering in the area of structural health monitoring of bridges the combination of finite element modelling, control designs and nondestructive testing and evaluation equipment in conducting a precise, successful and less costly

structural health monitoring, especially on old bridges and other structures detailed design and were as-built drawing are unavailable It has further demonstrated the elimination of data input error in finite element modelling by creating control designs using the applicable design code for old structures that do not have as built details.

With this combination demonstrated in the research, it is possible to completely model (physically or numerically) the behavior of full-large scale structures in-situ and accurately perform periodic structural health monitoring unlike adhoc testing and analysis which is more commonly performed on small-scale specimens, which represent only small portions of the actual structures, subjected to idealized loads. The study has further provided a wealth of information on how real structures actually behave when subjected to actual structural and environmental loads. This information is critical to advance the future practice of structural engineering.

6.3 Limitations of the research

Although the objectives were met, a comprehensive structural health monitoring would have included corrosion monitoring to assess the extent of corrosion on rebar. This would have been used to determine average remaining cross section of rebar diameter for finite element modelling, and hence predicting current capacity more effectively.

The cost of the research was relatively high for a self-sponsored student in terms of funds to procure equipment, software and making frequent site visits to the bridge site.

6.4 Recommendations

1) As mentioned in chapter 1, excessive deterioration is due to poor maintenance caused by inefficient and limited methods of bridge inspections. Further, lack of an efficient decision making tool for planning maintenance in conducting bridge inspections. The method of structural health monitoring demonstrated in this research should be adopted and applied by RDA and other Road Authorities on several concrete bridges for conducting inspections and monitoring.
2) Further Research on structural health monitoring should be extended to composite and steel highway bridges. This may be undertaken by institutions or post graduate students under appropriate financial support.

3) Research on structural health monitoring should be sponsored and funded by organizations or interested parties as the cost may be too huge for self-sponsored students to bare. Approximately USD75, 000 (seventy five thousand United States dollars) was spent in conducting this research.

4) Continuous structural health monitoring to include corrosion monitoring should be carried out on cracked regions of the bridge in order to examine effects of corroded rebar in reinforced concrete under a moving load.

5) The bridge should be repaired by converting the cantilevered beams into simply supported beams that should seat on new elastomeric bearings. Carbon fibre reinforcement should be considered for further strengthening of the girders to stop the continuous growth of cracks.

6) The impact loads created by the potholes and rough approach between the bridge deck surface could be reduced if the road surface is repaired.

7) Based on the crack widths and depths, the current state of the bridge is poor and decisions should be made to adequately repair or replace the structure.

REFERENCES

Abdel-Wahab, M. M., and De Roeck, G., (1999). "Damage Detection in Bridges Using Modal Curvatures: Application to a Real Damage Scenario", J. Sound and Vibration, Vol. 226.

Abdo, M. A.-B., (2012) "Damage Detection in Plate-Like Structures using High-Order Mode Shape Derivatives", International J. Civil and Structural Engineering.

Abdo, M. A.-B.,(2002) "Structural Health Monitoring Using Changes in Dynamic Characteristics", Ph. D. Dissertation, The University of Tokyo, Japan.

Aktan, A. E., and Grimmelsman, K. A.(2006) "The Role of NDE in Bridge Health Monitoring", Part of SPIE Conference on Nondestructive Evaluation of Bridges and Highways III.

American Society of Civil Engineers, (2009) Report Card for America's Infrastructure.

Arias Pedro, Julia .A, Daniel .D .C (2007) Digital photogrammetry, GPR and computational analysis of structural damages in a mediaeval bridge Article in Engineering Failure Analysis.

Baran, I. (2009). Airborne InSAR and LiDAR compared.

Bisby, L. A. (2006), An Introduction to Structural Health Monitoring, ISIS Educational Module #5: IIS Canada.

British standard BS 5400-2: (1978) Steel, concrete and composite bridges Part 2: Specification for loads.

Bungey JH, Shaw MR, Millard SG, Molyneaux TCK (2013). Location ofsteel reinforcement in concrete using ground penetrating radar and neural networks. In: Forde MC, editor. Structural faults and repair.London: Engineering Technics Press.

Bungey, J. H. (2004). "Sub-surface radar testing of concrete: a review." Construction and Building Materials.

Caesar, B., (1986) "Update and Identification of Dynamic Mathematical Modes", Proc. 4th International Modal Analysis Conference.

Conyers L B, (2002). Ground Penetrating radar Published online: 15th of Jan 2002. DOI: 10.1002/0471443395.

Daniele Inaudi, (2009) 4th International Conference on Structural Health Monitoring on Intelligent Infrastructure (SHMII-4), Zurich, Switzerland.

Davison, N., G. K. Glass, A. C. Roberts, and J. M. Taylor. (2003). The Protective Effects of Electrochemical.

Day G S, Schoemaker P J H & Gunther R E, 2000. Wharton on Managing Emerging Technologies. Wiley, New Jersey. ISBN: 978-0-471-68939-3.

Djordjevich, A.,(1998) "Curvature Gauge as Torsional and Axial Load Sensor", Sensors and Actuators, Vol. 64.

Doebling, S. W., Farrar, C. R., Prime, M. P., and Shevitz, D. W.(1996) "Damage Identification and Health Monitoring of Structural and Mechanical Systems from Changes in Their Vibration Characteristics: A Literature review", ," Los Alamos National Laboratory report LA-13070-MS.

Doebling, S.W., C.R. Farrar, M.B. Prime, and D.W. Shevitz (1998) "A Review of Damage Identification Methods that Examine Changes in Dynamic Properties," Shock and Vibration Digest 30 (2), pp. 91–105.

Enckell M, (2006). Structural Health Monitoring using Modern Sensor Technology –Longterm Monitoring of the New Årsta Railway Bridge. Licentiate thesis, Royal Institute of Technology, KTH.

Enckell M, Glisic B, Myrvoll F & Bergstrand B., (2011). Evaluation of a large-scale bridge strain, temperature and crack monitoring with distributed fibre optic sensors. Journal of Civil Structural Health Monitoring. DOI: 10.1007/s13349-011-0004-x.

Enckell M, Glisic B, Myrvoll F and Bergstrand B. (2011), Evaluation of a large-scale bridge strain, temperature and crack monitoring with distributed fibre optic sensors. Journal of Civil Structural Health Monitoring. DOI: 10.1007/s13349-011-0004-x.

Enckell M. (2013), New and Emerging Technologies in Structural Health Monitoring Part I. Civil and Environmental Engineering https://doi.org/10.1002/9781118436707.hmse001.

Engstrom B. (2007) Simulation of shear-type cracking and failure with non-linear finite-element method, Department of Civil and Environmental Engineering, Chalmers University of Technology. Sweden.

Engström, B (2007): Design and analysis of continuous beams and columns. Chalmers University of Technology, Göteborg, Sweden.

Eurocode 1 CEN: (2002). Actions on structures – Part 2: Traffic loads on bridges, pr EN 1991-2, Brussels.

Eurocode 2 CEN: (2001). Design of concrete structures –Genaral Rules and Rules for Buildings, pr EN 1992-1, Brussels.

Eurocode 2: (1992) Design of concrete structures - Part 1-2: General rules - European committee for standardization.

Farrar C & and Worden K (2007), An introduction to structural health monitoring. Phil. Trans, R. Soc. A V 365;303–315doi:10.1098/rsta.2006.1928.

Ferenc Nemeth (2015) Crack analysis in FEM design, Technical University, BudaPest.

Friswell, M. I. And Mottershead, J. E., (1995)"Finite Element Model Updating in Structural Dynamics", Kluwer Academic Publishers, Dordrecht, The Netherlands.

G. A. Rombach (2004) Finite Element Design of Concrete Structures.

Geib D (2003) Multiplexing of Extrinsic Fabry-Perot Optical Fibre Sensors for Strain Measurements. M.S. Thesis, Virginia Polytechnic Institute and State University.

Gentile C, (2010). Deflection measurement on vibrating stay cables by non-contact microwave interferometer. NDT&E International 43:231–240.

Grattan K. T. V. and Meggitt, B. T., "Optical Fiber Sensor Technology: Applications and Systems", Vol. 3, Kluwer Academic Publishers, 322 PP., (1999).

Guan, H. and Karbhari, V. M.,(2008) "Vibration-Based Structural Health Monitoring of Highway Bridges", Report No. CA06-0081, University of California, USA, 330 PP.

Housner G.W., Bergman, L.A., Caughey, T.K., Chassiakos, A.G., Claus, R.O., Masri, S.F., Skelton, R.E.,Soong, T.T., Spencer, B.F., and Yao, J.T.P., (1997), "Structural Control: Past, Present and Future," ASCE Journal of Engineering Mechanics, (Special Issue), Vol 123.

http://www.infrastructurereportcard.org/sites/default/files/RC2009_full_report.pdf

Inaudi, D. (2009a), "Structural Health Monitoring of bridges: general issues and applications", in "Structural Health Monitoring of Civil Infrastructure Systems" edited by Vistasp M. Karbhari

Inaudi D, (19970. Fibre optic sensors network for the monitoring of civil engineering structures. Dissertation, Ecole Polytechnique Federale de Lausanne (EPFL).

Inaudi, D. and Glisic, B., (2008), Overview of 40 bridge monitoring using fiber optic sensors, IABMAS'08, Fourth International Conference on Bridge Maintenance, Safety and Management, Seoul, Korea.

Inaudi, D., (2009b), Overview of 40 Bridge Structural Health Monitoring Projects, International Bridge Conference, IBC 2010:June 15-17,Pittsburgh,USA.

Inaudi, D., (2010), Long-term static Structural Health Monitoring, ASCE Structures Congress, Orlando Florida.

Jaffrey D, 1982. Acoustic Emission Monitoring. Met. Forum. V 5: 154-157. Winter.

Karbhari, V.M., Guan, H. and Sikorsky, C. (2003). "Web-based structural health monitoring of a FRP composite bridge." Structural Health Monitoring and Intelligent Infrastructure.

Kijewski-Correa, T., Young, B., Baker, W. F., Sinn, R., Abdelrazaq, A.,Isyumov, N., and Kareem, (2005). "Full-scale validation of finite element models for tall buildings Chicago.

Kosmatka, J. B., and Ricles, J. M., “Damage Detection in Structures by Modal Vibration Blaauwendraad, J (2010): Plates and FEM: Surprises and Pitfalls. Springer Dordrecht Heidelberg. Davidson, M (2003): Struktur analyser av bro konstruktiner med FEM-fördelning av krafter och moment, Brosamverkan Väst. Göteborg.

Kovacevic, M., Djordjevich A., and Nikezic, D., (2008) “Analytical Optimization of Optical Fibre Curvature Gauges,” IEEE Sensors Journal, Vol. 8.

Lanticq, V., Gabet, G., Taillade, F., Delepine-Lesoille, S. (2009) Distributed Optical fiber sensors for structural health monitoring: upcoming challenges.“Optical Fiber, New Developments”

Lau J M,Glisic B, Inaudi D, & Fong C C, (2010). Real strain evolution in concrete columns,monitoring results and CEB-FIP Model Code 1990, 3rd fib International Congress - 2010, Washington D.C., USA.

Lee J. and Fenves G. L. (1998), A plastic- damage concrete model for earthquake analysis of dams, Earthquake engineering & structural dynamics.

Lee, J.-W., Choi, K.-H., and Huh, Y.-C., (2010) “Damage Detection Method for Large Structures Using Static and Dynamic Strain Data from Distributed Fiber Optic Sensor”, International J. Steel Structures.

Liu, W.Q., Chen, S.E. and Hauser, E. (2010). “LiDAR-Based Bridge Structure Defect Detection,” Experimental Techniques, DOI: 10.1111/j.1747-1567.2010.00644.x.

Ljung, L.,(1999) “System Identification: Theory for the User”, Prentice Hall Inc., Upper Saddle River, N. J., USA.

Lynch, J.P.(2006). "An overview of wireless structural health monitoring for civil structures." Philosophical Transactions ofthe Royal Society A: Mathematical,Physical and Engineering Sciences 365, (1851):345-372.

M.Enckell, (2007).Structural Health Monitoring of Bridges in Sweden, the 3rd International Conference on Structural Health Monitoring of Intelligent Infrastructure - SHMII-3, Sweden.

Marchesiello, S., and Gorman, D.J. (1999) “Bridge Dynamics Misinterpretations due to Low Spatial Resolution and Closeness of Frequencies,” Damage Assessment of Structures, Proceedings of the International Conference on Damage Assessment of Structures (DAMAS 99), Dublin, Ireland.

Mayer L, Yanev B, Olson L D, and Smyth A, (2010). Monitoring of the Manhattan Bridge for Vertical and Torsional Performance with GPS and Interferometric Radar Systems. Transportation Research Board Annual Meeting 2010. Paper #10-3183.

Measures M R, (2001). Structural monitoring with fibre optic technology. Academic Press, San Diego.

Meng, X., Dodson, A., and Roberts, G. (2007).“Detecting bridge dynamics with GPS and triaxial acclerometers.”Eng. Struct., 29(11), 3178–3184

Michigan Tech (2011), http://www.me.mtu.edu/~bettig/MEEM4405/Lecture12.pdf, MEEM4405 Introduction to Finite Element Analysis.

Mohamed abdel, Bessel Abdo (2014) structural health monitoring , A review book , History Application and future .Open Science Publishers S#45956, New York, NY 10003, U.S.A.

Mufti A. A., Tadros G. and Jones P. R. (1997), Field assessment of fibre-optic Bragg grating strain sensors in the Confederation Bridge, Canadian Journal of Civil Engineering.

Mufti, A., (2001), “Guidelines for Structural Health Monitoring,” ISIS Canada Design Manual No. www.isiscanada.com

Nakamura, M., Masri, S. F., Chassiakos, A. G., and Caughey, T. K., (1998) “A Method for Non-Parametric Damage Detection through the Use of Neural Networks”, Earthquake Engineering and Structural Dynamics.

O Brein, EJ, Gonzalez, A Znidaric, A and McNulty p.2002. ‘Testing of a Bridge weigh in Motion systems cold environmental conditions’ Orlando Florida.

Ottosen, N & Petersson, H. (1992): Introduction to the Finite Element Method. Prentice Hall, London, United Kingdom.

Park H., Lee H., Adeli H. and Lee I. (2007), A new approach for health monitoring of structures: terrestrial laser scanning, Computer Aided Civil and Infrastructure Engineering.

Patjawit and Nukulchai (2005), Synthesis of Current Knowledge of *Structural Health* Monitoring, R. Soc. A V 365;303–315doi:10.1098/rsta.

Pieraccini, M. (2013) Monitoring of civil infrastructures by interferometric radar: A review. Sci. World J.

Pieraccini, M.; Luzi, G.; Mecatti, D.; Fratini, M.; Noferini, L.; Carissimi, L.; Franchioni, G.; Atzeni, C.(20040 Remote sensing of building structural displacements using a microwave interferometer with imaging capability. NDT E Int.

Pines, D. and Aktan, A.E. (2002). “Status of structural health monitoring of long-span bridges in the United States.” Progress in Structural Engineering and Materials, 4(4), 372-380.

Quilligan M, (2003) weigh in motion systems, development of a 2D multi vehicle algorithm, Department of civil and architectural engineering, Royal Institute of Technology. Sweden.

Rice. C. High resolution Aerial photography .MS Thesis, Civil and Environmental engineering UNC Charlotte.

Rombach, G A. (2004): Finite element design of concrete structures. Thomas Telford Ltd, London, England.

Road Development Agency (2007) standard bidding document works, Republic of Zambia

Ross R M & Matthews S L, 1995. In-service structural monitoring—a state of the art review. Struct. Eng. V 73:23–31

Ruotolo, R. and Surace, C., (1997)"Damage Assessment of Multiple Cracked Beams: Numerical Results and Experimental Validation", J. Sound and Vibration, Vol. 206(4), pp. 567-588,)

Samuelsson, A & Wiberg, N. (1998): Finite Element Method- Basics. Studentlitterature, Lund, Sweden. Stockholm

Sikorsky, C., (1999). .Development of a Health Monitoring System for Civil Structures Using a Level IV Non-Destructive Damage Evaluation Method, Proceedings of the 2nd International Workshop on Structural Health Monitoring 2000, Stanford University, CA, USA.

Siringoringo D.M., and Fujino, Y, (2008) Structural Health Monitoring of bridges in Japan. University of Tokyo,Japan.

Sohn, H., Farrar, C. R., Hemez, F. M., and Czarnecki, J. J.. (2002)A Review of Structural Health Review of Structural Health Monitoring Literature.United States.

Sushil. D (2013), Structural Health Monitoring for in service High way bridges using smart sensors, University of Connectcut. USA.

Tomonori Nagayama (2007) structural health monitoring using smart sensors, University of Illinois at Urbana-Champaign.

Treatment in Reinforced Concrete, Corrosion (2003), NACE, Paper No. 03291, San Diego.

Uomoto, T. (2000) "Maintenance of Concrete Structures and Application of Non-Destructive Inspection in Japan", Proc. 5th International Symposium on Non-Destructive Testing in Civil Engineering.

V.M. Karbhari (2007). Structural Health Monitoring, a means to optimal design in the future, university of Alabama .Huntsvile. USA.

Vägverket (2009): TK Bro, Banverket: BVS 1583.10 Publikation Vägverket: 2009:27, ISSN: 1401-9612 Characterization", J. Structural Engineering, ASCE.

Whalen, T. M., (2008)"The Behaviour of Higher Order Mode Shape Derivatives in Damaged Beam-Like Structures", J. Sound and Vibration, Vol. 309 (3-5), pp. 426-464,

Wiberg J, (2009). Railway bridge response to passing trains. Measurements and FE model updating. Dissertation, Royal Institute of Technology (KTH).

Xu, M. G., Archambault, J. L., Reekie, L., and Dakin, J. P.,(1994) “Structural Bending Sensor Using Fiber Gratings”, Proc. of SPIE, Vol. 2292, pp. 407-413.

Yong tao and Ruiqiang (2010) Bridges structural Health Monitoring and deterioration detection. School of Engineering, Alaska University.

Yu, F. T. S. and Yin, S., (2002). “Fiber Optic Sensors”, Marcel Dekker, Inc, USA.

Zhou, H.F., Y.Q. Ni, and J.M. Ko. 2010b. “Structural Damage Alarming Using Auto-Associative Neural Network Technique: Exploration of Environment-Tolerant Capacity and Setup of Alarming Threshold,” submitted to Mechanical Systems and Signal Processing.

Zimmerman, D. C. and Kaouk, M.(2004) “Structural Damage Detection Using a Minimum Rank Update Theory”, J. Vibration and Acoustics.

Bibliography

Bohse, J. Acoustic (2013) Emission. In Handbook of Technical Diagnosis; Czichos, H., Ed.; Springer: Berlin, Germany; Chapter 8, pp. 137–160.

Boller, C.; Chang, F.-K.; Fujino, J. (2009) (Eds.) Encyclopedia of Structural Health Monitoring; J. Wiley: New York,USA, Volume 1–3, p. 2960.

Cong Zhou (2016) Efficient Hysteresis Loop Analysis Based Structural Health Monitoring of Civil Structures University of Canterbury, New Zealand

Gorman, M.R. Modal (2011) AE analysis of fracture and failure in composite materials, and the quality and life of high pressure composite pressure vessels.J. Acoust. Emiss.

Messervey T B, Zangani D & Withiam J L, (2010). Smarttextiles and their application in bridge engineering. The Fifth International Conference on Bridge Maintenance, Safety and Management, Philadelphia, PA, USA

Mikhail E M, Bethel J & McGlone J C, (2001). Introduction to Modern Photogrammetry. Wiley. ISBN: 978-0-471-30924-6

Miranda P, (2006).Evaluation of the structural behavior during retro fitting of the Traneberg Bridge by monitoring. M.S. Thesis, Royal Institute of Technology (KTH).

Ono, K.; Dobmann, G. (2014) Nondestructive Testing. In Ullmann's Encyclopedia of Industrial Chemistry; J. Wiley:New York, USA, Volume 24, pp. 471–584.

Rainieri ,C,G. Fabbrocino and E. Cosenza (2008) Structural health monitoring systems as a tool for seismic protection The 14th World Conference on Earthquake Engineering October 12-17, 2008, Beijing, China.

Vijaya Gopu, Ayman Okeil, Rogers seals (2018) Introduction of Structural Health monitoring to civil engineering education, Louisiana Transportation Research Center and University of Louisiana

Wiberg J & Enckell M, (2008). Monitoring of the New Årsta Railway Bridge. Presentation of measured data and report on the monitoring system over the period 2003-2007. Tec. Rep. Royal Institute of Technology, KTH.

Wiberg J, (2006). Bridge Monitoring to Allow for Reliable Dynamic FE Modelling: A Case Study of the New Årsta Railway Bridge. Licentiate thesis, Royal Institute of Technology, KTH.

Wiberg J, (2009). Railway bridge response to passing trains. Measurements and FE model updating. Dissertation, Royal Institute of Technology (KTH).

Wu, X. and Yao, K. (2011), "The effect analysis about creep and shrinkage for long-term deflection of long-span continuous rigid frame bridge". Electric Technology and Civil Engineering (ICETCE), International Conference. pp 2730 - 2733. Doi.10.1109/ICETCE.2011.5774695

Zhang H & Wu Z, (2008). Performance evaluation of BOTDR-based Distributed Fiber Optic Sensors for crack monitoring. Structural Health Monitoring. Vol. 7:143-156.

Zilberstein, V., K. Walrath, D. Grundy, D. Schlicker, N. Goldfine, E. Abramovici, T. Yentzer.(2003). "MWM eddy-current arrays for crack initiation and growth monitoring." International Journal of Fatigue25(9-11): 1147-115

APPENDICES

APPENDIX A

CONTROL DESIGN DEVELOPMENT NANSENGA BRIDGE

APPENDIX A .DESIGN CONTROL DEVELOPMENT

A.1 Determination of Extreme loading

Code of Practice: BS5400 - 1978

3.3.2.1.1.1.1.1.1 Table 4.5 Results of Extreme loading position analysis for HB axle spacing (11m, 16m, and 21m)

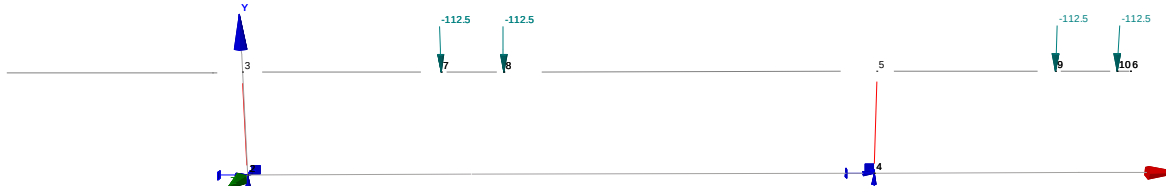

HB vehicle with 16m inner axle spacing figure 4.8a

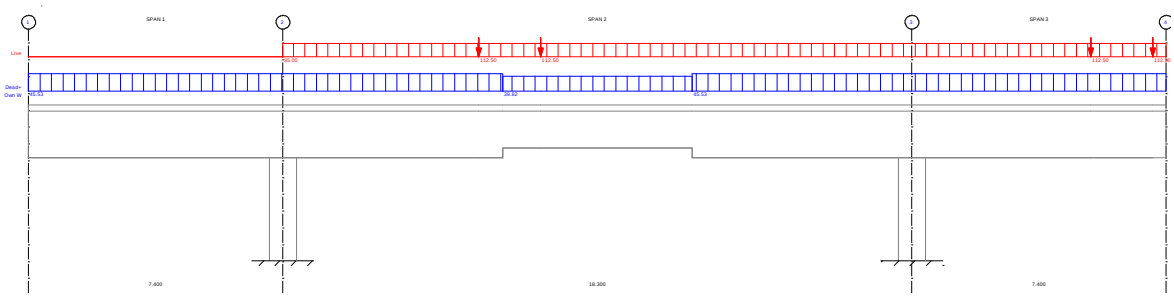

2 Figure 4.8b HB loading @ axle spacing of 16m with temperature loads

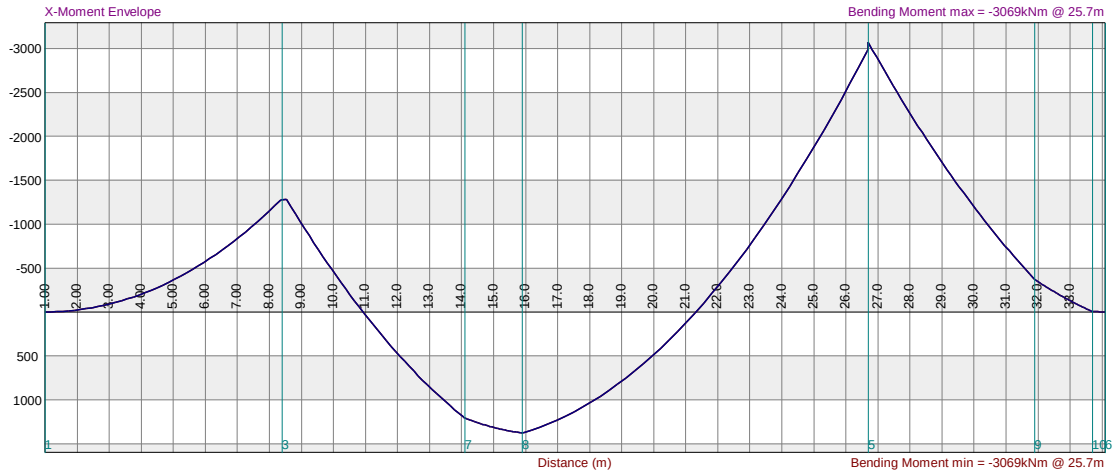

3 Figure 4.9a Ve Maximum Bending moment 3069KN.m @HB AXLE SPACING 16m LC1

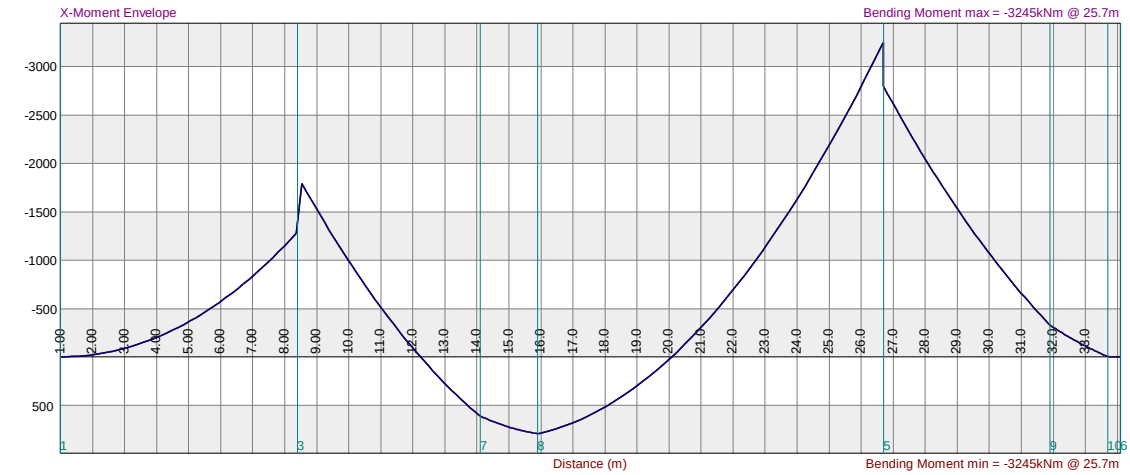

4 Figure 4.9b.Ve Maximum Bending moment **3245kN.m @HB AXLE SPACING 16m** LC3

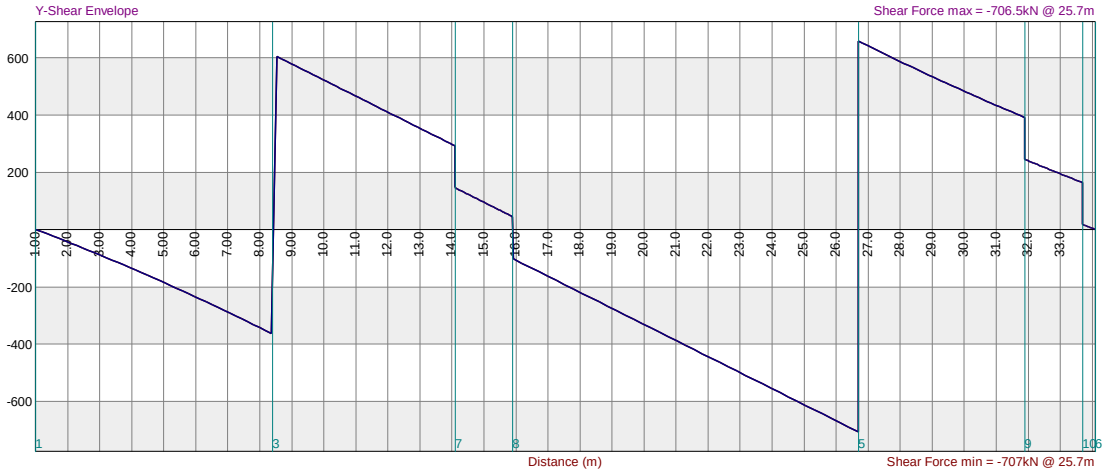

Figure 4.9c:Shear Force **Max706.5KN @HB AXLE SPACING 16m** Load combination C3

figure 4.10a:Analysis for HB vehicle with 21m axles spacing

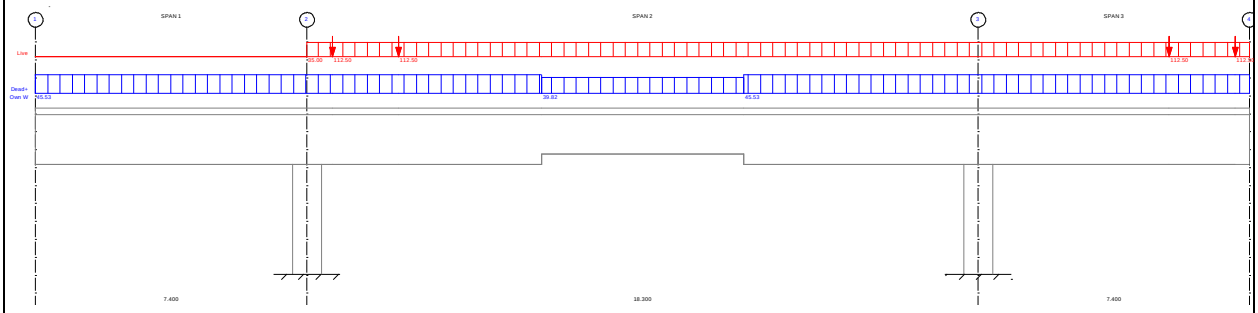

figure 4.10b HB loading @ axle spacing of 21m with tempreture loads

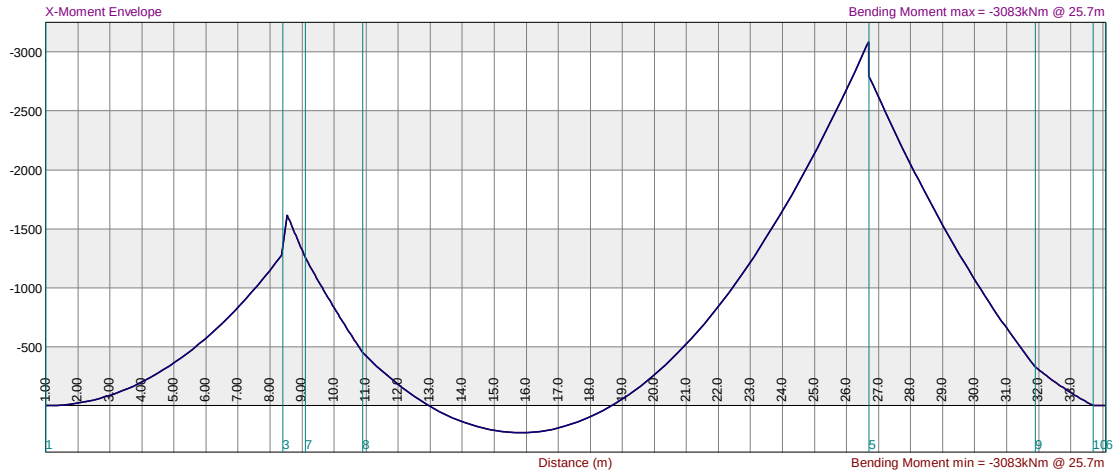

Figure 4.11 Ve Maximum Bending moment **3083kN.m** @HB AXLE SPACING 21m L C3

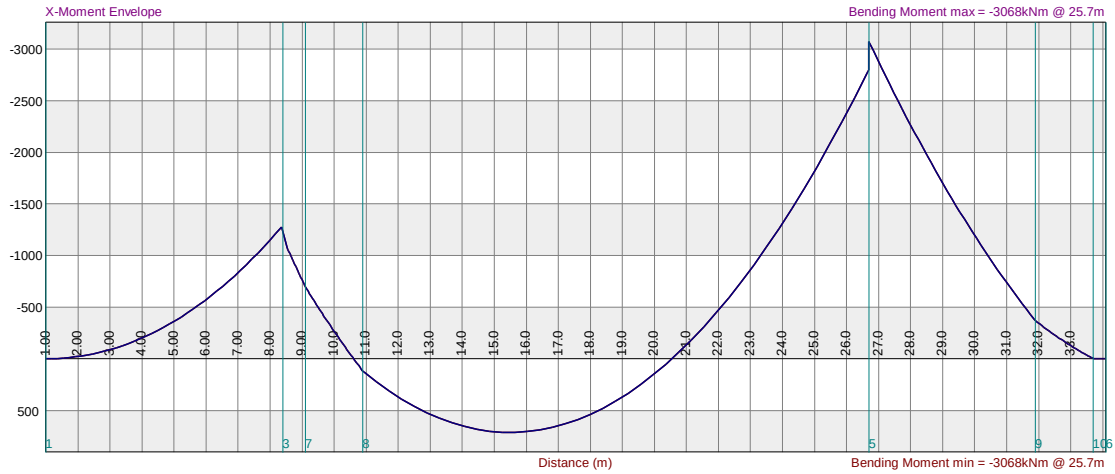

3 figure 4.11b:Ve Maximum Bending moment **3068kN.m** @HB AXLE SPACING 21m L C1

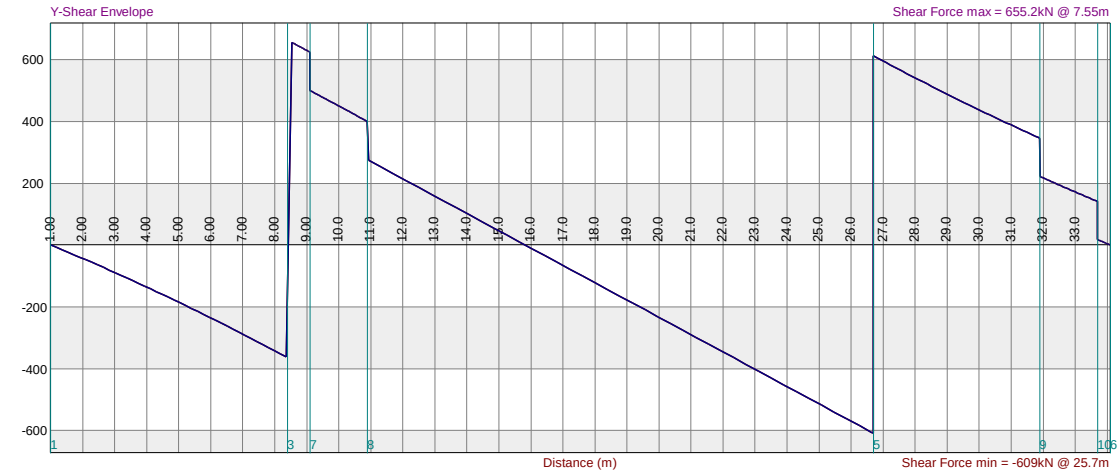

9 figure 4.11c Shear Force Max655.2kN @HB AXLE SPACING 21m L C3

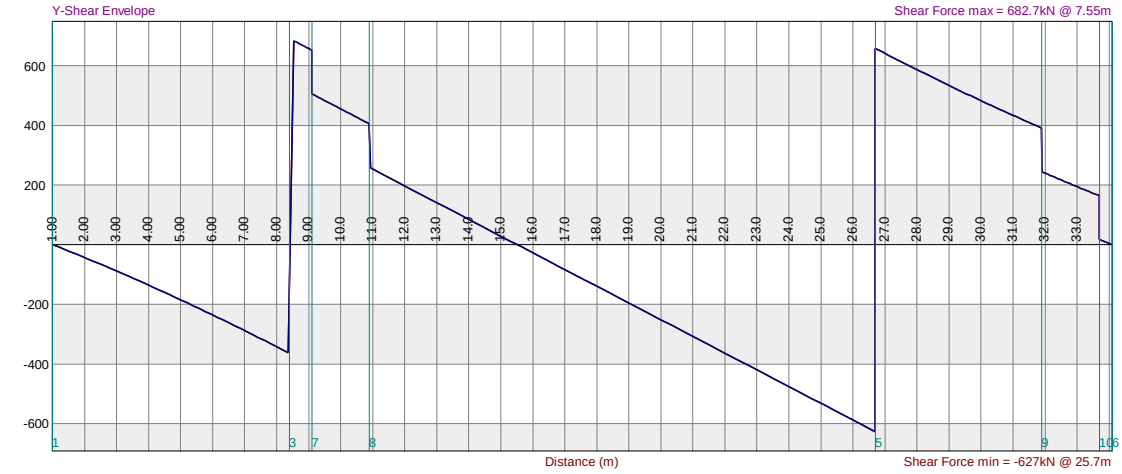

10 .....

figure 4.11d:Shear Force **Max682.7kN @HB AXLE SPACING 21m** L C1

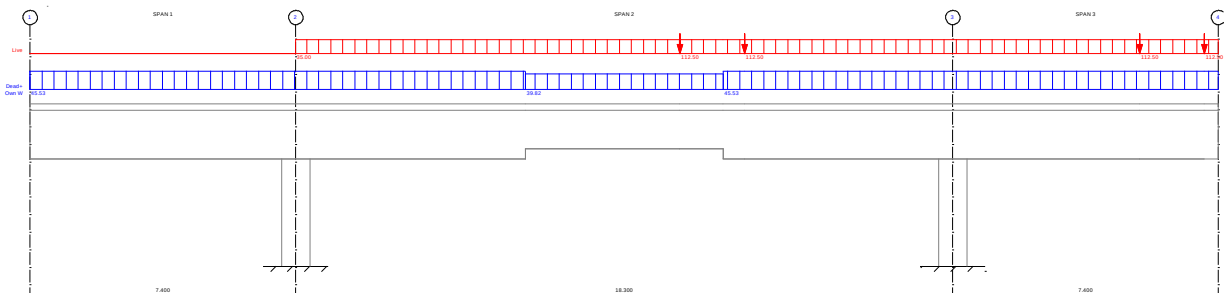

1 .....

igure 4.12a HB loading @ axle spacing of 11m with temperature loads

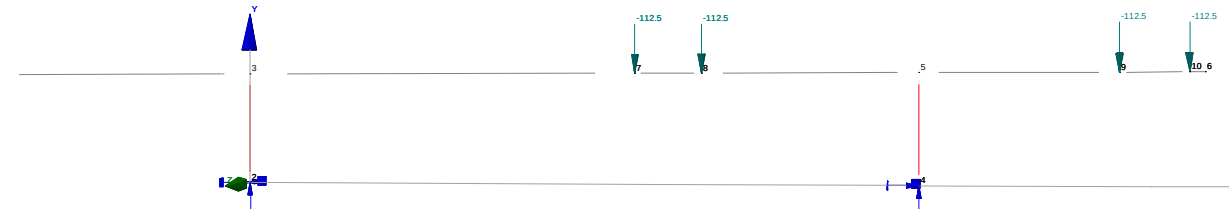

2 .....

igure 4.12b:Analysis for HB vehicle with 11m axles spacing moving 4

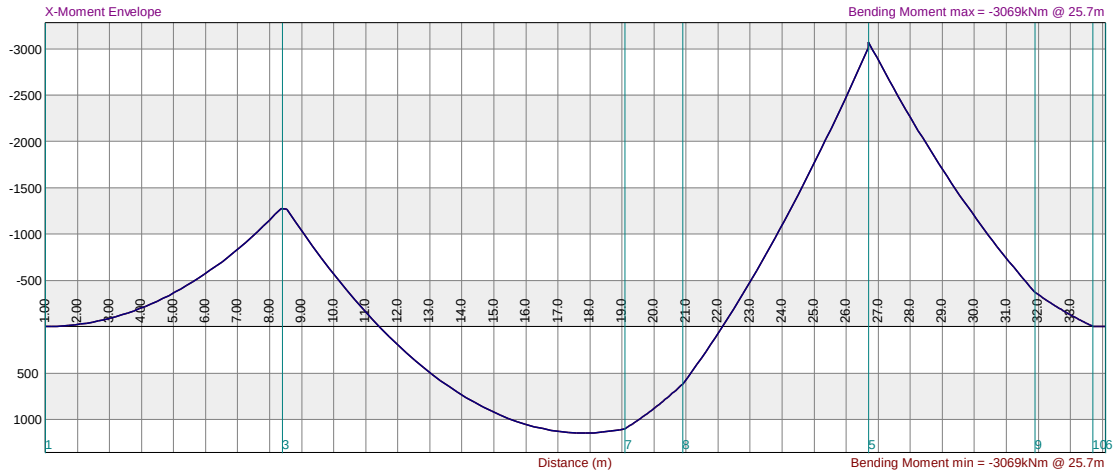

3 .....

igure 4.13a -Ve Maximum Bending moment **3069kN.m @HB AXLE SPACING 11m** L C1

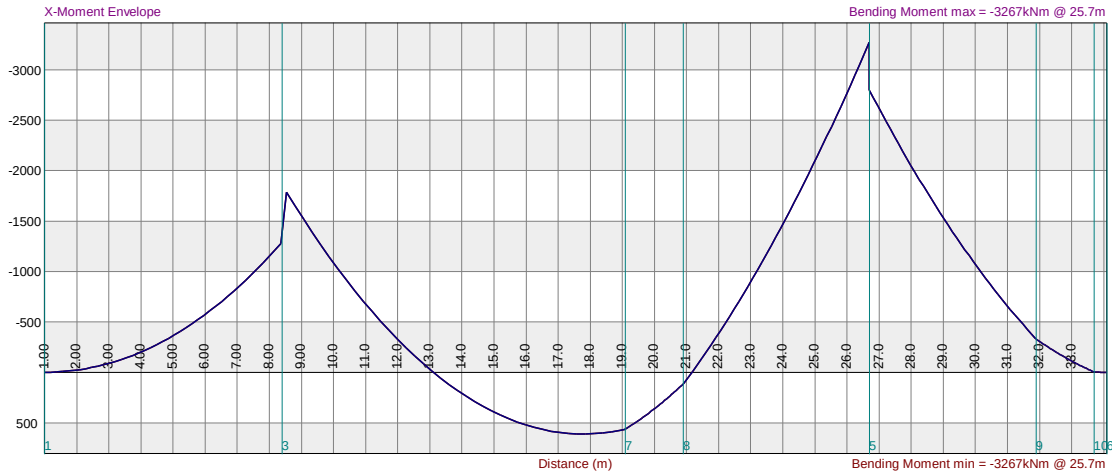

4 .....

igure 4.13b:-Ve Maximum Bending moment **3267KN.m @HB AXLE SPACING 11m** L C3

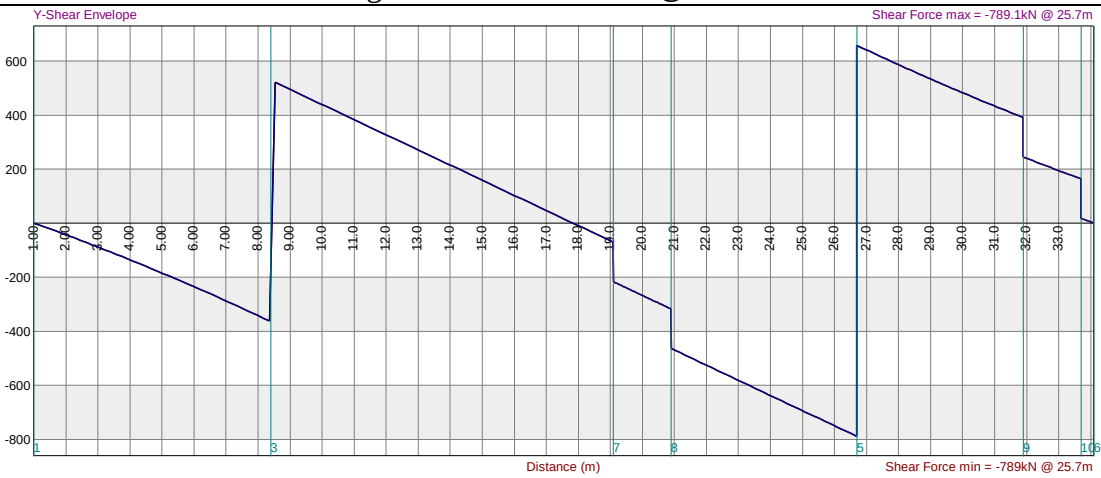

5 .....

igure 4.13:Shear Force Max=**789kN @HB AXLE SPACING 11m** L C1

==========NODAL POINT COORDINATES

Node No	X-coord m	Y-coord m	Z-coord m	Node No	X-coord m	Y-coord m	Z-coord m
1	-7.400	3.000	0.000	2	0.000	0.000	0.000
3	0.000	3.000	0.000	4	18.300	0.000	0.000
5	18.300	3.000	0.000	6	25.700	3.000	0.000
7	5.700	3.000	0.000	8	7.500	3.000	0.000

9 23.500 3.000 0.000 10 25.300 3.000 0.000

========== ELEMENT DATA ==========

Beam	Secn. type	Fixity	Length m	ß (°)	Group no.
1-3	1	00	7.400	0.00	0
3-7	1	00	5.700	0.00	0
7-8	1	00	1.800	0.00	0
5-8	1	00	10.800	0.00	0
5-9	1	00	5.200	0.00	0
9-10	1	00	1.800	0.00	0
6-10	1	00	0.400	0.00	0
2-3	2	00	3.000	0.00	0
4-5	2	00	3.000	0.00	0

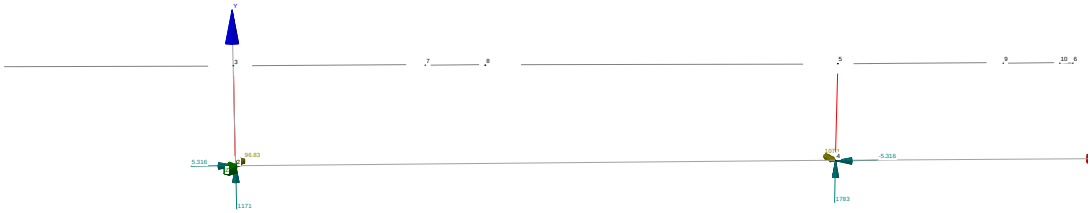

========== SECTION PROPERTIES ========

Section : 1 Section designation: nansec T UC

A	Ay	Ax	Ixx	Iyy	J	Material
m^2	m^2	m^2	m^4	m^4	m^4	
1.481	0.000	0.000	326E-3	164E-3	208E-3	Concrete:35MPa

Section : 2 Section designation: 750x750 RC

A	Ay	Ax	Ixx	Iyy	J	Material
m^2	m^2	m^2	m^4	m^4	m^4	
561.0E-3	0.000	0.000	26.2E-3	26.2E-3	44.6E-3	Concrete:35MPa

==========MATERIALS =======

Designation	E	poisson	Density	Exp. coeff.
	kPa		kN/m^3	
Concrete:35MPa	25.00E6	0.20	25.00	10.00E-6

==========SUPPORT DATA ==========

Prescribed displacements

Node	Fixity	X	Y	Z	X-Rot	Y-Rot	Z-Rot	Orien node
		m	m	m	rad.	rad.	rad.	
2	XYZxyz	0.00	0.00	0.00	0.00	0.00	0.00	0
4	XYZxyz	0.00	0.00	0.00	0.00	0.00	0.00	0

Spring constants

Node	Fixity	X	Y	Z	X-Rot	Y-Rot	Z-Rot
		kN/m	kN/m	kN/m	kNm/rad	kNm/rad	kNm/rad

A.2 LOADS

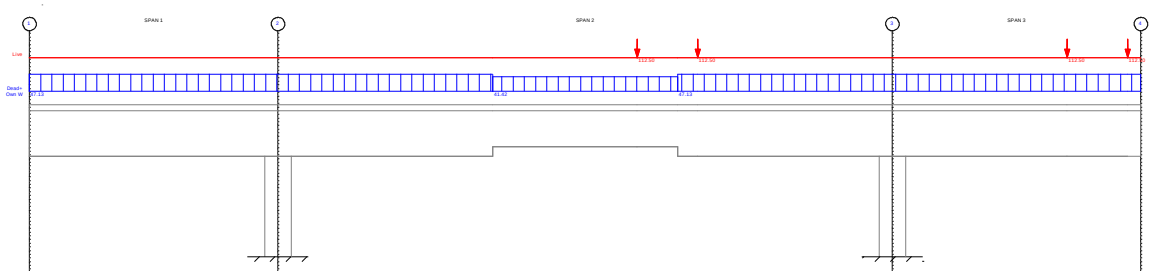

Load Case Description

HB
DEADL
SIDL
HA
TEMP

Add own weight to load case: DEADL

A2.1LOAD CASE HB

*** POINT LOADS ***

Node	Fx	Fy	Fz	Mx	My	Mz
	kN	kN	kN	kNm	kNm	kNm
7	0.00	-112.50	0.00	0.00	0.00	0.00
8	0.00	-112.50	0.00	0.00	0.00	0.00
9	0.00	-112.50	0.00	0.00	0.00	0.00
10	0.00	-112.50	0.00	0.00	0.00	0.00

A2.2 LOAD CASE DEADL

*** BEAM ELEMENT LOADS ***

Element	Direction	P	a	Wl	Wr	dT
		kN	m	kN/m	kN/m	°C
1-3	Y	0.00	0.00	-9.10	-9.10	0.00
3-7	Y	0.00	0.00	-9.10	-9.10	0.00
7-8	Y	0.00	0.00	-9.10	-9.10	0.00

5-8	Y	0.00	0.00	-9.10	-9.10	0.00
5-9	Y	0.00	0.00	-9.10	-9.10	0.00
9-10	Y	0.00	0.00	-9.10	-9.10	0.00
6-10	Y	0.00	0.00	-9.10	-9.10	0.00

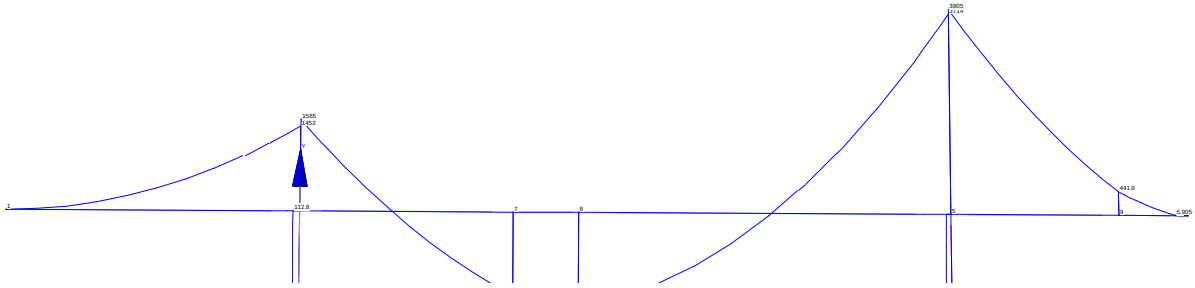

A2.3 LOAD CASE SIDL

*** BEAM ELEMENT LOADS ***

Element	Direction	P	a	Wl	Wr	dT
		kN	m	kN/m	kN/m	°C
7-8	Y	0.00	0.00	-1.71	-1.71	0.00
5-8	Y	0.00	0.00	-1.71	-1.71	0.00
5-9	Y	0.00	0.00	-1.71	-1.71	0.00
9-10	Y	0.00	0.00	-1.71	-1.71	0.00
6-10	Y	0.00	0.00	-1.71	-1.71	0.00

A2.4VLOAD CASE HA ==========

A2.5 BEAM ELEMENT LOADS ***

Element	Direction	P	a	Wl	Wr	dT
		kN	m	kN/m	kN/m	°C
3-7	Y	0.00	0.00	-13.67	-13.67	0.00
7-8	Y	0.00	0.00	-13.67	-13.67	0.00

5-8	Y	0.00	0.00	-13.67	-13.67	0.00
5-9	Y	0.00	0.00	-13.67	-13.67	0.00
9-10	Y	0.00	0.00	-13.67	-13.67	0.00
6-10	Y	0.00	0.00	-13.67	-13.67	0.00

A2.6 LOAD CASE TEMP

***** BEAM ELEMENT LOADS *****

Element	Direction	P	a	Wl	Wr	dT
		kN	m	kN/m	kN/m	°C
3-7	Y	0.00	0.00	0.00	0.00	27.00
7-8	Y	0.00	0.00	0.00	0.00	27.00
5-8	Y	0.00	0.00	0.00	0.00	27.00
5-9	Y	0.00	0.00	0.00	0.00	27.00
9-10	Y	0.00	0.00	0.00	0.00	27.00
6-10	Y	0.00	0.00	0.00	0.00	27.00

A2.7 LOAD COMBINATIONS

Load Comb Description

C1

C3

Comb. Load factor for each load case: Ultimate Limit State

	HB	**DEADL**	**SIDL**	**HA**	**TEMP**
C1	1.30	1.15	1.75	1.30	0.00
C3	1.10	1.15	1.75	1.10	1.00

Comb. Load factor for each load case: Serviceability Limit State

	HB	**DEADL**	**SIDL**	**HA**	**TEMP**

C1	1.00	1.00	1.00	1.00	0.00
C3	1.00	1.00	1.00	1.00	0.80

A2.8 OWN WEIGHT ACCELERATIONS ==

Direction	Acceleration (g)
X	0.00
Y	-1.00
Z	0.00

A2.9 OUTPUT: LINEAR ANALYSIS

=====NODAL POINT DISPLACEMENTS at SLS

Node	Lcase	X-disp. mm	Y-disp. mm	Z-disp. mm	X-rot. rad.	Y-rot. rad.	Z-rot. rad.
1	C1	0.54	0.38	0.00	0.0000	0.0000	0.0000
	C3	-1.35	-3.08	0.00	0.0000	0.0000	0.0005
2	C1	0.00	0.00	0.00	0.0000	0.0000	0.0000
	C3	0.00	0.00	0.00	0.0000	0.0000	0.0000
3	C1	0.54	-0.21	0.00	0.0000	0.0000	-0.0004
	C3	-1.35	-0.21	0.00	0.0000	0.0000	0.0001
4	C1	0.00	0.00	0.00	0.0000	0.0000	0.0000
	C3	0.00	0.00	0.00	0.0000	0.0000	0.0000
5	C1	0.53	-0.31	0.00	0.0000	0.0000	-0.0003
	C3	2.43	-0.31	0.00	0.0000	0.0000	-0.0008
6	C1	0.53	-8.48	0.00	0.0000	0.0000	-0.0014
	C3	4.02	-11.94	0.00	0.0000	0.0000	-0.0018
7	C1	0.54	-3.00	0.00	0.0000	0.0000	-0.0003
	C3	-0.18	-1.16	0.00	0.0000	0.0000	-0.0001
8	C1	0.54	-3.33	0.00	0.0000	0.0000	-0.0000
	C3	0.19	-1.26	0.00	0.0000	0.0000	0.0000

9	C1	0.53	-5.46	0.00	0.0000	0.0000	-0.0013
	C3	3.55	-7.89	0.00	0.0000	0.0000	-0.0018
10	C1	0.53	-7.93	0.00	0.0000	0.0000	-0.0014
	C3	3.94	-11.20	0.00	0.0000	0.0000	-0.0018

A.2.10 REACTIONS at ULS ==========

(In rotated axes where applicable)

Node	Lcase	X-force kN	Y-force kN	Z-force kN	X-moment kNm	Y-moment kNm	Z-moment kNm
2	C1	5.32	1171.43	0.00	0.00	0.00	96.83
	C3	439.03	1135.06	0.00	0.00	0.00	-696.20
4	C1	-5.32	1782.65	0.00	0.00	0.00	107.08
	C3	-439.03	1658.76	0.00	0.00	0.00	869.46

A2.11 EQUILIBRIUM CHECK AT ULS:

LC APPLIED LOADS & MOMENTS about (0.0, 0.0,0.0) in global axes

Sum of:	Px	Py	Pz	Mx	My	Mz
C1	0.00	-2954.09	0.00	0.00	0.00	-32826.49
C3	0.00	-2793.82	0.00	0.00	0.00	-30528.60

A2.12 LC REACTIONS & REACTION MOMENTS about (0.0,0.0,0.0) in global axes

Sum of:	Rx	Ry	Rz	MRx	MRy	MRz
C1	0.00	2954.09	0.00	0.00	0.00	32826.49
C3	0.00	2793.82	0.00	0.00	0.00	30528.60

REACTIONS AT SLS (Combinations only

(In rotated axes where applicable)

Node	Lcase	X-force kN	Y-force kN	Z-force kN	X-moment kNm	Y-moment kNm	Z-moment kNm
2	C1	3.66	992.30	0.00	0.00	0.00	74.44
	C3	349.79	992.30	0.00	0.00	0.00	-546.92
4	C1	-3.66	1454.10	0.00	0.00	0.00	81.50
	C3	-349.79	1454.10	0.00	0.00	0.00	702.85

A2.13 BEAM ELEMENT END FORCES IN LOCAL ELEMENT AXES at ULS =

Elem	Lcase	Axial kN	Y-Shear kN	X-Shear kN	Torsion kNm	M-yy kNm	M-xx kNm
1-3	C1	0.00	0.00	0.00	0.00	0.00	-0.00
		-0.00	392.52	0.00	0.00	0.00	-1452.34
	C3	-0.00	-0.00	0.00	0.00	0.00	0.00
		0.00	392.52	0.00	0.00	0.00	-1452.34
3-7	C1	5.32	730.52	0.00	0.00	0.00	1565.12
		-5.32	-326.88	0.00	0.00	0.00	1448.46
	C3	439.03	694.15	0.00	0.00	0.00	2073.21
		-439.03	-306.09	0.00	0.00	0.00	777.46
7-8	C1	5.32	180.63	0.00	0.00	0.00	-1448.46
		-5.32	-47.77	0.00	0.00	0.00	1654.02
	C3	439.03	182.34	0.00	0.00	0.00	-777.46
		-439.03	-54.41	0.00	0.00	0.00	990.54
5-8	C1	5.32	895.59	0.00	0.00	0.00	3713.96
		-5.32	-98.48	0.00	0.00	0.00	1654.02
	C3	439.03	836.93	0.00	0.00	0.00	3903.36
		-439.03	-69.34	0.00	0.00	0.00	990.54
5-	C1	0.00	838.67	0.00	0.00	0.00	3805.09

9		-0.00	-454.88	0.00	0.00	0.00	-441.86
	C3	0.00	773.44	0.00	0.00	0.00	3455.74
		-0.00	-403.86	0.00	0.00	0.00	-394.75
9-	C1	0.00	308.63	0.00	0.00	0.00	441.86
10		-0.00	-175.77	0.00	0.00	0.00	-5.90
	C3	0.00	280.11	0.00	0.00	0.00	394.75
		-0.00	-152.18	0.00	0.00	0.00	-5.69
6-	C1	0.00	0.00	0.00	0.00	0.00	0.00
10		-0.00	29.52	0.00	0.00	0.00	-5.90
	C3	0.00	0.00	0.00	0.00	0.00	-0.00
		-0.00	28.43	0.00	0.00	0.00	-5.69
2-	C1	1171.43	-5.32	0.00	0.00	0.00	96.83
3		-1123.04	5.32	0.00	0.00	0.00	-112.78
	C3	1135.06	-439.03	0.00	0.00	0.00	-696.20
		-1086.67	439.03	0.00	0.00	0.00	-620.88
4-	C1	1782.65	5.32	0.00	0.00	0.00	107.08
5		-1734.27	-5.32	0.00	0.00	0.00	-91.13
	C3	1658.76	439.03	0.00	0.00	0.00	869.46
		-1610.38	-439.03	0.00	0.00	0.00	447.62

A3.0 BENDING MOMENTS & REINFORCEMENT

SPAN 1

Position(m)	Min.Moment(kNm)	Max.Moment(kNm)	As-top(mm2)	As-bot(mm2)
0.000	0.00	0.00	0.00	0.00
0.250	-1.69	-1.47	3.08	0.00
0.500	-6.78	-5.89	12.31	0.00
0.750	-15.24	-13.26	27.71	0.00
1.000	-27.10	-23.57	49.26	0.00
1.250	-42.35	-36.82	76.97	0.00

1.500	-60.98	-53.02	110.83	0.00
1.750	-83.00	-72.17	150.86	0.00
2.000	-108.40	-94.26	197.04	0.00
2.250	-137.20	-119.30	249.37	0.00
2.500	-169.38	-147.29	307.87	0.00
2.750	-204.95	-178.22	372.52	0.00
3.000	-243.91	-212.09	443.33	0.00
3.250	-286.25	-248.92	520.30	0.00
3.500	-331.99	-288.68	603.42	0.00
3.700	-371.01	-322.62	674.35	0.00
3.950	-422.84	-367.69	768.56	0.00
4.200	-478.06	-415.70	868.93	0.00
4.450	-536.67	-466.67	975.45	0.00
4.700	-598.66	-520.57	1088.13	0.00
4.950	-664.04	-577.43	1206.96	0.00
5.200	-732.81	-637.22	1331.96	0.00
5.450	-804.96	-699.97	1463.11	0.00
5.700	-880.51	-765.66	1600.42	0.00
5.950	-959.44	-834.30	1743.88	0.00
6.200	-1041.76	-905.88	1893.51	0.00
6.450	-1127.47	-980.40	2049.29	0.00
6.700	-1216.56	-1057.88	2211.23	0.00
6.950	-1309.04	-1138.30	2379.32	0.00
7.200	-1404.91	-1221.66	2553.58	0.00
7.400	-1484.05	-1290.47	2697.41	0.00

Deflection, Shear, Moment and Steel diagrams. Span 1

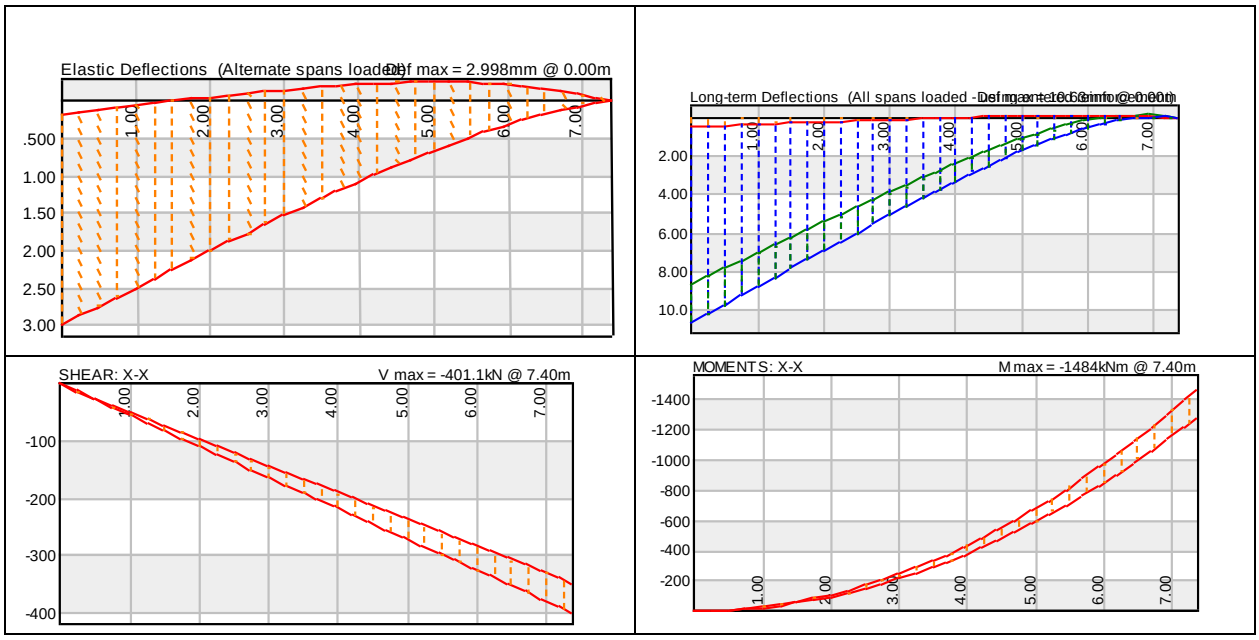

SPAN 2

Position(m) Min.Moment(kNm) Max.Moment(kNm) As-top(mm2) As-bot(mm2)

0.000	-1484.05	-1123.85	2697.41	0.00
0.250	-1359.56	-1038.11	2471.15	0.00
0.500	-1238.47	-955.31	2251.05	0.00
0.750	-1120.76	-875.47	2037.10	0.00
1.000	-1006.44	-798.57	1829.31	0.00
1.250	-895.51	-724.61	1627.68	0.00
1.500	-787.96	-653.60	1432.20	0.00
1.750	-683.80	-585.53	1242.88	0.00
2.000	-583.03	-471.99	1059.72	0.00
2.250	-485.65	-360.72	882.72	0.00
2.500	-399.02	-252.85	725.25	0.00
2.750	-342.73	-148.36	622.96	0.00
3.000	-289.40	-47.26	526.01	0.00
3.250	-239.01	50.45	434.42	91.71
3.500	-191.56	144.78	348.19	263.15
3.750	-147.07	235.72	267.31	428.44

4.000	-105.51	323.27	191.78	587.57
4.250	-66.91	407.43	121.61	740.55
4.500	-31.24	488.20	56.79	887.36
4.750	1.47	565.59	0.00	1028.02
5.000	31.24	639.59	0.00	1162.52
5.250	58.06	710.20	0.00	1290.87
5.500	81.94	777.43	0.00	1413.05
5.750	102.87	841.26	0.00	1529.08
6.000	120.86	901.71	0.00	1638.96
6.250	135.90	958.77	0.00	1742.67
6.400	143.51	991.38	0.00	2222.40
6.650	154.02	1043.23	0.00	2338.62
6.900	161.94	1092.10	0.00	2448.18
7.150	167.27	1137.99	0.00	2551.05
7.400	170.01	1180.91	0.00	2647.26
7.650	170.16	1220.85	0.00	2736.79
7.900	167.72	1257.81	0.00	2819.64
8.150	162.69	1291.79	0.00	2895.83
8.400	155.08	1322.80	0.00	2965.34
8.650	144.87	1350.83	0.00	3028.17
8.900	132.08	1375.88	0.00	3084.33
9.150	116.70	1397.96	0.00	3133.82
9.400	98.73	1417.05	0.00	3176.63
9.650	78.17	1433.18	0.00	3212.77
9.900	55.02	1446.32	0.00	3242.24
10.150	29.29	1456.49	0.00	3265.03
10.400	0.96	1463.68	0.00	3281.15
10.650	-29.95	1467.89	67.14	3290.60
10.700	-36.44	1468.38	81.70	3291.69
10.950	-70.46	1432.46	157.96	3211.16
11.200	-107.07	1393.56	240.03	3123.96
11.450	-146.27	1351.68	327.90	3030.09
11.700	-188.06	1306.83	421.57	2929.54
11.900	-223.35	1268.80	405.96	2306.19
12.150	-269.97	1218.39	490.71	2214.55
12.400	-319.55	1164.58	580.81	2116.75

12.500	-340.20	1142.11	618.35	2075.91
12.750	-393.89	1047.00	715.94	1903.04
13.000	-450.53	948.51	818.89	1724.01
13.250	-510.12	846.62	927.20	1538.83
13.500	-572.65	741.35	1040.85	1347.48
13.750	-638.13	632.69	1159.87	1149.98
14.000	-706.55	520.64	1284.23	946.32
14.250	-777.92	405.21	1413.95	736.51
14.500	-852.24	286.38	1549.03	520.53
14.750	-929.50	164.17	1689.46	298.40
15.000	-1009.70	38.58	1835.24	70.12
15.250	-1092.85	-90.41	1986.38	0.00
15.500	-1178.95	-222.78	2142.87	0.00
15.750	-1268.00	-358.54	2304.72	0.00
16.000	-1386.07	-497.69	2519.33	0.00
16.250	-1542.48	-640.23	2803.63	0.00
16.500	-1702.29	-786.15	3094.09	0.00
16.750	-1865.48	-935.46	3390.71	0.00
17.000	-2032.06	-1088.16	3693.49	0.00
17.250	-2202.03	-1244.25	4002.42	0.00
17.500	-2375.38	-1403.72	4317.51	0.00
17.750	-2552.13	-1566.58	4638.76	0.00
18.000	-2732.26	-1732.83	4966.17	0.00
18.250	-2915.77	-1902.47	5317.44	0.00
18.300	-2952.88	-1936.80	5389.20	0.00

Deflection, Shear, Moment and Steel diagrams. Span 2

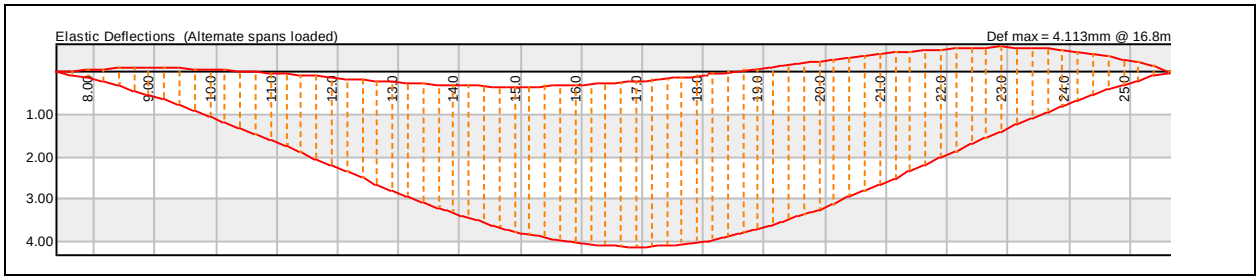

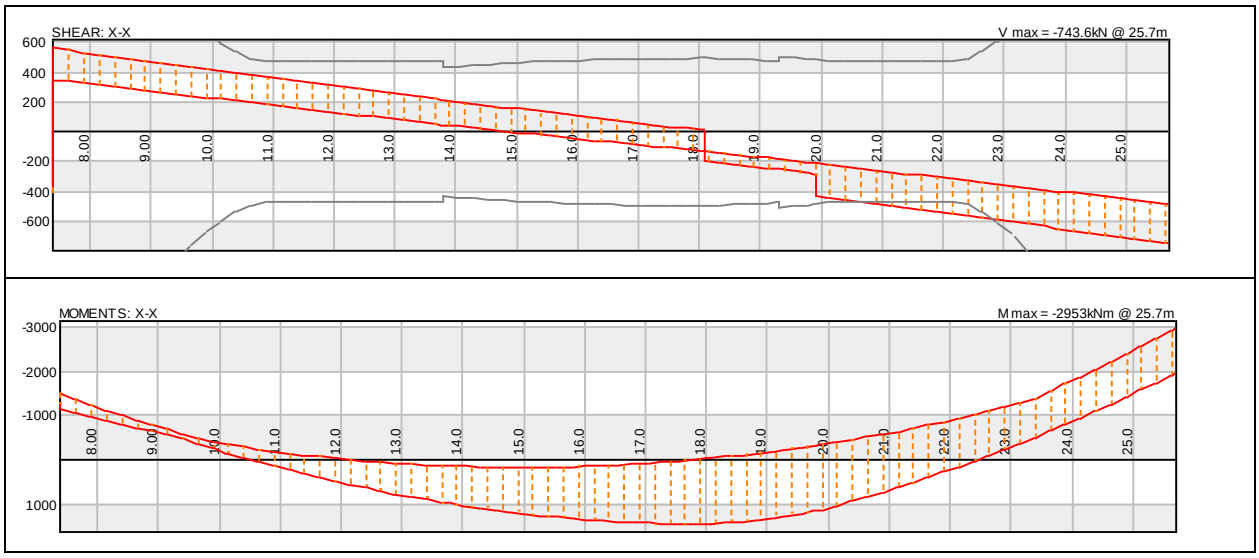

SPAN 3

Position(m) Min.Moment(kNm) Max.Moment(kNm) As-top(mm2) As-bot(mm2)

0.000	-3268.30	-1290.47	6003.85	0.00
0.250	-3096.59	-1204.75	5668.19	0.00
0.500	-2928.27	-1121.98	5341.60	0.00
0.750	-2763.34	-1042.15	5023.89	0.00
1.000	-2601.80	-965.26	4729.06	0.00
1.250	-2443.65	-891.33	4441.59	0.00
1.500	-2288.88	-820.33	4160.29	0.00
1.750	-2137.50	-752.29	3885.14	0.00
2.000	-1989.51	-687.18	3616.15	0.00
2.250	-1844.91	-625.03	3353.32	0.00
2.500	-1703.69	-565.82	3096.64	0.00
2.750	-1565.86	-509.56	2846.13	0.00
3.000	-1431.42	-456.24	2601.77	0.00
3.250	-1300.37	-405.87	2363.56	0.00
3.500	-1172.70	-358.44	2131.52	0.00
3.700	-1073.01	-322.62	1950.31	0.00
3.950	-951.44	-280.49	1729.35	0.00
4.200	-833.26	-241.32	1514.55	0.00
4.450	-718.47	-205.08	1305.90	0.00

4.700	-607.07	-171.80	1103.41	0.00
4.950	-499.05	-141.45	907.07	0.00
5.200	-394.42	-114.06	716.90	0.00
5.450	-329.74	-89.61	599.34	0.00
5.700	-268.45	-68.11	487.93	0.00
5.950	-210.54	-49.55	382.68	0.00
6.200	-156.03	-33.94	283.59	0.00
6.450	-104.90	-21.27	190.66	0.00
6.700	-57.15	-11.55	103.88	0.00
6.950	-12.80	-4.77	23.27	0.00
7.000	-4.34	-3.77	7.88	0.00
7.250	-0.61	-0.53	1.11	0.00
7.400	0.00	0.00	0.00	0.00

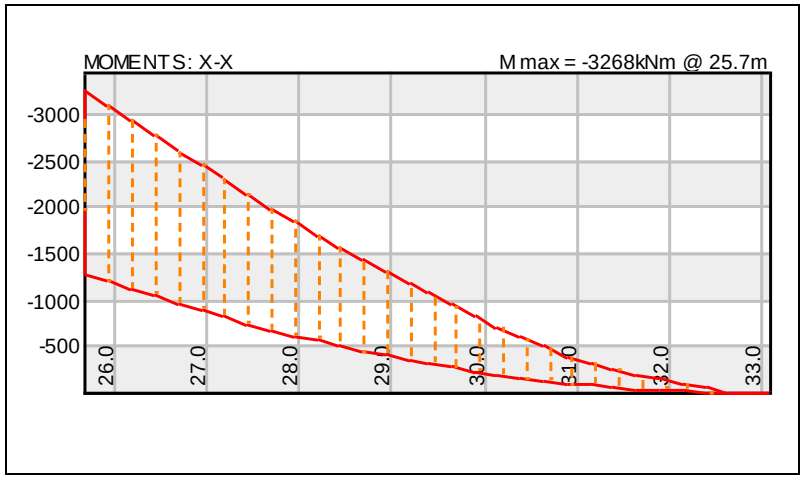

A4.0 SHEAR FORCES & REINFORCEMENT

SPAN 1

Position(m)	Minimum Shear(kN)	Maximum Shear(kN)	Capacity(kN)	Asv/Sv (mm2/mm)	Asv/Sv(nom) (mm2/mm)
0.000	-0.00	0.00	472.58	0.00	1.56
0.250	-13.55	-11.78	472.58	0.00	1.56
0.500	-27.10	-23.57	472.58	0.00	1.56
0.750	-40.65	-35.35	472.58	0.00	1.56
1.000	-54.20	-47.13	472.58	0.00	1.56
1.250	-67.75	-58.91	472.58	0.00	1.56

1.500	-81.30	-70.70	472.58	0.00	1.56
1.750	-94.85	-82.48	472.58	0.00	1.56
2.000	-108.40	-94.26	472.58	0.00	1.56
2.250	-121.95	-106.05	472.58	0.00	1.56
2.500	-135.50	-117.83	472.58	0.00	1.56
2.750	-149.05	-129.61	472.58	0.00	1.56
3.000	-162.61	-141.40	472.58	0.00	1.56
3.250	-176.16	-153.18	472.58	0.00	1.56
3.500	-189.71	-164.96	472.58	0.00	1.56
3.700	-200.55	-174.39	472.58	0.00	1.56
3.950	-214.10	-186.17	472.58	0.00	1.56
4.200	-227.65	-197.95	499.58	0.00	1.56
4.450	-241.20	-209.74	548.56	0.00	1.56
4.700	-254.75	-221.52	608.19	0.00	1.56
4.950	-268.30	-233.30	682.36	0.00	1.56
5.200	-281.85	-245.09	777.13	0.00	1.56
5.450	-295.40	-256.87	902.47	0.00	1.56
5.700	-308.95	-268.65	1076.02	0.00	1.56
5.950	-322.50	-280.44	1332.22	0.00	1.56
6.200	-336.05	-292.22	1750.54	0.00	1.56
6.450	-349.60	-304.00	2614.24	0.00	1.56
6.700	-363.15	-315.78	4915.83	0.00	1.56
6.950	-376.70	-327.57	5953.94	0.00	1.56
7.200	-390.25	-339.35	5953.94	0.00	1.56
7.400	-401.09	-348.78	5953.94	0.00	1.56

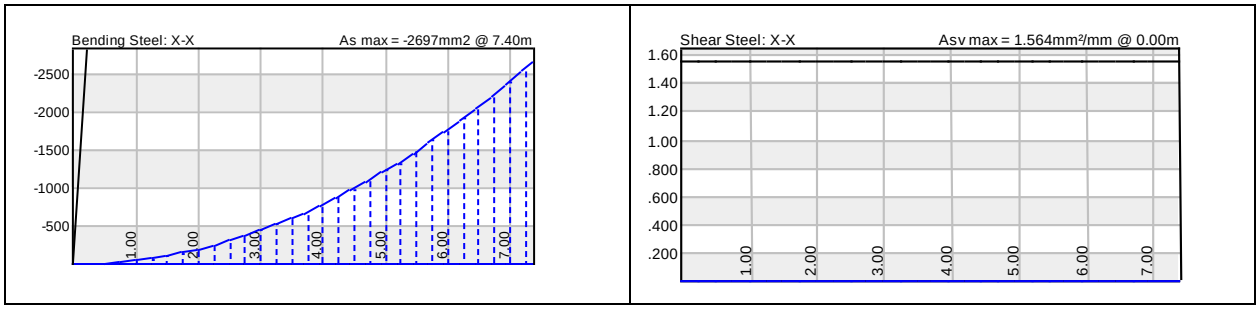

SPAN 2

Position(m)	Minimum Shear(kN)	Maximum Shear(kN)	Shear Capacity(kN)	Asv/Sv (mm2/mm)	Asv/Sv(nom) (mm2/mm)
0.000	348.85	560.23	5953.94	0.00	1.56
0.250	337.06	546.68	5953.94	0.00	1.56
0.500	325.28	533.13	5953.94	0.00	1.56
0.750	313.50	519.58	4099.93	0.00	1.56
1.000	301.72	506.03	2331.38	0.00	1.56
1.250	289.93	492.48	1645.68	0.00	1.56
1.500	278.15	478.93	1271.66	0.00	1.56
1.750	266.37	465.38	1036.17	0.00	1.56
2.000	254.58	451.83	874.27	0.00	1.56
2.250	242.80	438.28	756.12	0.00	1.56
2.500	231.02	424.73	666.11	0.00	1.56
2.750	219.23	411.18	595.25	0.00	1.56
3.000	207.45	397.63	538.01	0.00	1.56
3.250	195.67	384.08	490.82	0.00	1.56
3.500	183.89	370.53	472.58	0.00	1.56
3.750	172.10	356.97	472.58	0.00	1.56
4.000	160.32	343.42	472.58	0.00	1.56
4.250	148.54	329.87	472.58	0.00	1.56
4.500	136.75	316.32	472.58	0.00	1.56
4.750	124.97	302.77	472.58	0.00	1.56
5.000	113.19	289.22	472.58	0.00	1.56
5.250	101.40	275.67	472.58	0.00	1.56
5.500	89.62	262.12	472.58	0.00	1.56
5.750	77.84	248.57	472.58	0.00	1.56
6.000	66.06	235.02	472.58	0.00	1.56
6.250	54.27	221.47	472.58	0.00	1.56
6.400	47.20	213.34	433.95	0.00	1.56
6.650	36.85	201.43	441.38	0.00	1.56
6.900	26.49	189.52	448.17	0.00	1.56
7.150	16.14	177.62	454.36	0.00	1.56
7.400	5.78	165.71	460.00	0.00	1.56

7.650	-4.57	153.80	465.13	0.00	1.56
7.900	-14.93	141.89	469.78	0.00	1.56
8.150	-25.28	129.98	473.97	0.00	1.56
8.400	-35.64	118.07	477.73	0.00	1.56
8.650	-45.99	106.17	481.08	0.00	1.56
8.900	-56.35	94.26	484.04	0.00	1.56
9.150	-66.70	82.35	486.62	0.00	1.56
9.400	-77.06	70.44	488.82	0.00	1.56
9.650	-87.41	58.53	490.67	0.00	1.56
9.900	-97.77	46.62	492.16	0.00	1.56
10.150	-108.12	34.72	493.31	0.00	1.56
10.400	-118.48	22.81	494.12	0.00	1.56
10.650	-128.83	10.90	494.60	0.00	1.56
10.700	-130.90	8.52	494.65	0.00	1.56
10.700	-193.26	-130.90	494.65	0.00	1.56
10.950	-205.16	-141.26	490.59	0.00	1.56
11.200	-217.07	-151.61	486.10	0.00	1.56
11.450	-228.98	-161.97	481.19	0.00	1.56
11.700	-240.89	-172.32	475.80	0.00	1.56
11.900	-250.41	-180.61	505.26	0.00	1.56
12.150	-263.97	-192.39	498.48	0.00	1.56
12.400	-277.52	-204.17	491.03	0.00	1.56
12.500	-282.94	-208.89	487.85	0.00	1.56
12.500	-429.19	-208.89	487.85	0.00	1.56
12.750	-442.74	-220.67	473.91	0.00	1.56
13.000	-456.29	-232.45	472.58	0.00	1.56
13.250	-469.84	-244.24	472.58	0.00	1.56
13.500	-483.39	-256.02	472.58	0.03	1.56
13.750	-496.94	-267.80	472.58	0.08	1.56
14.000	-510.49	-279.58	472.58	0.12	1.56
14.250	-524.04	-291.37	472.58	0.16	1.56
14.500	-537.59	-303.15	472.58	0.20	1.56
14.750	-551.14	-314.93	472.58	0.24	1.56
15.000	-564.69	-326.72	482.36	0.26	1.56
15.250	-578.24	-338.50	536.97	0.13	1.56
15.500	-591.79	-350.28	608.08	0.00	1.56

15.750	-605.34	-362.07	695.46	0.00	1.56
16.000	-618.89	-373.85	810.68	0.00	1.56
16.250	-632.44	-385.63	967.38	0.00	1.56
16.500	-645.99	-397.41	1178.21	0.00	1.56
16.750	-659.54	-409.20	1478.79	0.00	1.56
17.000	-673.09	-420.98	1944.21	0.00	1.56
17.250	-686.64	-432.76	2765.04	0.00	1.56
17.500	-700.20	-444.55	4608.12	0.00	1.56
17.750	-713.75	-456.33	5953.94	0.00	1.56
18.000	-727.30	-468.11	5953.94	0.00	1.56
18.250	-740.85	-479.90	5953.94	0.00	1.56
18.300	-743.56	-482.25	5953.94	0.00	1.56

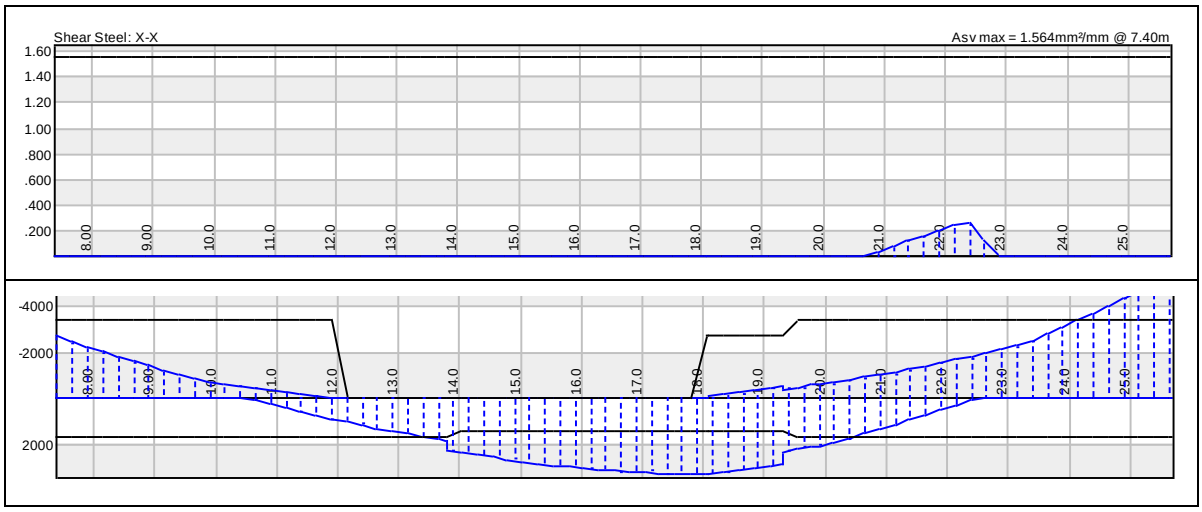

SPAN 3

Position(m)	Minimum Shear(kN)	Maximum Shear(kN)	Shear Capacity(kN)	Asv/Sv (mm2/mm)	Asv/Sv(nom) (mm2/mm)
0.000	348.78	693.59	5953.94	0.00	1.56
0.250	336.99	680.04	5953.94	0.00	1.56
0.500	325.21	666.49	5953.94	0.00	1.56
0.750	313.43	652.94	5539.25	0.00	1.56
1.000	301.64	639.39	3166.74	0.00	1.56
1.250	289.86	625.84	2189.11	0.00	1.56

1.500	278.08	612.29	1655.09	0.00	1.56
1.750	266.30	598.74	1318.18	0.00	1.56
2.000	254.51	585.19	1085.93	0.00	1.56
2.250	242.73	571.64	915.85	0.00	1.56
2.500	230.95	558.09	785.69	0.00	1.56
2.750	219.16	544.54	682.64	0.00	1.56
3.000	207.38	530.99	598.81	0.00	1.56
3.250	195.60	517.44	529.08	0.00	1.56
3.500	183.81	503.89	492.17	0.04	1.56
3.700	174.39	493.05	477.80	0.05	1.56
3.950	162.61	479.50	472.58	0.02	1.56
4.200	150.82	465.95	472.58	0.00	1.56
4.450	139.04	452.40	472.58	0.00	1.56
4.700	127.26	438.84	472.58	0.00	1.56
4.950	115.47	425.29	472.58	0.00	1.56
5.200	103.69	411.74	472.58	0.00	1.56
5.200	103.69	265.49	472.58	0.00	1.56
5.450	91.91	251.94	472.58	0.00	1.56
5.700	80.12	238.39	472.58	0.00	1.56
5.950	68.34	224.84	472.58	0.00	1.56
6.200	56.56	211.29	472.58	0.00	1.56
6.450	44.78	197.74	472.58	0.00	1.56
6.700	32.99	184.19	472.58	0.00	1.56
6.950	21.21	170.64	472.58	0.00	1.56
7.000	18.85	167.93	472.58	0.00	1.56
7.000	18.85	21.68	472.58	0.00	1.56
7.250	7.07	8.13	472.58	0.00	1.56
7.400	-0.00	-0.00	472.58	0.00	1.56

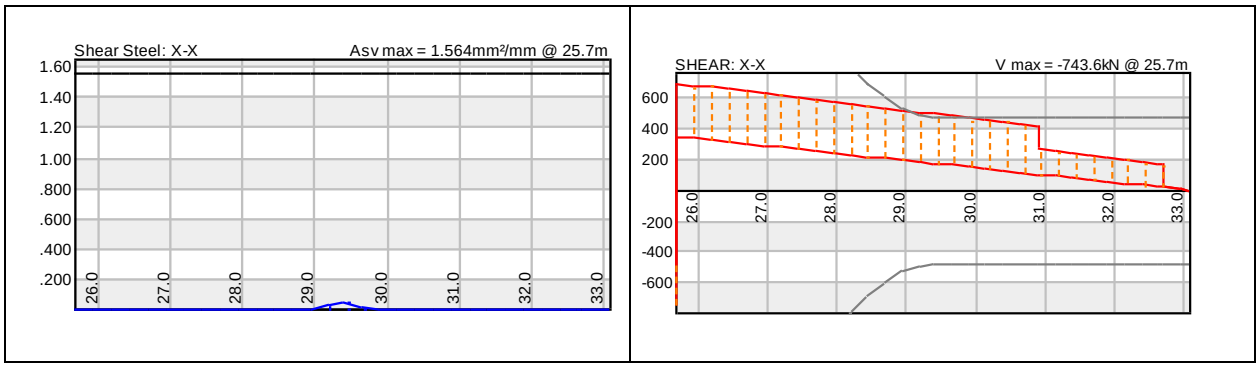

COLUMN REACTIONS

Support	Dead Load(kN)	Live Load(kN)	Dead + Live(kN)	Ultimate(kN)
1	0.00	0.00	0.00	0.00
2	764.33	26.43	790.75	909.01
3	764.33	423.57	1187.90	1437.15
4	0.00	0.00	0.00	0.00

Support	Bending Moment(kNm)		Shear Force (kN)	
No.	Min.	Max.	Min.	Max.
1	0.00	0.00	0.00	0.00
2	-535.92	360.20	-267.96	180.10
3	-923.79	646.33	-461.90	323.17
4	0.00	0.00	0.00	0.00

A5.0 ELASTIC DEFLECTIONS (Alternate spans loaded - positive downward)

Modulus of elasticity: Ec = 20 + fcu/5 = 27.0 Gpa

SPAN 1

Position(m)	Min.Deflection(mm)	Max.Deflection(mm)
0.000	0.17	3.00

0.250	0.14	2.87
0.500	0.12	2.75
0.750	0.09	2.63
1.000	0.06	2.50
1.250	0.03	2.38
1.500	0.00	2.25
1.750	-0.03	2.13
2.000	-0.05	2.01
2.250	-0.08	1.89
2.500	-0.10	1.77
2.750	-0.13	1.65
3.000	-0.15	1.53
3.250	-0.17	1.41
3.500	-0.19	1.30
3.700	-0.21	1.21
3.700	-0.21	1.21
3.950	-0.22	1.09
4.200	-0.24	0.99
4.450	-0.25	0.88
4.700	-0.25	0.78
4.950	-0.26	0.68
5.200	-0.26	0.58
5.450	-0.25	0.49
5.700	-0.24	0.41
5.950	-0.23	0.33
6.200	-0.20	0.25
6.450	-0.18	0.19
6.700	-0.14	0.13
6.950	-0.10	0.07
7.200	-0.05	0.03
7.400	-0.00	0.00

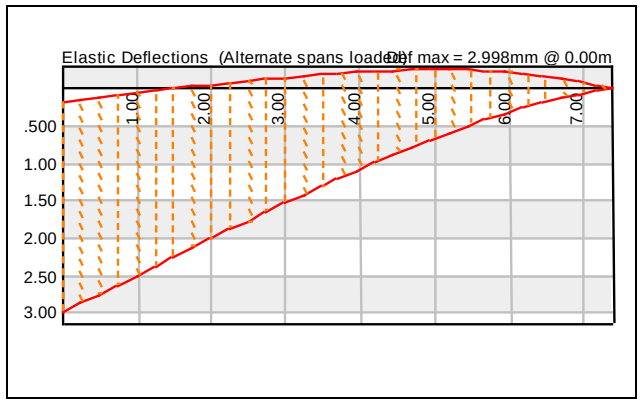

SPAN 2

Position(m) Min.Deflection(mm) Max.Deflection(mm)

0.000	-0.00	0.00
0.250	-0.03	0.07
0.500	-0.05	0.14
0.750	-0.07	0.23
1.000	-0.08	0.32
1.250	-0.09	0.43
1.500	-0.09	0.54
1.750	-0.09	0.65
2.000	-0.08	0.77
2.250	-0.07	0.90
2.500	-0.06	1.03
2.750	-0.04	1.17
3.000	-0.02	1.31
3.250	-0.00	1.45
3.500	0.02	1.60
3.750	0.05	1.75
4.000	0.07	1.90
4.250	0.10	2.04
4.500	0.13	2.19
4.750	0.15	2.34
5.000	0.18	2.49
5.250	0.21	2.64
5.500	0.23	2.78
5.750	0.25	2.92
6.000	0.27	3.06
6.250	0.29	3.19
6.400	0.30	3.26
6.400	0.30	3.26
6.650	0.32	3.39
6.900	0.33	3.50
7.150	0.33	3.61
7.400	0.34	3.71
7.650	0.34	3.79
7.900	0.33	3.87
8.150	0.33	3.94

8.400	0.32	4.00
8.650	0.30	4.04
8.900	0.28	4.08
9.150	0.26	4.10
9.150	0.26	4.10
9.400	0.24	4.11
9.650	0.21	4.11
9.900	0.18	4.10
10.150	0.14	4.07
10.400	0.10	4.03
10.650	0.07	3.98
10.700	0.06	3.97
10.700	0.06	3.97
10.950	0.02	3.90
11.200	-0.03	3.82
11.450	-0.07	3.73
11.700	-0.11	3.63
11.900	-0.15	3.53
11.900	-0.15	3.53
12.150	-0.19	3.41
12.400	-0.23	3.28
12.500	-0.25	3.23
12.500	-0.25	3.23
12.750	-0.29	3.10
13.000	-0.34	2.96
13.250	-0.38	2.81
13.500	-0.41	2.66
13.750	-0.45	2.50
14.000	-0.48	2.35
14.250	-0.51	2.19
14.500	-0.54	2.03
14.750	-0.56	1.87
15.000	-0.57	1.71
15.250	-0.58	1.55
15.500	-0.59	1.40
15.750	-0.58	1.24

16.000	-0.57	1.09
16.250	-0.55	0.95
16.500	-0.52	0.80
16.750	-0.48	0.67
17.000	-0.44	0.54
17.250	-0.38	0.42
17.500	-0.31	0.30
17.750	-0.22	0.20
18.000	-0.13	0.10
18.250	-0.02	0.02
18.300	-0.00	0.00

SPAN 3

Position(m)	Min.Deflection(mm)	Max.Deflection(mm)
0.000	-0.00	0.00
0.250	-0.07	0.13
0.500	-0.14	0.27
0.750	-0.20	0.43
1.000	-0.25	0.61
1.250	-0.29	0.80
1.500	-0.33	1.00
1.750	-0.36	1.22
2.000	-0.38	1.45
2.250	-0.40	1.69
2.500	-0.42	1.95
2.750	-0.43	2.21
3.000	-0.44	2.48
3.250	-0.44	2.76
3.500	-0.45	3.05
3.700	-0.45	3.29
3.700	-0.45	3.29
3.950	-0.44	3.59
4.200	-0.44	3.89
4.450	-0.44	4.20

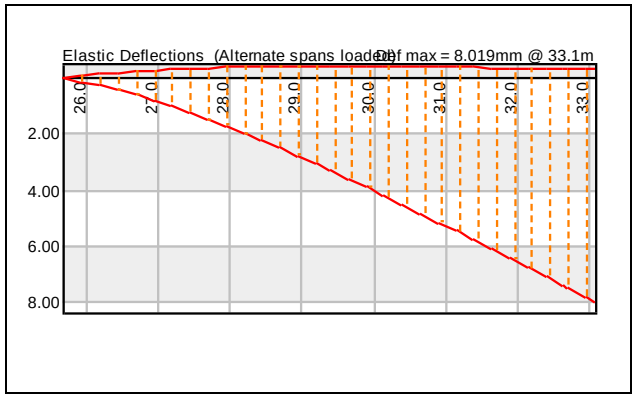

4.700	-0.43	4.51
4.950	-0.42	4.83
5.200	-0.41	5.15
5.200	-0.41	5.15
5.450	-0.40	5.47
5.700	-0.39	5.79
5.950	-0.38	6.12
6.200	-0.37	6.44
6.450	-0.35	6.77
6.700	-0.34	7.10
6.950	-0.33	7.43
7.000	-0.33	7.49
7.000	-0.33	7.49
7.250	-0.32	7.82
7.400	-0.31	8.02

A 5.0 LONGTERM DEFLECTIONS (All spans loaded - positive downward)

Symbols: DS : Shrinkage deflection.

DL : Long-term deflection under permanent load.

DI : Instantaneous deflection under short-term load.

DT : Total long-term deflection.

SPAN 1

Position(m)	DS(mm)	DL(mm)	DI(mm)	DT(mm)
0.000	0.66	10.13	-2.05	8.74
0.250	0.62	9.69	-1.98	8.33
0.500	0.58	9.26	-1.91	7.93
0.750	0.54	8.83	-1.85	7.52
1.000	0.50	8.39	-1.78	7.12
1.250	0.46	7.96	-1.71	6.71
1.500	0.42	7.53	-1.64	6.31
1.750	0.38	7.09	-1.57	5.91

2.000	0.35	6.66	-1.50	5.51
2.250	0.31	6.24	-1.43	5.12
2.500	0.27	5.81	-1.36	4.72
2.750	0.24	5.39	-1.29	4.33
3.000	0.20	4.97	-1.22	3.95
3.250	0.17	4.55	-1.15	3.56
3.500	0.13	4.14	-1.08	3.19
3.700	0.11	3.81	-1.03	2.89
3.700	0.11	3.81	-1.03	2.89
3.950	0.08	3.41	-0.96	2.53
4.200	0.04	3.02	-0.89	2.17
4.450	0.02	2.63	-0.82	1.83
4.700	-0.01	2.26	-0.75	1.50
4.950	-0.04	1.90	-0.68	1.19
5.200	-0.06	1.57	-0.61	0.90
5.450	-0.07	1.25	-0.54	0.64
5.700	-0.08	0.96	-0.47	0.40
5.950	-0.09	0.70	-0.40	0.21
6.200	-0.09	0.47	-0.33	0.05
6.450	-0.08	0.28	-0.26	-0.06
6.700	-0.07	0.14	-0.19	-0.13
6.950	-0.05	0.04	-0.12	-0.14
7.200	-0.03	-0.01	-0.06	-0.09
7.400	-0.00	0.00	0.00	-0.00

SPAN 2

Position(m)	DS(mm)	DL(mm)	DI(mm)	DT(mm)
0.000	-0.00	0.00	0.00	
-0.00				
0.250	0.04	0.06	0.07	0.18
0.500	0.09	0.19	0.14	0.42
0.750	0.15	0.36	0.22	0.73
1.000	0.21	0.59	0.30	1.09
1.250	0.28	0.85	0.38	1.51
1.500	0.36	1.15	0.46	1.96

1.750	0.44	1.48	0.54	2.45
2.000	0.52	1.83	0.62	2.97
2.250	0.61	2.20	0.70	3.52
2.500	0.71	2.59	0.78	4.08
2.750	0.80	2.99	0.87	4.65
3.000	0.90	3.39	0.95	5.24
3.250	0.99	3.81	1.03	5.83
3.500	1.09	4.22	1.11	6.42
3.750	1.19	4.64	1.19	7.02
4.000	1.29	5.06	1.28	7.62
4.250	1.39	5.48	1.36	8.23
4.500	1.48	5.90	1.44	8.83
4.750	1.59	6.32	1.52	9.43
5.000	1.69	6.74	1.60	10.03
5.250	1.79	7.15	1.68	10.62
5.500	1.89	7.56	1.76	11.21
5.750	1.99	7.97	1.84	11.80
6.000	2.08	8.36	1.92	12.37
6.250	2.18	8.75	2.00	12.93
6.400	2.23	8.98	2.05	13.26
6.400	2.23	8.98	2.05	13.26
6.650	2.32	9.33	2.12	13.78
6.900	2.39	9.66	2.19	14.25
7.150	2.46	9.95	2.25	14.67
7.400	2.52	10.22	2.31	15.04
7.650	2.56	10.44	2.36	15.36
7.900	2.60	10.63	2.40	15.63
8.150	2.62	10.78	2.43	15.83
8.400	2.64	10.89	2.45	15.98
8.650	2.64	10.97	2.46	16.07
8.900	2.63	11.00	2.46	16.10
9.150	2.61	11.00	2.46	16.07
9.150	2.61	11.00	2.46	16.07
9.400	2.58	10.96	2.44	15.98
9.650	2.54	10.88	2.42	15.84
9.900	2.49	10.76	2.38	15.63

10.150	2.42	10.60	2.34	15.36
10.400	2.35	10.41	2.28	15.04
10.650	2.27	10.18	2.21	14.67
10.700	2.25	10.14	2.20	14.59
10.700	2.25	10.14	2.20	14.59
10.950	2.16	9.87	2.12	14.15
11.200	2.07	9.58	2.03	13.68
11.450	1.97	9.26	1.93	13.16
11.700	1.87	8.91	1.82	12.60
11.900	1.79	8.62	1.73	12.13
11.900	1.79	8.62	1.73	12.13
12.150	1.68	8.23	1.61	11.53
12.400	1.58	7.84	1.49	10.92
12.500	1.54	7.69	1.45	10.67
12.500	1.54	7.69	1.45	10.67
12.750	1.43	7.29	1.33	10.05
13.000	1.33	6.88	1.21	9.43
13.250	1.23	6.47	1.09	8.80
13.500	1.14	6.06	0.98	8.18
13.750	1.04	5.65	0.86	7.56
14.000	0.95	5.24	0.75	6.94
14.250	0.86	4.83	0.63	6.33
14.500	0.78	4.42	0.52	5.72
14.750	0.69	4.01	0.41	5.11
15.000	0.61	3.61	0.30	4.52
15.250	0.53	3.22	0.19	3.94
15.500	0.45	2.83	0.10	3.37
15.750	0.38	2.45	0.00	2.83
16.000	0.31	2.08	-0.08	2.32
16.250	0.24	1.74	-0.14	1.84
16.500	0.19	1.41	-0.20	1.40
16.750	0.14	1.11	-0.23	1.01
17.000	0.09	0.83	-0.25	0.67
17.250	0.06	0.59	-0.25	0.39
17.500	0.03	0.38	-0.23	0.18
17.750	0.01	0.21	-0.18	0.04

18.000	-0.00	0.08	-0.11	-0.03
18.250	-0.00	0.01	-0.02	-0.01
18.300	0.00	0.00	0.00	0.00

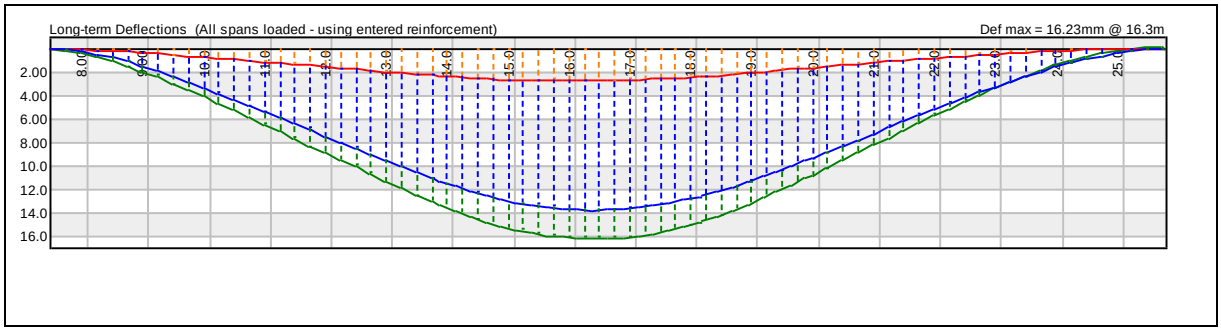

SPAN 3

Position(m)	DS(mm)	DL(mm)	DI(mm)	DT(mm)
0.000	-0.00	0.00	0.00	-0.00
0.250	0.01	-0.01	0.13	0.13
0.500	0.03	0.03	0.29	0.35
0.750	0.06	0.12	0.48	0.66
1.000	0.10	0.25	0.69	1.05
1.250	0.15	0.43	0.94	1.51
1.500	0.21	0.64	1.21	2.05
1.750	0.27	0.88	1.50	2.65
2.000	0.34	1.15	1.82	3.31
2.250	0.42	1.45	2.16	4.03
2.500	0.50	1.78	2.52	4.80
2.750	0.59	2.12	2.90	5.61
3.000	0.69	2.48	3.29	6.46
3.250	0.79	2.86	3.69	7.35
3.500	0.90	3.26	4.11	8.27
3.700	0.99	3.58	4.45	9.02
3.700	0.99	3.58	4.45	9.02
3.950	1.10	3.99	4.89	9.98
4.200	1.22	4.41	5.33	10.95
4.450	1.34	4.83	5.77	11.94

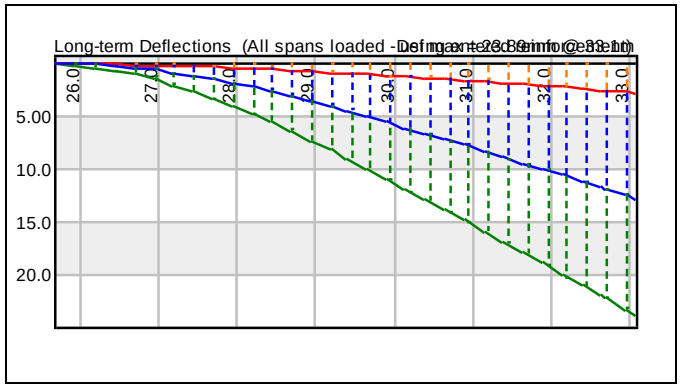

4.700	1.46	5.26	6.22	12.94
4.950	1.58	5.70	6.66	13.94
5.200	1.71	6.13	7.11	14.95
5.200	1.71	6.13	7.11	14.95
5.450	1.84	6.57	7.56	15.97
5.700	1.97	7.02	8.01	16.99
5.950	2.10	7.46	8.46	18.02
6.200	2.23	7.91	8.91	19.05
6.450	2.37	8.35	9.36	20.09
6.700	2.51	8.80	9.82	21.13
6.950	2.65	9.25	10.27	22.17
7.000	2.68	9.34	10.36	22.38
7.000	2.68	9.34	10.36	22.38
7.250	2.82	9.79	10.81	23.42
7.400	2.91	10.06	11.08	24.05

APPENDIX B

CONROL DESIGN RESULTS

B 1 DETAILLED DRAWING DEVELOPED DURING CONTROL DESIGN

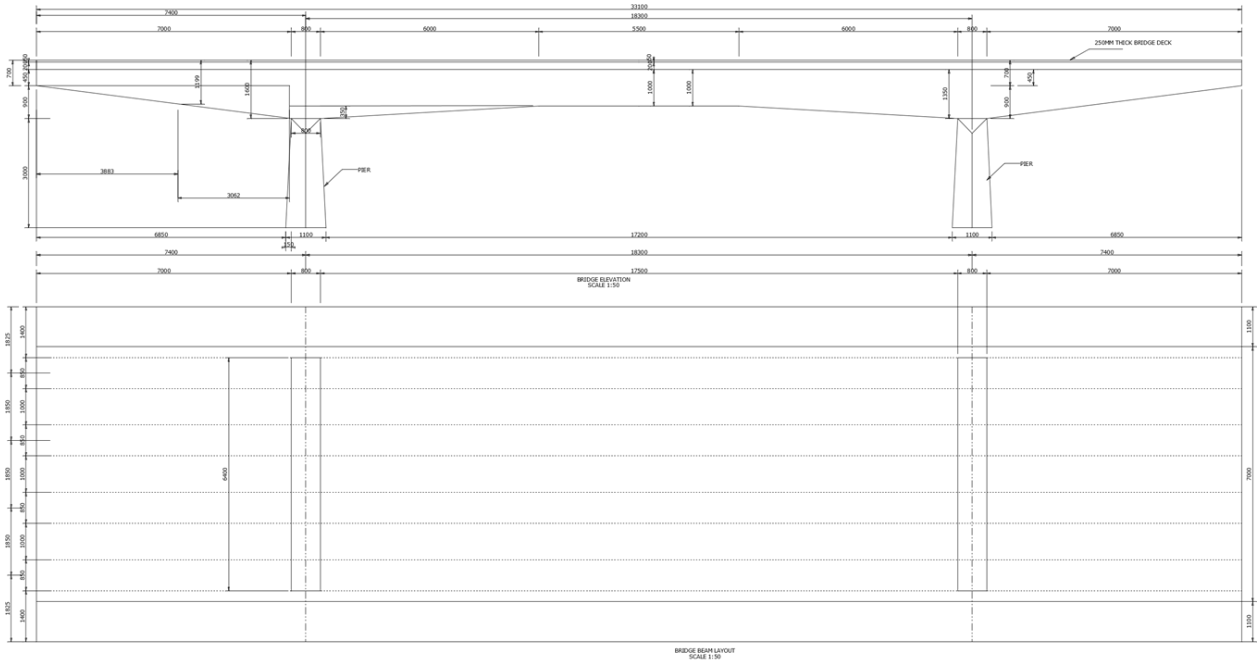

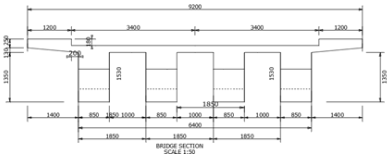

B 2.0 DETAILLED REINFORCEMENT LAYOUT

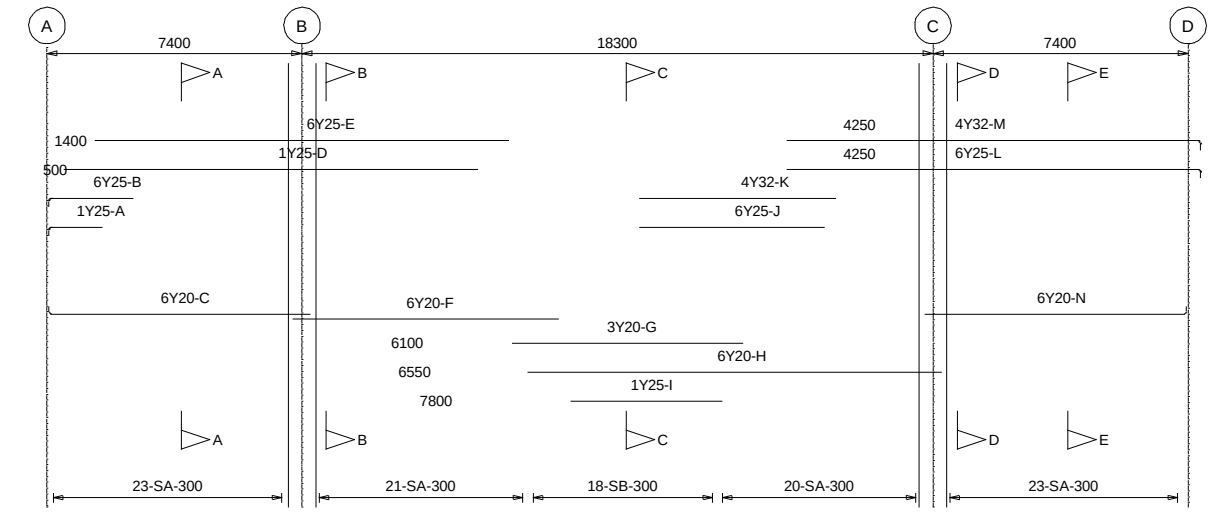

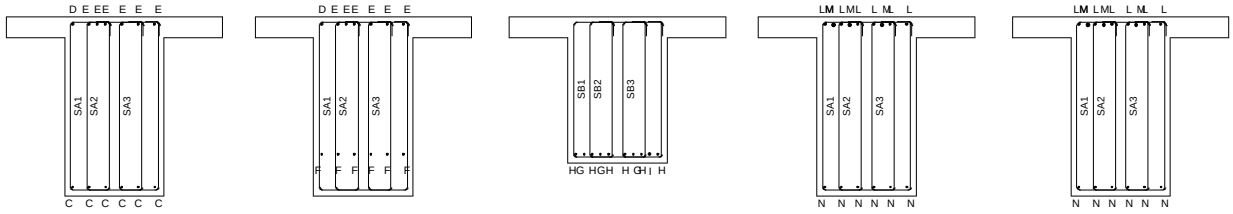

SECTION A-A SECTION B-B SECTION C-C SECTION D-D SECTION E-E

APPENDIX C:

FINITE ELEMENT MODELLING

APPENDIX C FINITE ELEMENT MODELLING

C1.0 Finite element modelling and analysis

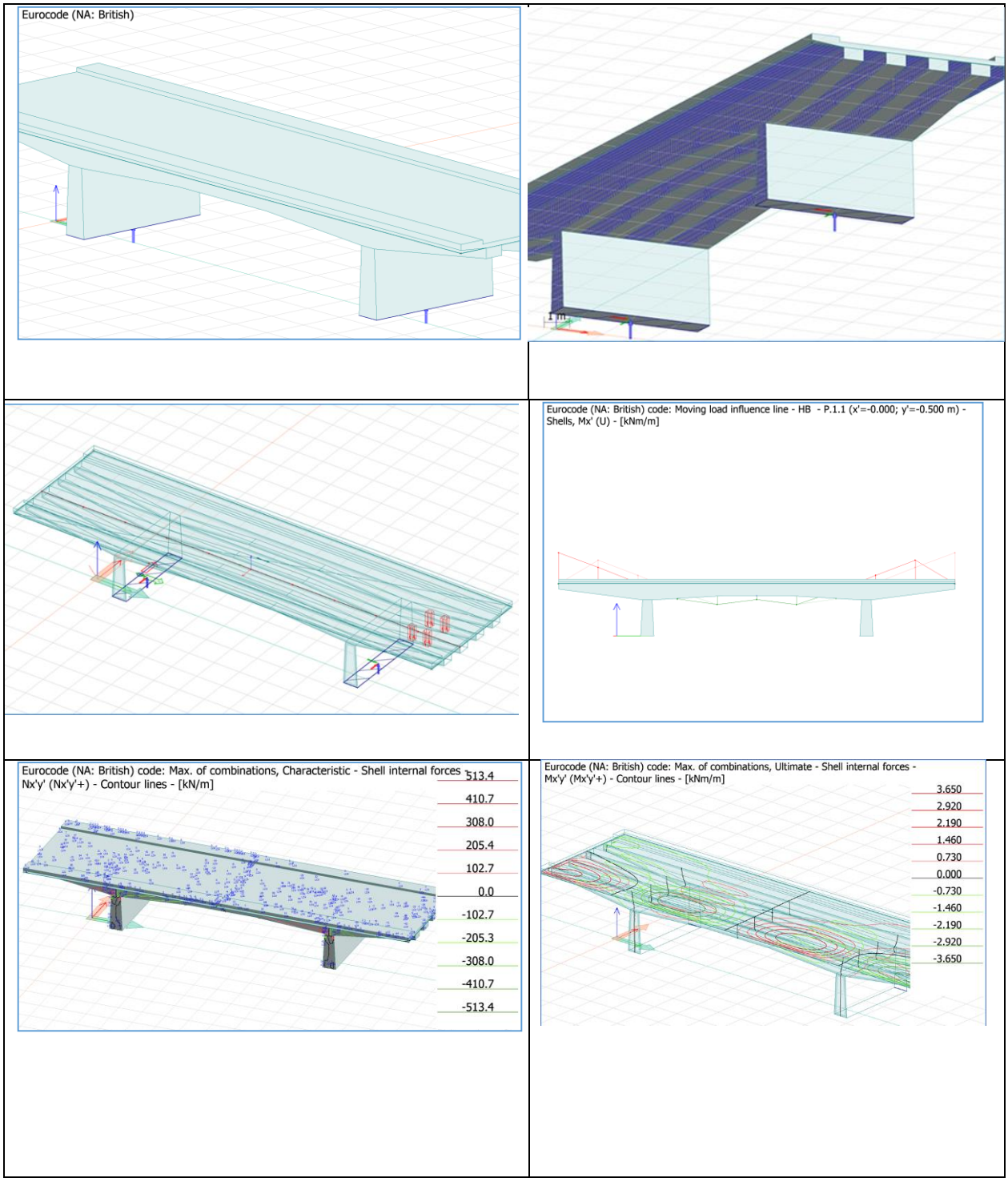

Finite element Tables C .1 Nodes (49419 items) table extends to more than 350pages,therefore only the last part has been included in this appendix

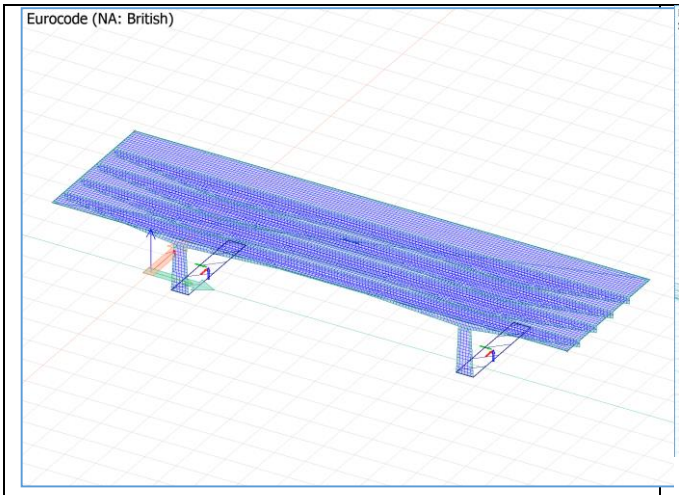
Eurocode (NA: British)

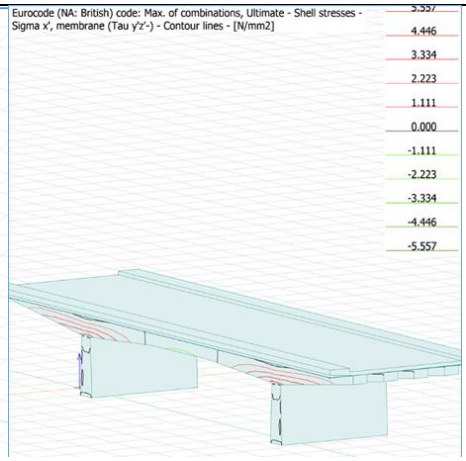
Eurocode (NA: British) code: Max. of combinations, Ultimate - Shell stresses - Sigma x', membrane (Tau y'z'-) - Contour lines - [N/mm2]
4.446
3.334
2.223
1.111
0.000
-1.111
-2.223
-3.334
-4.446
-5.557

49383	**28.250**	**4.759**	**4.350**
49384	28.250	4.861	4.350
49385	28.250	4.861	4.350
49386	28.250	4.964	4.350
49387	28.250	4.964	4.350
49388	28.250	5.066	4.350
49389	28.250	5.066	4.350
49390	28.250	5.168	4.350
49391	28.250	5.168	4.350
49392	28.250	5.270	4.350
49393	28.250	5.270	4.350
49394	28.250	5.373	4.350
49395	28.250	5.373	4.350
49396	28.250	5.475	4.350
49397	28.250	5.475	4.350
49398	28.250	5.577	4.350
49399	28.250	5.577	4.350
49400	28.250	5.680	4.350
49401	28.250	5.680	4.350
49402	28.250	5.782	4.350
49403	28.250	5.782	4.350
49404	28.250	5.884	4.350
49405	28.250	5.884	4.350
49406	28.250	5.986	4.350
49407	28.250	5.986	4.350
49408	28.250	6.089	4.350
49409	28.250	6.089	4.350
49410	28.250	6.191	4.350
49411	28.250	6.191	4.350
49412	28.250	6.293	4.350
49413	28.250	6.293	4.350
49414	28.250	6.395	4.350

Seismic load, horizontal sp.,

Value	Quantity
Type	1
Ground	A
ag [m/s2]	0.500
S	1.000
TB [s]	0.150
TC [s]	0.400
TD [s]	2.000
q	1.000
beta	0.200

Seismic load, vertical sp.,

Value	Quantity
Type	1
agv/ag [m/s2]	0.900
S	1.000
TB [s]	0.050
TC [s]	0.150
TD [s]	1.000
q	1.000
beta	0.200

Seismic load, structure information

Value	Quantity
Structure type	Bridge structure
xi (damping factor) [%]	5.000
qd (behaviour factor for displacements)	1.000

Site and load information (8 items)

Value	Quantity
Wind speed [m/s]	26
Characteristic snow load [kN/m2]	0.0
Terrain type[-]	II

Value	Quantity
Extent [m]	9x33.1
Building height [m]	0.00
Building width x-dir [m]	33.1
Building width y-dir [m]	9
Ground level [m]	1

No. -	x m	y m	z m	
1	-4.850	-2.600	4.350	
2	-4.850	-2.600	4.350	
3	-4.850	-2.500	4.350	
4	-4.850	-2.500	4.350	
5	-4.850	-2.400	4.350	
6	-4.850	-2.400	4.350	
7	-4.850	-2.300	4.350	**standard (9 items)**
8	-4.850	-2.300	4.350	
9	-4.850	-2.200	4.350	
10	-4.850	-2.200	4.350	
11	-4.850	-2.100	4.350	
12	-4.850	-2.100	4.350	
13	-4.850	-2.000	4.350	
14	-4.850	-2.000	4.350	
15	-4.850	-1.900	4.350	
16	-4.850	-1.900	4.350	
17	-4.850	-1.800	4.350	
18	-4.850	-1.800	4.350	
19	-4.850	-1.700	4.350	
20	-4.850	-1.700	4.350	
21	-4.850	-1.600	4.350	
22	-4.850	-1.600	4.350	
23	-4.850	-1.500	4.350	
24	-4.850	-1.500	4.350	**standard (8 items)**
25	-4.850	-1.200	4.350	
26	-4.850	-1.200	4.350	
27	-4.850	-1.200	4.350	
28	-4.850	-1.097	4.350	
29	-4.850	-1.097	4.350	
30	-4.850	-1.400	4.350	
31	-4.850	-1.400	4.350	
32	-4.850	-1.300	4.350	
33	-4.850	-1.300	4.350	
34	-4.850	-0.994	4.350	
35	-4.850	-0.994	4.350	
36	-4.850	-0.892	4.350	
37	-4.850	-0.892	4.350	
38	-4.850	-0.789	4.350	
39	-4.850	-0.789	4.350	

(3 items)

Load combinations analysis setup (8 items)

Table C2.Crack presence predictions due to load combinations

No	Type	Load combination	Non-linear elements	Plastic elements	Non-linear soil	Cracked section	2nd order	Imperfection shape
1	U	1.15*Dead load + 1.75*super imposed + HB live load	Yes	Yes	No	No	Yes	-
2	Sq	Dead load + super imposed + HB live load	Yes	Yes	No	No	No	-
3	Sf	Dead load + super imposed + HB live load	Yes	Yes	No	No	No	-
4	Sc	Dead load + super imposed + HB live load	Yes	Yes	No	Yes	No	-
5	U	1.15*Dead load + 1.75*super imposed + HB Truck moving live load	Yes	Yes	No	No	No	-
6	Sq	Dead load + super imposed + HB live load + truck moving load	Yes	Yes	No	Yes	Yes	-
8	Sc	Dead load + super imposed + HB truck moving load	Yes	Yes	No	Yes	Yes	-

Table C 3 Shell Crack width predictions due to load combination

ID	Elem	Face	Width 1	Direction 1	Width 2	Direction 2	Combination
-	-	-	mm	rad	mm	rad	-
P.1.1	1	bottom	0.000	0.548	0.000	2.119	Dead load + super imposed + HB live load
		top	0.000	0.724	0.000	2.295	Dead load + super imposed + HB live load
	11	bottom	03	2.384	0.000	3.955	Dead load + super imposed + HB live load
		top	0.213	2.418	0.111	3.988	Dead load + super imposed + HB live load
	12	bottom	0.34	0.491	0.412	2.061	Dead load + super imposed + HB live load
		top	0.311	0.477	0.288	2.048	Dead load + super imposed + HB live load
	13	bottom	0.294	1.095	0.237	2.666	Dead load + super imposed + HB live load
		top	0.311	1.074	0.241	2.645	Dead load + super imposed + HB live load

14	bottom	0.000	0.859	0.000	2.430	Dead load + super imposed + HB live load
	top	0.000	0.822	0.000	2.393	Dead load + super imposed + HB live load
15	bottom	0.000	2.283	0.000	3.854	Dead load + super imposed + HB live load

Moving loads (2 items) table 3.0

No.	Name	Vehicle	Return	Lock direction	Cut loads to path extent
-	-	-	-	-	-
1	HB	EC LM1 Lane 1. (Truck) [Distributed]	Yes	Yes	No
2	moving load	EC LM1 Lane 1. (Truck) [Concentrated]	Yes	Yes	No

Load groups (48 items) Table C 4.0

No.	Load group	Included load cases
1	dead load (Permanent, 1.00, 1.15, 1.00, 1.00, 0.85)	Dead load (+Struc. dead load)
2	super imposed dead (Permanent, 1.00, 1.75, 1.00, 1.00, 0.85)	super imposed (+Struc. dead load)
3	HB (Stress, 1.00, 1.30)	HB live load
4	moving truck (Stress, 1.00, 1.30)	truck moving load
5	HB (Temporary, 1.50, 0.70, 0.50, 0.30, L, --)	HB -1
		HB -2
		HB -3
		HB -4
		HB -5
		HB -6
		HB -7
		HB -8
		HB -9
		HB -10
		HB -11
		HB -12
		HB -13
		HB -14
		HB -15
		HB -16
		HB -17
		HB -18
		HB -19
		HB -20
		HB -21
		HB -22

C2.0 CRACK ANALYSIS

Longterm deflection: Permanent load

B2.2 Instantaneous deflection: Total load

Effective Elasticity Modulus(GPa): 27.00

	Uncracked		Cracked			fc-top	fc-bot
Pos(m)	M(kNm)	I(E9mm4)	NA(mm)	Cracked	I(E9mm4) NA(mm)	M/EI	(MPa) (MPa)
0.000	0.000	326.740	682.989	FALSE	326.740 682.989	0.000	0.000 -0.000
0.250	-1.473	333.892	681.939	FALSE	333.892 681.939	-0.000	-0.003 0.004
0.500	-5.892	337.983	681.664	FALSE	337.983 681.664	-0.001	-0.011 0.014
0.750	-13.256	341.870	680.962	FALSE	341.870 680.962	-0.001	-0.024 0.031
1.000	-23.566	342.703	680.089	FALSE	342.703 680.089	-0.003	-0.043 0.055
1.250	-36.822	342.703	680.089	FALSE	342.703 680.089	-0.004	-0.068 0.086
1.500	-53.024	342.703	680.089	FALSE	342.703 680.089	-0.006	-0.097 0.124
1.750	-72.171	342.703	680.089	FALSE	342.703 680.089	-0.008	-0.133 0.168
2.000	-94.264	342.703	680.089	FALSE	342.703 680.089	-0.010	-0.173 0.220
2.250	-119.303	342.703	680.089	FALSE	342.703 680.089	-0.013	-0.219 0.278
2.500	-147.288	342.703	680.089	FALSE	342.703 680.089	-0.016	-0.271 0.344
2.750	-178.218	342.703	680.089	FALSE	342.703 680.089	-0.019	-0.328 0.416
3.000	-212.094	342.703	680.089	FALSE	342.703 680.089	-0.023	-0.390 0.495
3.250	-248.916	342.703	680.089	FALSE	342.703 680.089	-0.027	-0.458 0.581
3.500	-288.684	342.703	680.089	FALSE	342.703 680.089	-0.031	-0.531 0.674
3.700	-322.619	342.703	680.089	FALSE	342.703 680.089	-0.035	-0.593 0.753
3.700	-322.619	342.703	680.089	FALSE	342.703 680.089	-0.035	-0.593 0.753

3.950-367.689 342.703 680.089 FALSE 342.703 680.089 -0.040 -0.676 0.858

4.200-415.704 342.703 680.089 FALSE 342.703 680.089 -0.045 -0.764 0.970

4.450-466.666 342.703 680.089 FALSE 342.703 680.089 -0.050 -0.858 1.089

4.700-520.573 342.703 680.089 FALSE 342.703 680.089 -0.056 -0.957 1.215

4.950-577.426 342.703 680.089 TRUE 306.822 728.505 -0.070 -1.000 1.414

5.200-637.225 342.703 680.089 TRUE 253.266 806.156 -0.093 -1.000 1.695

5.450-699.969 342.703 680.089 TRUE 210.180 874.745 -0.123 -1.000 2.016

5.700-765.659 342.703 680.089 TRUE 176.818 932.931 -0.160 -1.000 2.369

5.950-834.295 342.703 680.089 TRUE 151.536 980.939 -0.204 -1.000 2.748

6.200-905.877 342.703 680.089 TRUE 132.4751020.019 -0.253 -1.000 3.145

6.450-980.405 342.703 680.089 TRUE 118.0051051.766 -0.308 -1.000 3.558

6.700-1057.878 342.703 680.089 TRUE 106.8671077.691 -0.367 -1.000 3.982

6.950-1138.297 340.983 678.669 TRUE 97.5421097.526 -0.432 -1.000 4.463

7.200-1221.661 339.256 677.244 TRUE 90.1461113.560 -0.502 -1.000 4.966

7.400-1290.474 339.256 677.244 TRUE 85.6641125.593 -0.558 -1.000 5.339

7.400-1400.835 339.256 677.244 TRUE 79.9711141.418 -0.649 -1.000 5.931

7.650-1291.814 339.256 677.244 TRUE 85.5841125.809 -0.559 -1.000 5.346

7.900-1185.738 341.414 679.024 TRUE 93.5651108.446 -0.469 -1.000 4.709

8.150-1082.608 342.703 680.089 TRUE 103.9271084.783 -0.386 -1.000 4.117

8.400-982.424 342.703 680.089 TRUE 117.6711052.523 -0.309 -1.000 3.569

8.650-885.186 342.703 680.089 TRUE 137.3721009.707 -0.239 -1.000 3.030

8.900-790.894 342.703 680.089 TRUE 166.551 951.962 -0.176 -1.000 2.507

9.150-699.547 342.703 680.089 TRUE 210.430 874.328 -0.123 -1.000 2.013

9.400-611.146 342.703 680.089 TRUE 275.018 773.736 -0.082 -1.000 1.569

9.650-525.691 342.703 680.089 FALSE 342.703 680.089 -0.057 -0.967 1.227

9.900-443.181 342.703 680.089 FALSE 342.703 680.089 -0.048 -0.815 1.034

10.150-363.618 342.703 680.089 FALSE 342.703 680.089 -0.039 -0.669 0.849

10.400-287.000 342.703 680.089 FALSE 342.703 680.089 -0.031 -0.528 0.670

10.650-213.327 342.703 680.089 FALSE 342.703 680.089 -0.023 -0.392 0.498

10.900-142.601 342.703 680.089 FALSE 342.703 680.089 -0.015 -0.262 0.333

11.150 -74.820 342.703 680.089 FALSE 342.703 680.089 -0.008 -0.138 0.175

11.400 -9.985 342.675 680.118 FALSE 342.675 680.118 -0.001 -0.018 0.023

11.650 51.904 342.398 680.409 FALSE 342.398 680.409 0.006 0.096 -0.121

11.900 110.847 342.120 680.700 FALSE 342.120 680.700 0.012 0.204 -0.259

12.150 166.845 341.842 680.991 FALSE 341.842 680.991 0.018 0.308 -0.390

12.400 219.897 340.727 682.160 FALSE 340.727 682.160 0.024 0.408 -0.515

12.650 270.003 338.934 684.039 FALSE 338.934 684.039 0.030 0.505 -0.634

12.900 317.164 337.243 685.810 FALSE 337.243 685.810 0.035 0.598 -0.747

13.150 361.379 335.543 687.591 FALSE 335.543 687.591 0.040 0.687 -0.853

13.400 402.647 334.038 689.169 FALSE 334.038 689.169 0.045 0.770 -0.953

13.650 440.971 334.667 689.702 TRUE 307.900 657.012 0.053 0.869 -1.000

13.800 462.551 335.295 690.234 TRUE 280.525 621.847 0.061 0.943 -1.000

13.800 462.551 188.948 554.611 TRUE 70.186 305.440 0.244 1.683 -1.000

14.050 496.339 189.646 555.471 TRUE 66.459 294.028 0.277 1.822 -1.000

14.300 527.539 190.342 556.329 TRUE 64.765 287.991 0.302 1.939 -1.000

14.550 556.150 190.620 556.671 TRUE 61.969 279.486 0.332 2.060 -1.000

14.800 582.172 190.620 556.671 TRUE 58.651 269.826 0.368 2.182 -1.000

15.050 605.606 190.620 556.671 TRUE 56.108 262.260 0.400 2.291 -1.000

15.300	626.451	190.736	556.814	TRUE	54.745	257.887	0.424	2.379	-1.000
15.550	644.707	191.025	557.170	TRUE	54.684	257.052	0.437	2.441	-1.000
15.800	660.374	191.313	557.526	TRUE	54.906	257.081	0.445	2.491	-1.000
16.050	673.452	191.602	557.881	TRUE	55.361	257.820	0.451	2.528	-1.000
16.300	683.942	191.890	558.236	TRUE	56.014	259.164	0.452	2.554	-1.000
16.550	691.843	191.918	558.272	TRUE	55.613	257.875	0.461	2.586	-1.000
16.550	691.843	191.918	558.272	TRUE	55.613	257.875	0.461	2.586	-1.000
16.800	697.155	191.918	558.272	TRUE	55.262	256.799	0.467	2.609	-1.000
17.050	699.879	191.918	558.272	TRUE	55.085	256.257	0.471	2.621	-1.000
17.300	700.014	192.591	557.225	TRUE	55.225	255.262	0.469	2.602	-1.000
17.550	697.560	194.579	554.132	TRUE	55.824	252.911	0.463	2.536	-1.000
17.800	692.517	196.542	551.077	TRUE	56.596	251.164	0.453	2.461	-1.000
18.050	684.885	198.482	548.058	TRUE	57.566	250.056	0.441	2.380	-1.000
18.100	683.049	198.867	547.459	TRUE	57.787	249.917	0.438	2.363	-1.000
18.100	683.049	198.867	547.459	TRUE	57.787	249.917	0.438	2.363	-1.000
18.350	644.186	200.676	544.643	TRUE	61.433	256.595	0.388	2.166	-1.000
18.600	602.734	201.398	543.108	TRUE	65.237	265.530	0.342	1.991	-1.000
18.850	558.693	201.236	542.539	TRUE	69.659	277.555	0.297	1.825	-1.000
19.100	512.064	200.933	542.186	TRUE	76.570	295.803	0.248	1.644	-1.000
19.300	472.897	200.691	541.903	TRUE	85.164	317.275	0.206	1.484	-1.000
19.300	472.897	354.019	676.512	TRUE	308.111	622.178	0.057	0.878	-1.000
19.550	421.429	352.482	675.269	FALSE	352.482	675.269	0.044	0.748	-0.962
19.800	367.016	351.304	674.316	FALSE	351.304	674.316	0.039	0.652	-0.842
19.900	344.426	350.868	673.964	FALSE	350.868	673.964	0.036	0.613	-0.791

19.900 344.426 350.868 673.964 FALSE 350.868 673.964 0.036 0.613 -0.791

20.150 257.764 349.777 673.082 FALSE 349.777 673.082 0.027 0.459 -0.595

20.400 168.156 349.559 672.905 FALSE 349.559 672.905 0.018 0.300 -0.388

20.650 75.602 349.559 672.905 FALSE 349.559 672.905 0.008 0.135 -0.175

20.900 -19.898 349.559 672.905 FALSE 349.559 672.905 -0.002 -0.035 0.046

21.150-118.343 349.559 672.905 FALSE 349.559 672.905 -0.013 -0.211 0.273

21.400-219.734 349.559 672.905 FALSE 349.559 672.905 -0.023 -0.392 0.507

21.650-324.071 349.559 672.905 FALSE 349.559 672.905 -0.034 -0.577 0.748

21.900-431.353 349.559 672.905 FALSE 349.559 672.905 -0.046 -0.769 0.996

22.150-541.582 349.559 672.905 FALSE 349.559 672.905 -0.057 -0.965 1.250

22.400-654.756 349.559 672.905 TRUE 276.227 774.991 -0.088 -1.000 1.671

22.650-770.875 349.559 672.905 TRUE 217.784 866.776 -0.131 -1.000 2.171

22.900-889.941 349.559 672.905 TRUE 181.262 930.999 -0.182 -1.000 2.695

23.150-1011.952 349.559 672.905 TRUE 157.614 976.502 -0.238 -1.000 3.233

23.400-1136.909 349.559 672.905 TRUE 141.5251009.735 -0.298 -1.000 3.778

23.650-1264.812 349.559 672.905 TRUE 130.0521034.810 -0.360 -1.000 4.330

23.900-1395.661 349.559 672.905 TRUE 121.5351054.294 -0.425 -1.000 4.889

24.150-1529.455 349.559 672.905 TRUE 114.9981069.823 -0.493 -1.000 5.455

24.400-1666.195 349.559 672.905 TRUE 109.8421082.461 -0.562 -1.000 6.030

24.650-1805.881 349.559 672.905 TRUE 105.6811092.936 -0.633 -1.000 6.614

24.900-1948.512 349.559 672.905 TRUE 102.2601101.745 -0.706 -1.000 7.207

25.150-2094.089 348.684 672.197 TRUE 99.1841108.269 -0.782 -1.000 7.848

25.400-2242.612 346.490 670.423 TRUE 96.2521112.207 -0.863 -1.000 8.569

25.650-2394.081 346.050 670.067 TRUE 94.1051117.288 -0.942 -1.000 9.228

25.700-2424.729 346.050 670.067 TRUE 93.7321118.319 -0.958 -1.000 9.356

25.700-2662.974 346.050 670.067 TRUE 91.1931125.398 -1.082 -1.000 10.355

25.950-2521.003 346.050 670.067 TRUE 92.6321121.369 -1.008 -1.000 9.760

26.200-2381.977 348.246 671.843 TRUE 94.7601119.417 -0.931 -1.000 9.064

26.450-2245.897 349.559 672.905 TRUE 96.9311115.857 -0.858 -1.000 8.437

26.700-2112.763 349.559 672.905 TRUE 99.0711110.130 -0.790 -1.000 7.888

26.950-1982.575 349.559 672.905 TRUE 101.5411103.621 -0.723 -1.000 7.349

27.200-1855.332 349.559 672.905 TRUE 104.4131096.180 -0.658 -1.000 6.820

27.450-1731.036 349.559 672.905 TRUE 107.7941087.583 -0.595 -1.000 6.302

27.700-1609.685 349.559 672.905 TRUE 111.8211077.568 -0.533 -1.000 5.793

27.950-1491.279 349.559 672.905 TRUE 116.6871065.759 -0.473 -1.000 5.294

28.200-1375.820 349.559 672.905 TRUE 122.6691051.653 -0.415 -1.000 4.804

28.450-1263.306 349.559 672.905 TRUE 130.1661034.554 -0.359 -1.000 4.323

28.700-1153.738 349.559 672.905 TRUE 139.7801013.469 -0.306 -1.000 3.851

28.950-1047.115 349.559 672.905 TRUE 152.440 986.964 -0.254 -1.000 3.387

29.200-943.439 349.559 672.905 TRUE 169.623 952.948 -0.206 -1.000 2.931

29.400-862.619 349.559 672.905 TRUE 188.177 918.331 -0.170 -1.000 2.575

29.400-862.619 349.559 672.905 TRUE 188.177 918.331 -0.170 -1.000 2.575

29.650-764.244 349.559 672.905 TRUE 220.393 862.420 -0.128 -1.000 2.142

29.900-668.816 349.559 672.905 TRUE 267.491 788.021 -0.093 -1.000 1.730

30.150-576.333 349.559 672.905 TRUE 335.721 691.294 -0.064 -1.000 1.354

30.400-486.796 349.559 672.905 FALSE 349.559 672.905 -0.052 -0.867 1.124

30.650-400.205 349.559 672.905 FALSE 349.559 672.905 -0.042 -0.713 0.924

30.900-316.559 349.559 672.905 FALSE 349.559 672.905 -0.034 -0.564 0.731

30.900	-316.559	349.559	672.905	FALSE	349.559	672.905	-0.034	-0.564	0.731
31.150	-263.985	349.559	672.905	FALSE	349.559	672.905	-0.028	-0.470	0.610
31.400	-214.356	349.559	672.905	FALSE	349.559	672.905	-0.023	-0.382	0.495
31.650	-167.673	349.559	672.905	FALSE	349.559	672.905	-0.018	-0.299	0.387
31.900	-123.935	349.559	672.905	FALSE	349.559	672.905	-0.013	-0.221	0.286
32.150	-83.143	349.559	672.905	FALSE	349.559	672.905	-0.009	-0.148	0.192
32.400	-45.297	349.438	672.869	FALSE	349.438	672.869	-0.005	-0.081	0.105
32.650	-10.397	345.701	672.726	FALSE	345.701	672.726	-0.001	-0.019	0.024
32.700	-3.771	344.661	673.006	FALSE	344.661	673.006	-0.000	-0.007	0.009
32.700	-3.771	344.661	673.006	FALSE	344.661	673.006	-0.000	-0.007	0.009
32.950	-0.530	339.457	674.419	FALSE	339.457	674.419	-0.000	-0.001	0.001
33.100	0.000	335.002	674.179	FALSE	335.002	674.179	0.000	0.000	-0.000

APPENDIX D:

EXPERIMENTAL FIELD (SHM) TESTS

APPENDIX D EXPERIMENTAL FIELD (SHM) TESTS

D1.0

Total cracks: 2

Intercept: -217.89mm

Velocity: 1.949km/s

Correlation coefficient: 0.6679

D 1 Crack No.: 1

Component name: bm0001

Strength grade: C20

Crack name: NonCross

Operator: Eng.Hopeson

Total Points: 5

Whether crossing or not: Non-cross-over crack

Starting distance: 50.00mm

Distance Interval: 50.00mm

Calculation method: Auto.

Depth of Crack 1: 0.00mm

Depth of Crack 2: 0.00mm

No.	Time 1(us)	Distance(mm)	Depth of Crack(mm)
001-01	176.00	50.00	0.00
001-02	150.00	100.00	0.00
001-03	198.40	150.00	0.00

001-04 222.00 200.00 0.00

001-05 197.20 250.00 0.00

D2.Crack No: 2

Component name: bm0001

Crack name: LF-1

Strength grade: C20

Total Points: 5

Whether crossing or not: Cross-over crack

Starting distance: 50.00mm

Distance Interval: 50.00mm

Calculation method: Auto.

Depth of Crack 1: -1.00mm

Depth of Crack 2: 94.36mm

No. Time 1(us) Distance(mm) Depth of Crack(mm)

002-01 59.60 50.00 -1.00

002-02 200.00 100.00 112.86

002-03 222.00 150.00 113.96

002-04 222.00 200.00 56.25

002-05 222.00 250.00 -1.00

Total cracks: 3

Intercept: -64.24mm

Velocity: 1.214km/s

Correlation coefficient: 0.8764

D3 Crack No.: 3

Component name: bm02

Crack name: NonCross

Strength grade: C20

Operator: Eng.Hopeson

Total Points: 4

Whether crossing or not: Non-cross-over crack

Starting distance: 50.00mm

Distance Interval: 50.00mm

Calculation method: Auto.

Depth of Crack 1: 0.00mm

Depth of Crack 2: 0.00mm

No.	Time 1(us)	Distance(mm)	Depth of Crack(mm)
001-01	113.20	50.00	0.00
001-02	149.20	100.00	0.00
001-03	139.20	150.00	0.00
001-04	222.00	200.00	0.00

D4 Crack No.:4

Component name: bm06

Crack name: LF-1

Strength grade: C20

Total Points: 3

Whether crossing or not: Cross-over crack

Starting distance: 50.00mm

Distance Interval: 50.00mm

Calculation method: Auto.

Depth of Crack 1: -1.00mm

Depth of Crack 2: 51.76mm

No.	Time 1(us)	Distance(mm)	Depth of Crack(mm)
002-01	127.60	50.00	52.30
002-02	157.60	100.00	49.05
002-03	198.00	150.00	54.47

D4.0 Crack No.: 5

Component name: bm02

Crack name: LF-2

Strength grade: C20

Operator:Eng Hopeson

Total Points: 5

Whether crossing or not: Cross-over crack

Starting distance: 50.00mm

Distance Interval: 50.00mm

Calculation method: Auto.

Depth of Crack 1: -1.00mm

Depth of Crack 2: 65.63mm

No. Time 1(us) Distance(mm) Depth of Crack(mm)

003-01	200.00	50.00	107.11
003-02	158.00	100.00	49.52
003-03	222.00	150.00	81.73
003-04	222.00	200.00	26.44
003-05	222.00	250.00	-1.00

APPENDIX E:

DATA COLLECTION METHODS

APPENDIX E: DATA COLLECTION METHODS

E.1 WAVE FORM COMPRESSIVE TEST RESULTS BY ULTRASONIC PULSE VELOCITY

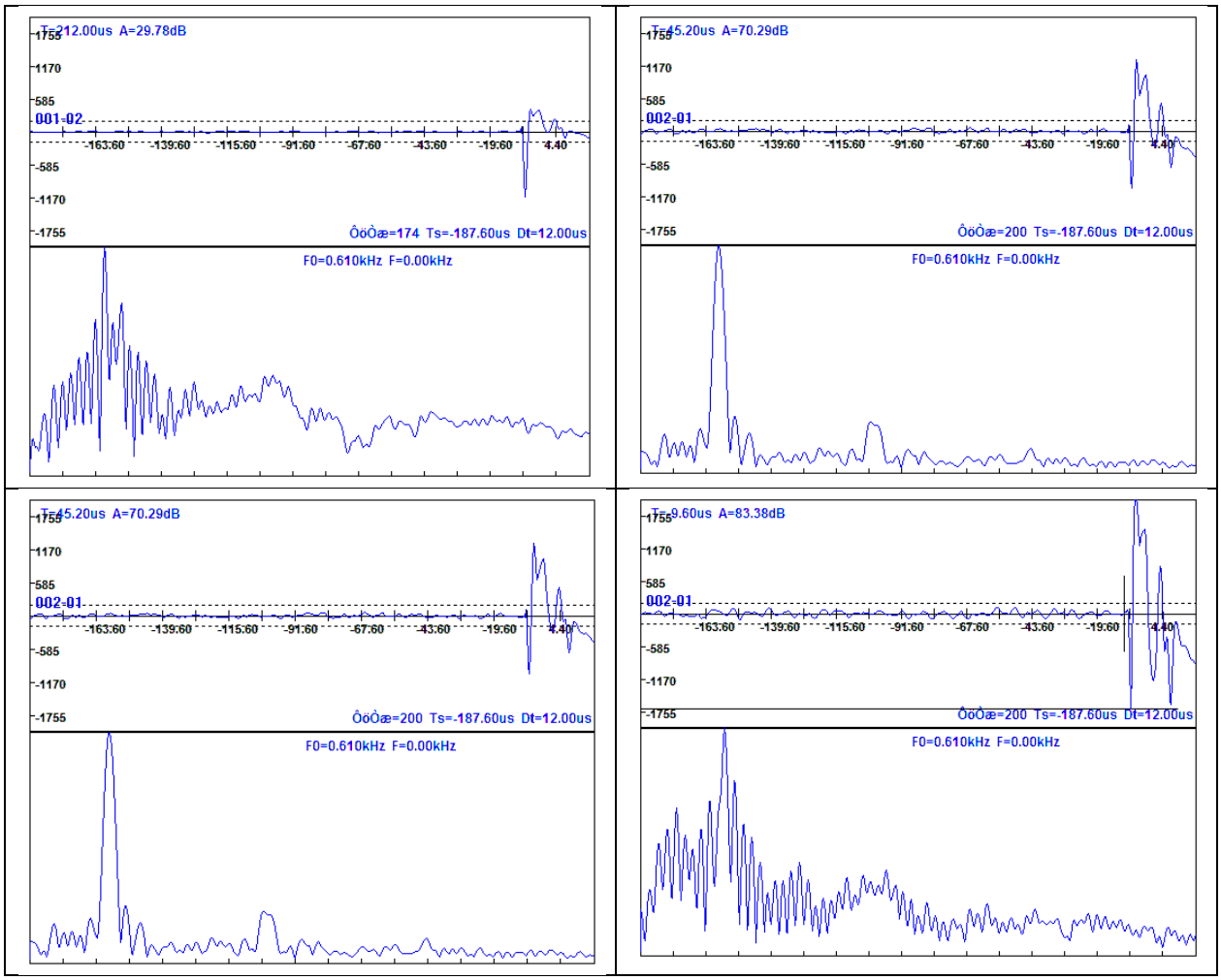

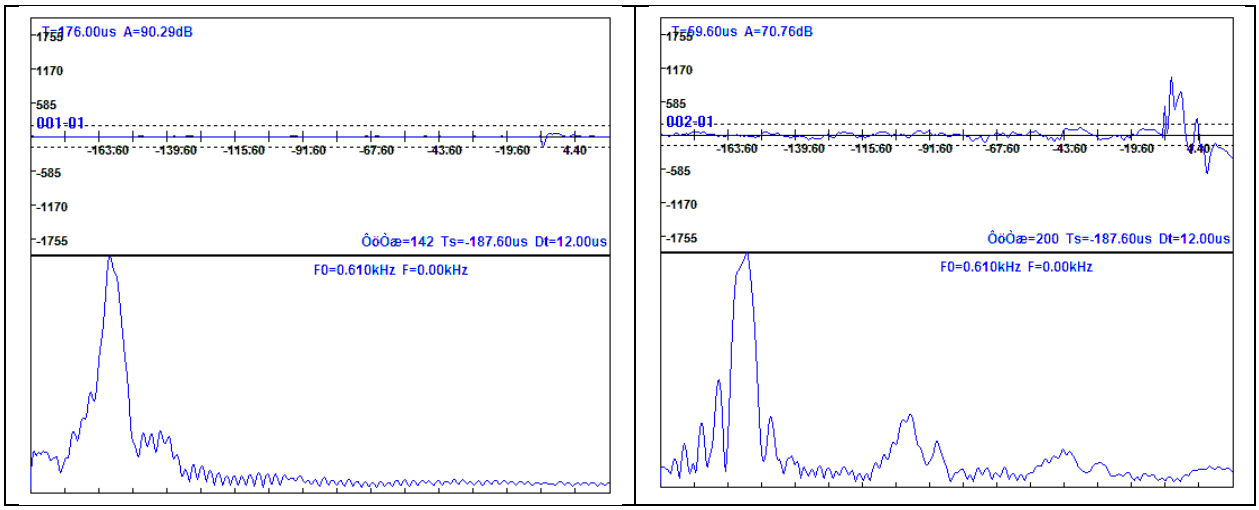

E2.0 compressive strength UT

E.2.1 BEAM 04

Total number of points: 3

Curve types: Standard

Aggregate types: crushed

Concrete types: Common

Processing methods: Country

Curve coefficients: A=0.005600,B=1.439000,C=1.769000,D=0.000000

Correction method: None

Process mode: Single

Component name : **BEAM 04**

Validity: Valid

Strength grade: 36.2**MPa**

Age :over 90days

Coarse aggregate size grading: 5to20mm

Ultrasonic operator: Eng.Hopeson

Transducer frequency: 50kHz

UT method: Opposite

Velocity correction factor: 1.00

Number of testing areas: 3

Test angle: 0

Test surface type: Side

Average strength of each test area (MPa): 36.2

Standard deviation of strength of each test area(MPa): 0.00

Minimum strength of each test area(MPa): 36.2

Constructive strength of component(MPa): 36.2

E2.2 BEAM 02

Total number of points: 3

Curve types: Standard

Aggregate types: crushed

Concrete types: Common

Processing methods: Country

Curve coefficients: A=0.005600,B=1.439000,C=1.769000,D=0.000000

Correction method: None

Process mode: Single

Component name: BEAM 02

Validity: Valid

Strength grade: **35.9MPa**

Age of concrete: over 90days

Coarse aggregate size grading: 5to20mm

Ultrasonic operator: Eng.Hopeson

Transducer frequency: 50kHz

UT method: Opposite

Velocity correction factor: 1.00

Number of testing areas: 3

Test angle: 0

Test surface type: Side

Average strength of each test area(MPa): 35.9

Standard deviation of strength of each test area(MPa): 0.00

Minimum strength of each test area(MPa): 35.9

Constructive strength of component(MPa): 35.9

E2.3 BEAM 01

Total number of points: 3

Curve types: Standard

Aggregate types: Crushed

Concrete types: Common

Processing methods: Country

Process mode: Single

Component name: **BEAM 01**

Validity: Valid

Strength grade:43.1**MPa**

Age of concrete : over 90days

Coarse aggregate size grading: 5to20mm

Ultrasonic operator: Eng.Hopeson

Transducer frequency: 50kHz

UT method: Opposite

Velocity correction factor: 1.00

Number of testing areas: 3

Test angle: 0

Test surface type: Side

Concrete type: Non pumping# Average carbonized depth of component (mm): 0.0

Average strength of each test area (MPa): 43.1

Standard deviation of strength of each test area (MPa): 0.00

Minimum strength of each test area (MPa): 43.1

Constructive strength of component (MPa): 43.1

E.2.4 BEAM 03

Total number of points: 3``

Curve types: Standard

Aggregate types: Crushed

Concrete types: Common

Processing methods: Country

Curve coefficients: A=0.005600,B=1.439000,C=1.769000,D=0.000000

Correction method: None

Process mode: Single

Component name: **BEAM 03**

Validity: Valid

Strength grade: **36.9Mpa**

Age of concrete: over 90days

Coarse aggregate size grading: 5to20mm

Ultrasonic operator: Eng.Hopeson

Transducer frequency: 50kHz

UT method: Opposite

Velocity correction factor: 1.00

Number of testing areas: 3

Test angle: 0

Test surface type: Side

Concrete type: Non pumpingzzz#Average carbonized depth of component(mm): 0.0

Average strength of each test area(MPa): 36.9

Standard deviation of strength of each test area(MPa): 0.00

Minimum strength of each test area(MPa): 36.9

Constructive strength of component(MPa): 36.9

E 3.0 REBAR SCANNING, SPACING, COVER TO REINFORCEMENT

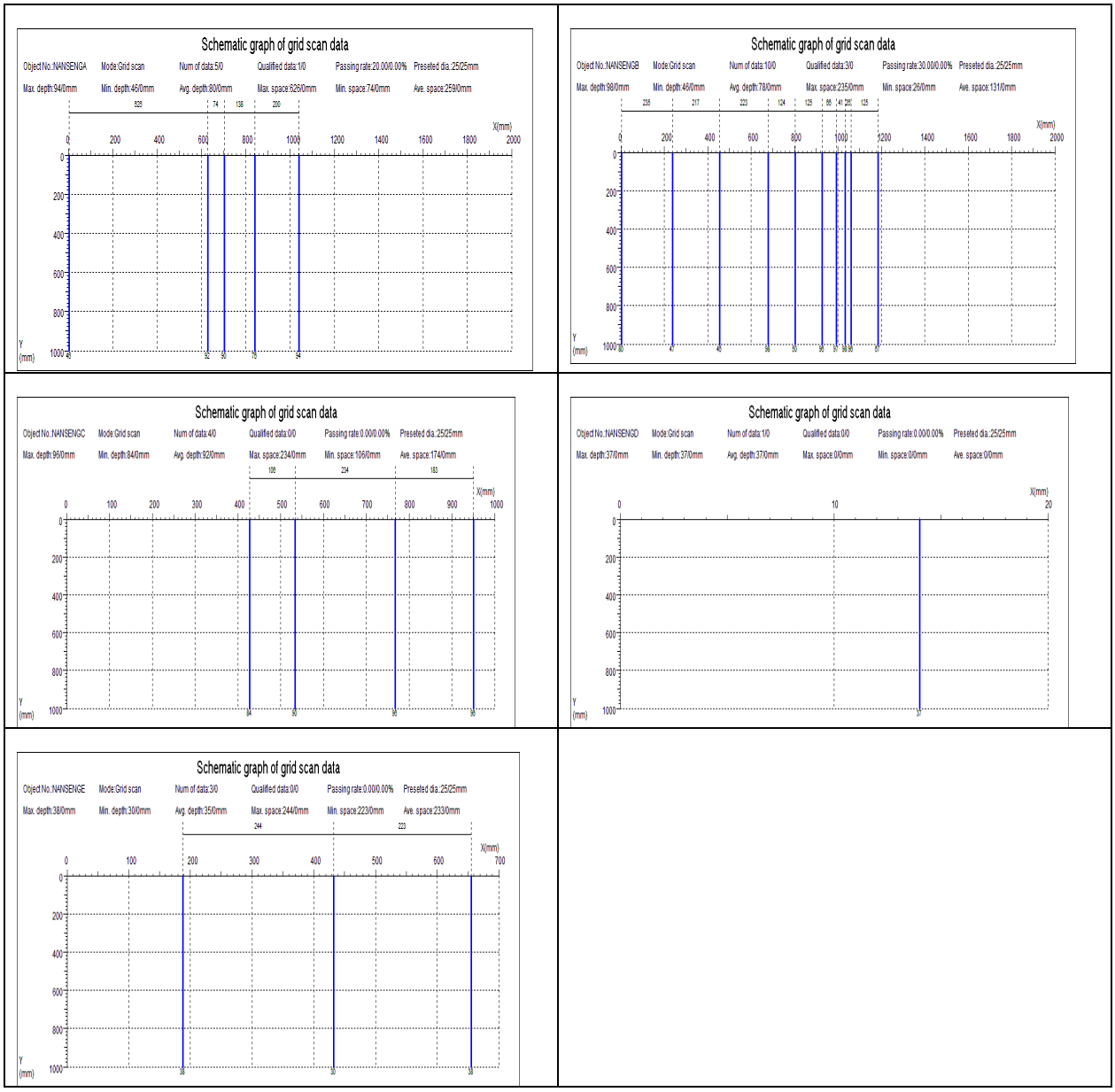

d